AD_____

The Effects of Blast Trauma (Impulse Noise) on Hearing: A Parametric Study

Report No. ARL 91-2

Final Report

Roger P. Hamernik
William A. Ahroon
George A. Turrentine
Robert I. Davis
Keng D. Hsueh
Sheau-Fang Lei

The Research Foundation of the
State University of New York

State University of New York at Plattsburgh
Plattsburgh, NY 12901

May 1991

Supported by

U.S. Army Medical Research and Development Command
Fort Detrick, Frederick, Maryland 21702-5012

SECURITY CLASSIFICATION OF THIS PAGE

REPORT DOCUMENTATION PAGE

Form Approved
OMB No. 0704-0188
Exp. Date: Jun 30, 1986

1a. REPORT SECURITY CLASSIFICATION Unclassified	1b. RESTRICTIVE MARKINGS
2a. SECURITY CLASSIFICATION AUTHORITY	3. DISTRIBUTION/AVAILABILITY OF REPORT Approved for public release; distriubtion unlimited
2b. DECLASSIFICATION/DOWNGRADING SCHEDULE	
4 PERFORMING ORGANIZATION REPORT NUMBER(S) ARL 91-2	5. MONITORING ORGANIZATION REPORT NUMBER(S)
6a. NAME OF PERFORMING ORGANIZATION The Research Foundation of the State University of New York 6b. OFFICE SYMBOL (If applicable)	7a. NAME OF MONITORING ORGANIZATION
6c. ADDRESS (City, State, and ZIP Code) P.O. Box 9 Albany, NY 12201-0009	7b. ADDRESS (City, State, and ZIP Code)
8a. NAME OF FUNDING/SPONSORING ORGANIZATION U.S. Army Medical Research & Development Command 8b. OFFICE SYMBOL (If applicable)	9. PROCUREMENT INSTRUMENT IDENTIFICATION NUMBER DAMD17-86-C-6172
8c. ADDRESS (City, State, and ZIP Code) Fort Detrick Frederick, Maryland 21702-5012	10. SOURCE OF FUNDING NUMBERS PROGRAM ELEMENT NO. 61102A; PROJECT NO. 3M1-61102BS15; TASK NO. CB; WORK UNIT ACCESSION NO 011

11. TITLE (Include Security Classification)

(U) The Effects of Blast Trauma (Impulse Noise) on Hearing: A Parametric Study

12. PERSONAL AUTHOR(S) Roger P. Hamernik, William A. Ahroon, George Turrentine, Robert I. Davis, Keng D. Hsueh and Sheau-Fang Lei

13a. TYPE OF REPORT	13b. TIME COVERED	14. DATE OF REPORT (Year, Month, Day)	15. PAGE COUNT
Final	FROM 4/1/86 TO 5/31/91	1991 May	124

16. SUPPLEMENTARY NOTATION

17. COSATI CODES			18. SUBJECT TERMS (Continue on reverse if necessary and identify by block number)
FIELD	GROUP	SUB-GROUP	
20	01		RA 3,
24	01		Blast Trauma Impulse Noise Hearing

19. ABSTRACT (Continue on reverse if necessary and identify by block number)

The primary goal of this research project was to produce a data base from which one could estimate the hazards to hearing associated with a wide variety of non-reverberant (free-field) blast wave exposures. To achieve this objective four different blast wave generation devices were designed. Three of these sources are based upon shock tube methods and one uses a high energy electrical discharge to produce a shock wave. The four sources produce pressure-time waveforms whose A-weighted amplitude spectra peak at four different regions of the audible spectrum. The conventional shock tube (Source I) has maximum A-weighted energy in the 0.250 kHz octave band; the 5-inch "Lamont" rapid acting valve driven shock tube (Source II) has its energy maxima in the 1 kHz octave band; the 3-inch "Lamont" tube (Source III) has its energy maxima in the 2 kHz octave band; while the spark discharge energy (Source IV) is concentrated in the 4 and 8 kHz octave band. These sources in anechoic surroundings produce non-reverberant waves that approximate the ideal Friedlander wave. By varying the exposure variables such as peak sound pressure level (SPL), number of impulses and the presentation rate, the relation between these variables

20. DISTRIBUTION/AVAILABILITY OF ABSTRACT ☐ UNCLASSIFIED/UNLIMITED ☒ SAME AS RPT ☐ DTIC USERS	21 ABSTRACT SECURITY CLASSIFICATION Unclassified
22a. NAME OF RESPONSIBLE INDIVIDUAL Mary Frances Bostian	22b TELEPHONE (Include Area Code) 301-663-7325 22c. OFFICE SYMBOL SGRD-RMI-S

DD FORM 1473, 84 MAR 83 APR edition may be used until exhausted
All other editions are obsolete.

SECURITY CLASSIFICATION OF THIS PAGE

19. Abstract (continued)

and auditory system trauma can be established. In summary, the results, based upon data from 423 experimental animals, indicate that (1) as the total energy of the exposure event increases so does the trauma to the auditory system. The increase in energy may occur as the result of an increase in the peak sound pressure level of the impulse or from an increase in the number of impulses. (2) The effects of the impulse repetition rate are less clear, but in general, the highest repetition rate when coupled with the more severe exposures produced the greatest amount of trauma. (3) The effects of the energy spectrum of the impulse are more subtle. The impulse from Source I produced the most severe low frequency PTS while Source IV produced a PTS which affected the highest frequencies the most. The other sources, II and III produced broad losses in the mid to high frequency range of the audiogram. There were also different patterns of cell loss produced which were related to the spectral content of the impulses. A general approach to developing a direct relation between frequency specific measures of acoustic trauma and the frequency domain representation of the impulse is presented. (4) Based upon over 3500 pre- and postexposure tuning curves, there are consistent relations between tuning curves parameters and the audiometric and histological measures of hearing trauma.

AD_____

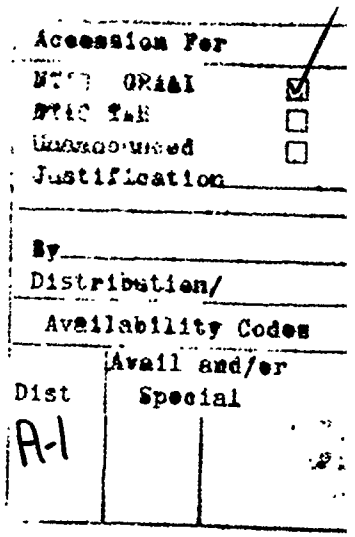

The Effects of Blast Trauma (Impulse Noise) on Hearing: A Parametric Study

Report No. ARL 91-2

Final Report

Roger P. Hamernik
William A. Ahroon
George A. Turrentine
Robert I. Davis
Keng D. Hsueh
Sheau-Fang Lei

The Research Foundation of the
State University of New York

State University of New York at Plattsburgh
Plattsburgh, NY 12901

May 1991

Supported by

U.S. Army Medical Research and Development Command
Fort Detrick, Frederick, Maryland 21702-5012

FOREWORD

Disclaimer:

Citations of commercial organizations and trade names in this report do not constitute an official Department of the Army endorsement or approval of the products or services of these organizations.

Animal Use:

In conducting the research described in this report, the investigators adhered to the "Guide for the Care and Use of Laboratory Animals," prepared by the Committee on Care and Use of Laboratory Animals of the Institute of Laboratory Animal Resources, National Research Council (DHHS Publication No. (NIH) 86-23, revised 1985).

TABLE OF CONTENTS

LIST OF TABLES

LIST OF FIGURES

I. INTRODUCTION

Blast waves, resulting from the sudden release of energy into the atmosphere (e.g., gun fire, cannon discharge, etc.), are one of the primary sources of high level impulse noise exposure in the military. These noise impulses are brief acoustic transients which have a very high intensity (often in excess of 180 dB peak SPL) and a relatively broad distribution of energy within the audible frequency spectrum. The blast waves that are typically encountered in military environments constitute a serious health hazard because of their damaging effects on hearing and other organ systems of the body. With a continuing increase in the sophistication and power of weapon systems, there has been a concomitant increase in the peak noise (pressure) levels to which personnel are exposed. While there exists a body of knowledge on the effects of continuous noise exposure on hearing, as well as to some extent the effects of impact noise on hearing, there is very little literature on the effects of blast wave and impulse noise exposure on hearing function. The paucity of data is due, in part, to the difficulty of producing well-controlled blast waves in a laboratory setting, and in part, because of the inherent difficulties associated with animal research. Direct laboratory studies on unprotected humans are usually not possible because of the excessive noise levels that must be used.

There are at present no generally accepted guidelines for predicting the adverse effects of blast wave exposures on hearing. What is needed before any predictive schemes can be developed, is a data base resulting from parametric studies of blast waves and their effects on hearing function. Because of the comparative delicacy of the cochlea and its associated conductive mechanism, such a data base may also be useful in providing an early indication of impending blast-induced trauma to other organ systems of the body.

II. BACKGROUND

There are a number of different suggested standards for exposure to impulse/impact noise [e.g. Coles, et al. (1968), Smoorenburg (1982), and Pfander, et al. (1980)]. Although each of these criteria has its proponents, there is a consensus that there is, in fact, an extremely limited empirical data base upon which a standard can be built. The difficulties associated with generating a data base are compounded by the extremely broad range of high intensity noise transients that exist in various industrial and military environments. For example, in industry, impacts often occur as a pseudorandom sequence, having variable peak intensities, that are superimposed on a continuous noise background. This combination produces a highly non-Gaussian noise of variable character often with a very high kurtosis. While rms SPLs' might be within the limits of hearing conservation standards, peaks in excess of 130 dB or more can be very common but irregular in their temporal spacing. At the other extreme, the diversity of military weapon systems produce impulses which originate as the result of a process of shock wave formation and propagation following high energy discharges. These waves, which can have peak levels in excess of 180 dB, can be either reverberant or non-reverberant in nature depending upon the environment in which they are encountered and they also may be superimposed on a background noise. Trying to develop a single standard to cover this broad range of "acoustic" signals is a formidable task.

The following paragraphs provide some background information which highlights the existing body of knowledge on impulse noise effects. The first section deals briefly with some of the fundamental differences between impulse and continuous noise. Later sections describe some of the relations between

the acoustic parameters of the impulse noise exposure and the magnitude of hearing loss and the last section presents some background on the role of tuning curves in the assessment of normal and pathological hearing function. These introductory comments are intended only to focus attention on studies that bear a direct relation to the data in this report and are not intended as a comprehensive review of the subject. The reader should keep in mind that many of the issues and relations that are discussed are poorly understood and tenuous at best, since they are based upon very limited data.

A. Impulse Versus Continuous Noise: There is a temptation to view the mechanisms of impulse* noise trauma as being essentially the same as those of continuous noise. Recent data, however, clearly differentiates impulse noise from other forms of noise. In the first instance, blast waves are different in a physical sense from tone bursts or noise impacts. They are characterized by a very rapid rise time (i.e., on the order of a microsecond or less) as a consequence of the shock front leading the pressure wave, and they obey an entirely different set of physical principles than conventional acoustic auditory stimuli. In addition, the waveforms contain a large amount of acoustic energy that is almost instantaneously applied to the conductive and sensory structures of the ear. Such an impulsive loading greatly increases the mechanical stresses that the peripheral auditory system must endure, and often results in mechanical damage to not only the middle ear structures, but to the delicate sensory structures of the inner ear as well. Thus, a basic difference between impulse and continuous noise is that in the former case we are dealing with a stimulus that can cause significant mechanical damage in the cochlea (Hamernik et al., 1984a), while in the latter case the stimulus, at levels normally encountered, causes damage primarily through cumulative metabolic effects over relatively long periods of time. Comparatively little is known about the physiological effects of mechanical disruption of the membranous labyrinth and the ensuing intermixing of endolymph and perilymph (Hamernik et al., 1984b). In general, however, both mechanisms, mechanical and metabolic, are always active to some extent. Spoendlin (1976) has suggested that at intensities around 125 dB, direct mechanical destruction and metabolic exhaustion are competing mechanisms in cochlear pathologies.

Bohne (1974) has shown that a fracture of the reticular lamina leads to an intermixing of endolymph and perilymph producing a potassium rich milieu for the sensory cells. This mixing of cochlear fluids leads to the ultimate demise of the hair cells and to changes in the nerve fibers innervating the organ of Corti. The effects on more central structures, such as spiral ganglion cells and the central auditory pathways, have not been extensively studied (Morest, 1982). Hamernik et al. (1984b) have shown that following a severe mechanically-induced lesion in the organ of Corti caused by blast exposure, the cells of the inner sulcus become extremely active. These cells begin to develop an unusual system of pseudopodia and villi. How these and other changes relate to recovery processes or to alterations of psychoacoustic hearing performance is not known.

Audiologically, the results of impulse noise exposure have also been atypical. Luz and Hodge (1971) have reported that for chinchilla, monkey, and human, the threshold recovery curve following exposure to reverberant impulses

---

* Impulse noise is being used here as a generic term to include both impact noise and blast waves (Friedlander waves). The former, usually being associated with industrial environments, are often caused by the impact of two objects; while the latter are, of necessity, very intense (> 140 dB), and usually caused by the non-linear processes of shock wave propagation following an explosive discharge.

is non-monotonic, i.e., there is an initial fast recovery, a rebound to higher levels of temporary threshold shift (TTS), such that the maximum TTS may occur several hours after the impulse noise exposure. This second peak in the TTS function is followed by a slower recovery that is approximately linear in log time. This non-monotonic pattern is distinctly different from the "classic" linear-in-log-time recovery pattern that typically results from lower level continuous noise exposure in humans. The same type of non-linear recovery has been found in the chinchilla after an impulse noise exposure (Henderson et al., 1974; Patterson et al., 1985, 1986; Hamernik et al., 1988). Furthermore, the data of Hamernik et al., (1988) indicate that this complex recovery pattern is frequently associated with a developing cochlear lesion. The practical consequence of the non-monotonic recovery following impulse noise exposure is that a single measurement of threshold shift (TS) during the early postexposure period is probably not a good index of acoustic trauma from high-level impulse noise. Thus, human experimentation which often relies on using TTS_2 (i.e., TTS measured 2 minutes after noise exposure) as a predictor of noise trauma is of questionable utility, and the CHABA (1965) postulate that TTS_2 is an accurate index of the hazard of a noise is of limited value. The corollary that all exposures that produce an equal TTS_2 are equally hazardous is therefore also of questionable validity.

B. Relation Between Hearing Loss and Impulse Noise Parameters:

1. Intensity-Duration Tradeoff: In the current industrial noise regulations, no consideration is given to the specific characteristics of the impulse (e.g., spectrum, repetition rate, etc.). The Coles et al. (1968) criteria attempts to include parameters other than just peak intensity. Briefly, the Coles et al. damage risk criteria (DRC) utilizes a tradeoff between the intensity and the duration of an impulse noise. The DRC is designed to protect 95% of the exposed population and is intended for 100 impulses presented over a period of a few minutes to "several" hours per day. A correction factor is applied to adjust the DRC curve for more or fewer impulses using a 5 dB trade-off per tenfold change in the number of impulses. The intensity-duration trading relation proposed by Coles et al. was evaluated in our laboratories using chinchillas exposed to impulses varying in intensity from 113 dB to 170 dB, and having durations of 40 µsec through 200 msec (Henderson and Hamernik, 1978). The chinchillas exposed to impulses lying on the DRC line (50 impulses, 1/min), developed large hair cell losses. These cochlear lesions may or may not be accompanied by parallel losses in hearing sensitivity. The amount of damage could be increased by either increasing the total number of impulses, or by holding the number of impulses constant and decreasing, within limits, the interstimulus interval. One general idea that reemerged from these studies was the notion of a "critical exposure" level (Ward, 1968). Exposures below the critical exposure were not excessively traumatic, while those above it generated significant cochlear pathologies, often far beyond what might be predicted by the DRC. The critical level probably varies with exposure parameters (Roberto et al., 1985). Since the duration or temporal structure of an impulse is closely related to its energy spectrum, the effect of impulse duration is further discussed in Section 5, spectral effects. In fact, an evaluation of the impulse in terms of its energy spectrum is probably the more preferable approach.

2. Impulse Noise and Variability: Hodge and McCommons (1966) reported that the variability in TTS following impulse noise exposure was too large to permit generalized statements based upon mean data. Kryter and Garinther (1966) also say essentially the same thing in summarizing their own data; however, they go one step further and suggest that the large variability is

the result of "tough" and "tender" ears. McRobert and Ward (1973) suggest that each ear has a critical intensity for a given non-reverberant impulse. Impulses below the critical level induce little or no TTS, regardless of the number of impulses (N); impulses above the critical level produce a TTS that grows by 5 dB for each tenfold increase in N. (See Price, 1981 for additional discussion of the critical level). To further complicate the issue, we have also found that as the threshold of damage is approached, animals will divide into two "Kryter-like" groups, i.e., "tough" and "tender" ears. Above and below the critical level, the amount of damage was relatively homogeneous; however, tremendous variability between subjects was usually associated with the transition region. Spoendlin (1976) has also commented on the extreme variability resulting from impulse noise exposure.

Some of our early data (Eames et al., 1975) suggests that there is also a critical intensity that is related to a conductive failure of the middle ear; i.e., tympanic membrane rupture or other conductive changes occur in the chinchilla at approximately 160 to 166 dB for free-field impulses having a first positive over-pressure duration of 1 msec. Thus, in reviewing the literature on impulse noise, there appears to be at least two major sources of variability: (a) the critical level for developing PTS and cochlear pathology and (b) the critical level for developing a pathological change in the conductive mechanism of the ear.

3. Number of Impulses: The original Coles et al. (1968) DRC recognized the importance of the number of impulses in estimating the potential trauma from an impulse noise exposure. Their basic curve was designed for an exposure of 100 impulses per day with a 5 dB shift of the curve for a tenfold change in N. Before relying too heavily on these figures, perhaps we should consider how this trading relationship originated. In the words of Coles et al., "where exposure is to an occasional single impulse only, it seems reasonable to raise the limits somewhat, and an estimate of 10 dB has been agreed upon for this. The exact adjustment for different numbers of impulses has not been defined since there are obviously an infinite number of variations in the pattern and amount of noise exposure." Thus, the 5 dB for tenfold change in N took hold and is to be found today in the CHABA (1968) report. The point of the above is that this relationship which has been often quoted and accepted is only a best guess and without experimental foundation. Data of McRobert and Ward (1973) show that the function relating hearing loss to the number of impulses is not simple and that each individual may have a critical level for a given impulse. If the impulse exceeds the critical level, then hearing loss with repeated exposure will develop faster than would be predicted. On the other hand, if the impulse is below the critical level, the auditory system appears to be able to withstand many more impulses. The findings of McRobert and Ward are for the TTS state. We have obtained similar results for the chinchilla when PTS and hair cell counts were measured (Roberto, et al., 1985). More recently, Patterson et al. (1985) have shown, using chinchilla, that, over a limited range of impulse parameters, a more defensible trading relation is a 10 dB change in intensity for a tenfold change in the number of impulses. Experiments such as this need to be extended in order to establish the generality of this latter result.

4. Repetition Rate: The Coles et al. DRC, as well as criteria that are based upon equal energy considerations neglect the rate of presentation of the impulses as a factor in the production of hearing loss. With repetition rates less than 1/sec, the acoustic reflex can exert a protective effect. Ward et al. (1961) exposed human subjects to impulses presented at interstimulus intervals (ISI) of 1, 3, 9, or 30 seconds. Because there was no difference between the level of TTS for each group, it was concluded that when the ISI is

greater than 1/sec the repetition rate has little or no effect on PTS. The conclusions of Ward et al. (1961) may not be generalized to all impulse presentations. Perkins et al. (1975), using blast waves, compared the hearing loss produced by 50 impulses of 155 dB and 1 msec A-duration; the impulses were presented at either 1/min or 10/min. There were distinct differences between groups; the faster repetition rates produced much larger amounts of threshold shift, (TS), PTS, and hair cell loss than the lower repetition rates. The effects are almost certainly independent of the influence of the acoustic reflex because the ISI at the highest repetition rate is longer than the reflex decay time. While we are a long way from understanding the effects of temporal spacing of impulses on hearing loss, it seems likely that temporal sequencing is an important part of an impulse noise exposure.

5. Spectral Effects: One of the surprising features of the existing or proposed exposure criteria is the general lack of specific consideration that is given to the frequency domain representation of the impulse, a point frequently raised by Price (1983) and others. Some deference is, however, given to the spectrum in these criteria, but in a rather covert or indirect manner; e.g., through the use of A-weighting of the stimulus or through the handling of the A and B duration variables. The authors of the Coles, et al. (1968) proposal, for example, acknowledge the importance of the spectrum by recognizing that long A-duration Friedlander type waves, which transport relatively large amounts of energy at low frequencies, are less effective in producing acoustic trauma than are short duration A-waves. Thus, their criterion line for the "A-waves" is drawn horizontal for A-durations greater than approximately 1 ms. A more direct spectral approach to the evaluation of impulses and impacts was proposed by Kryter (1970). His suggestions, while based upon sound reasoning, never really caught on. The Kryter approach appeared attractive in its ability to predict the amount of temporary threshold shift measured two minutes after exposure (TTS_2) to a noise transient provided that the TTS_2 was not very large or alternatively that the levels of the transient in any given frequency band were not excessive. Price (1979, 1983, 1986) to some extent has tried to build upon and extend the Kryter approach by considering the spectral transmission characteristics of the peripheral auditory system. Price's reasoning led to the following conclusions. (a) There is a species specific frequency, f_o, at which the cochlea is most vulnerable and that impulses whose spectrum peaks at f_o will be most damaging. This would appear to be true, according to Price, regardless of the distribution of energy above and below f_o. For man the suggested frequency is 3.0 kHz. (b) Relative to the threshold for damage at f_o, the threshold for damage should rise at 6 dB/octave for $f_p<f_o$ and at 18 dB/octave for $f_p>f_o$ where f_p = spectral peak of the impulse. Thus, a model for permanent damage was developed which is amenable to experimental testing. In subsequent studies, Price (1983) has tried to relate, with varying degrees of success, experimental data obtained from the cat to the predictions of this model. A review of the literature indicates that, except for the Price studies, there are few published results obtained from experiments specifically designed to study the effects of the spectrum of an impulse on hearing trauma.

C. The Relation Among Hearing Loss, Sensory Cell Loss and Tuning Characteristics.

Attempts at correlating hearing loss with hair cell loss have met with varying degrees of success. Some investigators have found threshold shifts of 30 to 50 dB with outer hair cell loss (e.g., Moody et al., 1976; Ryan and Dallos, 1975) while others have reported little or no hearing loss with

significant OHC loss (Hunter-Duvar and Elliott, 1972; Henderson et al., 1974). Still others have reported hearing losses of 20 to 40 dB with little hair cell loss (Lindquist et al., 1954; Hunter-Duvar and Elliott, 1972). Some of the differences may be due to subtle forms of anatomical damage which are difficult to relate to hearing loss patterns, (e.g., isolated, mid-cochlear hair cell lesions versus lesions that extend continuously from base toward the apex of the cochlea). In the case of an isolated lesion, it is possible for the excitation pattern in the cochlea to spread from a damaged region of the cochlea into one that is normal as intensity increases. Thus, the spread of excitation could potentially obscure the correlations between hair cell loss and hearing loss.

The psychophysical tuning curve (TC), which represents the envelope of the set of intensities and frequencies of a tone that effectively masks a second low level probe signal that is fixed in frequency, is a useful measure of the peripheral frequency resolution capabilities of the auditory system. This masked threshold function, which tends to increase in a fairly monotonic fashion as the tone (masker) frequency is systematically moved farther away from the probe signal frequency, has an asymmetric 'V' shape especially at the higher frequencies, which presumably reflects the excitation pattern of the masker (Zwicker et al., 1974). From the TC quantitative estimates of the auditory filter characteristics such as the $Q_{10\ dB}$ and the low- and high-frequency slopes can be obtained as a function of the characteristic (probe) frequency (CF). These TC variables have often been used as measures of the effects that cochlear damage has on frequency selectivity.

Animal studies have shown that certain characteristics of the TC may be altered (e.g., broadened tip, sensitization effects, and shifts of the CF toward lower frequencies, etc.) when there is sensory cell loss with a concomitant threshold shift. However, tuning curves measured in animal models using psychoacoustic methods or various gross electrical recordings have not, in general, been shown to be particularly sensitive to the histological status of the cochlea. In the relatively limited number of studies that included a histological documentation, the consensus has been that the changes seen in frequency selectivity were associated primarily with missing outer hair cells (Ryan et al., 1979; Smith et al., 1987; Harrison et al., 1981). On the basis of these psychophysical studies, it would appear that threshold shifts in excess of 30 dB are required before tuning is altered. This is in contrast (not surprisingly) to the high degree of sensitivity of TCs, obtained from single VIII nerve neurons, to the conditions of very localized groups of sensory cells (Liberman and Dodds, 1984). These authors, for example, have shown that normal TCs require that the stereocilia of both the inner and outer hair cells be normal. Even units innervating completely normal regions of the cochlea basalward of a small lesion can exhibit changes such as hypersensitivity of the tail region. Changes in tuning, measured using physiological techniques, may also be dependent upon the region of the cochlea where damage is sustained. Harrison and Evans (1977), for instance, reported a decrease in the sharpness of tuning (i.e., 10 dB bandwidth) for cochlear neurons with CFs above 2.0 kHz once the threshold shift began to approximate 30 dB. However, for CFs below 2.0 kHz, tuning was affected by thresholds shifts much less than 30 dB. Thus there are distinct differences in the sensitivity of tuning curve measures obtained from pathological cochleas using physiological and psychoacoustic methods. In humans with sensorineural hearing losses, psychophysical TCs also show a reduction in $Q_{10\ dB}$ and in some cases a shallow low-frequency tail with a sharp high-frequency slope (i.e., upward spread of masking) or, less commonly, a shallow high-frequency slope with a sharp low-frequency slope (i.e., downward spread of masking) (Wightman et al., 1977; Tyler et al., 1980: Florentine et al., 1980; Ritsma et al., 1980;

Klein and Mills, 1981; Tyler et al., 1984). The sensitivity of the TC to changes in threshold in humans, however, can be quite good with consistent changes in tuning being found with temporary thresholds shifts as little as 10 dB (Mills, 1982). While changes in psychophysical tuning characteristics similar to those found in humans have been observed following cochlear damage induced by noise and drugs in various animal models, the total number of animals published is very small and the range of permanent threshold shift (PTS) examined is limited. Thus, there is a need for further studies correlating tuning curve shape with a variety of cochlear histopathologies induced with noise and drugs. The blast wave exposures that we have used generated a variety of complex patterns of inner and outer hair cell loss. Such cochleas present a unique opportunity to study the frequency selectivity of the cochlea and how it is changed by various types of hair cell loss. The shapes of psychological tuning curves in hearing impaired persons may ultimately be used to predict the pattern or type of cochlear pathology (i.e., OHC versus IHC loss). The results are also relevant to theoretical problems in auditory research, namely the role of OHC's and IHC's in hearing, i.e., is frequency selectivity determined at the level of the IHC or are the OHC involved with frequency resolution? This, then, is the rationale for obtaining TC's on the animals from this study. The TC data in this report were obtained from 298 impulse noise exposed chinchillas from which more than 3,500 TC's were obtained.

III. METHODS

The basic experimental protocol that is common to all of the experiments consists of the following steps: (a) Preexposure evoked response audiograms and tuning curves (TC's) are measured on each animal. (b) The animals are exposed to noise under well controlled conditions. The temporal and spectral characteristics of the noise are recorded. (c) The animal's evoked response thresholds are determined immediately after exposure and at regular intervals after exposure. At 30 days postexposure, the audiogram is again measured to establish the animal's permanent threshold shift, (PTS), and postexposure TC's are once again collected at all audiometric test frequencies. (d) The animals are euthanized and their cochleas are then prepared for microscopic analysis. Cochleograms, which provide a quantitative description of the extent and location of the hair cell lesions are prepared for each cochlea.

A. Subjects: The experimental animal was the chinchilla. There is no one "best" animal for all aspects of the project. A number of common laboratory animals used in hearing research were considered. Primates, whose auditory function is similar to humans are extremely expensive to purchase and care for and have been ruled out because of the large number of animals that were required in this project. Cats and guinea pigs are prone to middle ear pathologies which could contaminate the interpretation of the experiments. Given the range of measures to be explored, the chinchilla was the logical choice for a number of reasons. (a) The chinchilla is resistant to middle ear disease. (b) The chinchilla has previously been used in a large number of experiments on noise-induced hearing loss involving continuous and impulse noise so that there is an existing data base on which to rationally plan new experiments (Henderson, 1969; Eldredge et al., 1973; Carder and Miller, 1972; Mills, 1973; Burdick et al., 1977; Patterson et al., 1985). Further research on the chinchilla will provide additional data for modeling the effects of noise. (c) Related to the issue of susceptibility; the chinchilla seems to be more susceptible to noise than humans. However, the difference in susceptibility can be compensated for by using a constant which varies with the frequency of the exposure. Mills et al. (1978) has analyzed the asymptotic threshold shift (ATS) data from chinchillas, monkeys and humans and

found that one equation could be used to describe the relationship between the level of noise and the amount of ATS [i.e., ATS = 1.7 (OBL - C) where OBL is the octave band level and C is a frequency and species dependent constant; C is 5-30 dB smaller for chinchilla than for man]. Similar results have been found for impulse noise by Henderson and Hamernik (1982) to describe the effects of an impulse noise exposure. In summary, there are differences in susceptibility between species, but the differences appear to depend on a single frequency dependent constant. (d) The chinchilla has been used in numerous psychophysical experiments, consequently, much is known about its threshold (Miller, 1970; Salvi et al., 1978), psychophysical tuning curves (McGee et al., 1976; Salvi et al., 1982c), threshold for gap detection (Giraudi et al., 1980) and amplitude modulated noise (Salvi et al., 1982a). These psychophysical results indicate that the chinchilla's hearing capabilities are quite similar to those of man. For the above reasons the chinchilla was considered to be a reasonable animal model for the blast waves experiments described here.

Four hundred and twenty-three (423) chinchillas were used in this study. Each animal used with Sources I and II was anesthetized with an IM injection of Ketamine (12.86 mg/kg), Acepromazine (0.43 mg/kg) and Xylazine (2.57 mg/kg) and made monaural by the surgical destruction of the left cochlea. The animals used with Sources III and IV were anesthetized with Telazol© (IM injection - Tiletamine-Zolazepan 30 mg/kg). A chronic electrode was implanted near the inferior colliculus for single-ended, near-field recording of the evoked potential (Henderson et al., 1973; Salvi et al., 1982b). Each animal was given Amoxicillin© (100 mg/kg, subcutaneous) to reduce the possibility of postoperative infection. The animals were allowed to recover for at least two weeks before evoked potential testing began.

B. Host Computer - Hardware Description: A Digital Equipment Corporation (DEC) MicroPDP-11/73 supports all the other computers used in the laboratories. A block diagram describing the host computer system is shown in Figure 1. The host is configured with 2.0 MB of memory, 9-track magnetic tape, a 31 MB fixed, 340 MB fixed and 80 MB removable Winchester-technology disk storage and a dual 0.4 MB floppy disk drive. The host computer is configured as a time-sharing system and is connected by a serial line to each of the other microcomputers which are discussed in detail below. Other peripherals which are used by the laboratory systems include two eight-pen digital plotters (Nicolet Zeta-8, Soltec 281), laser printer (DEC LN03), and dot-matrix printer (DEC LA-50). A color-graphics terminal (DEC VT 241) and four other video terminals also are also served by the host.

Acquired initially to support only the two other MicroPDP-11/73 laboratory computers as well as two LSI-11/23-based systems, the host's operating system is TSX+. TSX+ allows us to develop software on the time-sharing system and move modules to the laboratory units via floppy disk or serial line transfer (KERMIT or VTCOM/TRANSF) which will then run without modification. Data files are easily (although not quickly) transferred from the laboratory system to the host using the same methods. This arrangement allows us to transfer data to and from any computer system in the laboratory and therefore gives us more flexibility in the laboratory than would be possible without the host system. The host is also connected to a ROLM data switch via a DTI to allow access to the campus Data General MV/10000 minicomputer and Burroughs A10D mainframe (replaced during the period of this project by a DEC VAX 6420) and to commercial statistical packages.

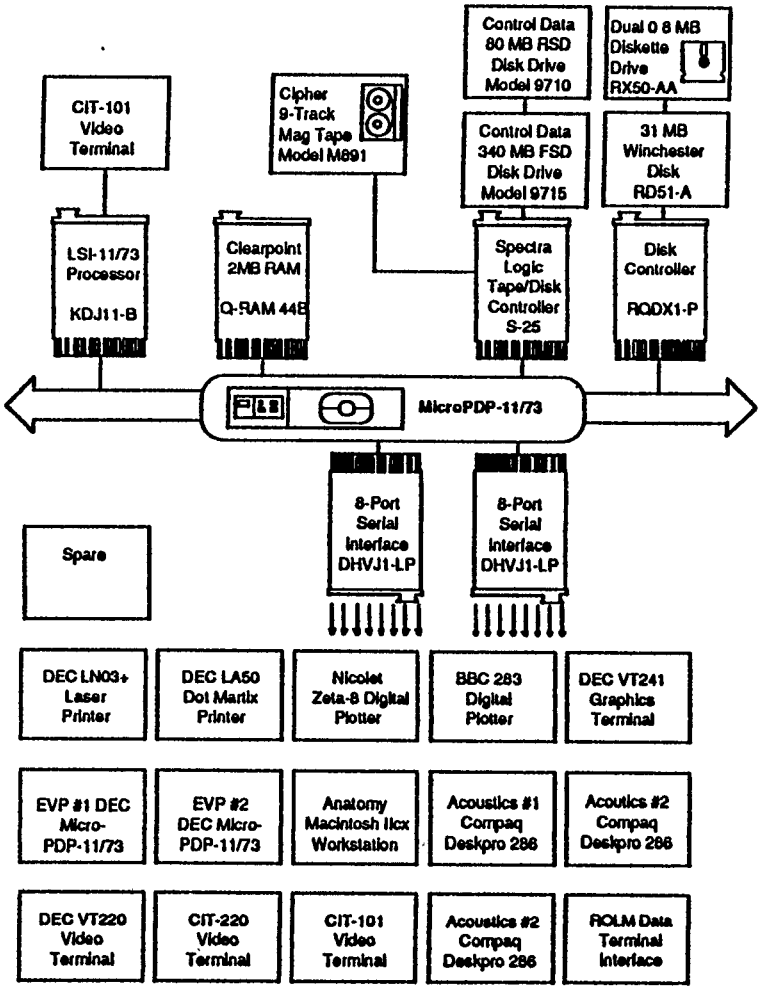

Figure 1. Schematic representation of the time-sharing host computer system.

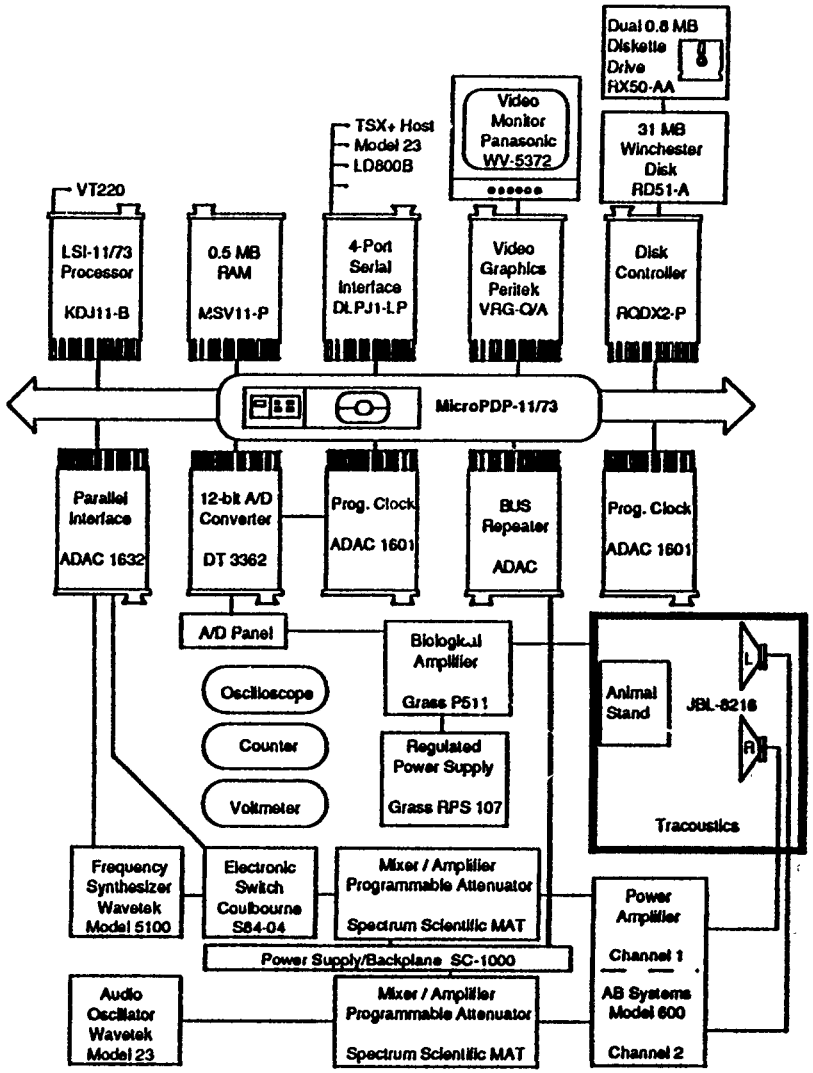

Figure 2. Schematic representation of the auditory evoked potential computer system.

The laboratory data base described below runs on the host system. In addition, the host runs a number of other programs required for the operation of the laboratory and support of the project which include, but are not limited to, word processing, data bases, statistical procedures, data transformations, printing and plotting.

C. Preexposure Testing: Hearing thresholds were estimated on each animal using the auditory evoked potential (AEP). A schematic of the AEP system is shown in Figure 2. The AEP has been shown to be a valid index of hearing threshold in the chinchilla. The correlation between the behavioral and evoked response measures has been strengthened by directly comparing, in the same animal, estimates of noise-induced behavioral and evoked potential threshold shifts (Henderson et al., 1983; Davis and Ferraro, 1984). There is a close correlation between the behavioral and evoked response thresholds before, during, and after acoustic overstimulation. In other words, the evoked potential threshold estimation procedure provides a good estimate of the magnitude of noise-induced hearing loss. The animals were awake during testing and restrained in a yoke-like apparatus to maintain the animal's head in a constant position within the calibrated sound field. AEP's were collected to 20 msec tone bursts (5 msec rise/fall time) presented at a rate of 10 per second. A general-purpose computer (Digital Equipment Corporation MicroPDP-11/73) with 12-bit A/D converter (Data Translation 3362), timer (ADAC 1601) and digital interface (ADAC 1632) was used to acquire the evoked potential data and control the frequency, intensity and time of the stimulus via a programmable oscillator (Wavetek 5100), programmable attenuator (Spectrum Scientific MAT) and electronic switch (Coulbourn Instruments S84-04). The electrical signal from the implanted electrode was amplified (50,000x) and filtered (30 Hz to 3000 Hz) by a Grass P511J biological amplifier and led to the input of the A/D converter where it was sampled at 20 kHz (50 msec period) over 500 points to obtain a 25 msec sampling window. Each sampled waveform was analyzed for large amplitude artifacts; and if present, the sample was rejected from the average and another sample taken. Averaged AEP's were obtained from 250 presentations of the 20 msec signal. Each waveform was stored on disk for later analysis.

Thresholds were measured using an intensity series with 5 dB steps at octave intervals from 0.5 to 16.0 kHz and at the half-octave frequency of 11.2 kHz. Threshold was determined to be one half step size (2.5 dB) below the lowest intensity that showed a "response" consistent with the responses seen at higher intensities. The intensity resolution of our method is 5 dB. The average of at least three separate threshold determinations at each frequency obtained on different days was used to obtain the preexposure audiogram.

Tone-on-tone masking functions (i.e., AEP tuning curves, see e.g., Salvi et al., 1982c) were measured on three to five animals in each group at six probe frequencies between 0.5 and 11.2 kHz presented at 15 dB above the preexposure threshold. A simultaneous masking paradigm was used (McGee et al., 1976). The probe tone had a duration of 20 ms and the intensity was set at 15 dB sensation level at the given test frequency. A simultaneous pure tone masker was presented at increasing levels until the masker just abolished the evoked potential elicited by the probe tone. The procedure was repeated over a range of masker frequencies around the probe tone to yield a "V" shaped masking function. The AEP has been shown to provide as good an estimate of the frequency selectivity as that obtained by behavioral techniques (Salvi et al., 1982c). It also shows that a small population of neurons within a restricted frequency band are contributing to the AEP at near threshold intensities. The advantage of the AEP tuning curves is that they provide an

independent method of assessing frequency selectivity and a method that is much easier to apply than behavioral techniques. Ten masker frequencies (from a Wavetek Model 23 programmable frequency synthesizer) distributed in frequency above and below the probe tone frequency were presented in an intensity series with 5 dB steps. The masked threshold was taken as one half a step size (2.5 dB) above the last masker intensity that resulted in a "response". TC's were run on a total of 298 chinchillas from which 1788 preexposure TC's and 1788 postexposure TC's were obtained. Table 1 presents the masking frequencies used for each probe tone.

Table 1

Evoked potential tuning curve probe and masker frequencies

Probe (kHz)	Masker Frequencies (kHz)									
0.5	0.15	0.20	0.30	0.40	0.52*	0.60	0.65	0.75	1.30	2.20
1.0	0.15	0.20	0.40	0.55	0.80	1.05*	1.30	1.70	1.90	2.50
2.0	0.30	0.75	0.90	1.30	1.70	2.05*	2.20	3.00	3.50	4.00
4.0	0.45	1.30	2.20	3.00	3.50	4.10*	4.50	5.00	5.60	6.00
8.0	0.45	1.30	2.50	5.90	7.00	8.10*	9.30	11.00	12.70	14.00
11.2	1.00	4.00	7.00	9.00	11.00	11.50*	12.00	13.00	14.50	16.00

*Indicates the frequency used as CF for calculations of tuning curve statistics.

D. Impedance Measures: The measurement of tympanometric functions and impedance was not part of the original protocol for this study. However, when it became obvious that individual variability might be quite large, the decision was made to try and assess middle ear function before and after exposure since damage to the middle ear conductive structures could be one source of variability (Eames et al., 1975).

Prior to each exposure, and immediately following the first postexposure threshold measurement, tympanometry was performed on 64 animals that were exposed to the Source I blast waves in order to monitor middle ear function. Tympanometric measurements were performed by monitoring the acoustic conductance (Ga) and acoustic susceptence (Ba) outputs of an acoustic admittance meter (Grason Stadler 1723) with a strip-chart recorder. Tympanograms were individually recorded at two probe frequencies (220 and 660 Hz) with decreasing ear canal air pressure (+200 to -300mm H_2O). During testing, the animal was restrained in a specially designed holder to prevent head and body movement. All data were corrected to the plane of the tympanic

membrane using the MAX/MIN procedure (Margolis and Smith, 1977a). Tympanograms reflecting the acoustic conductance and susceptence, at various canal pressures were converted to acoustic resistance (Ra), reactance (Xa), and impedance (Za) using the relations derived by Margolis and Popelka (1977b).

The result of these measurements were presented in our annual report ADA 206-180. Since impedance measures were time consuming and proved to be of no practical value in exlaining the variability in the dependent measures following exposures, they were not continued and the results will not be repeated in this report.

E. Blast Wave Generation: One of the primary requirements of this project was to develop blast wave sources which would reliably generate blast waves whose intensity, frequency spectrum and presentation rate could be varied and kept under experimental control. The blast waves employed in this study were generated by one of the following four methods: (a) conventional Shock Tube, Source I; (b) a 5-inch diameter valve-controlled shock tube ("Lamont driver"), Source II; (c) a 3-inch diameter Lamont Driver, Source III; and (d) an Electrical Spark Discharge, Source IV.

(1) The Conventional Shock Tube (Source I): The conventional shock tube shown schematically in Figure 3, in its most simple form, is a device in which a plane shock wave is produced by the bursting of a diaphragm which separates the high pressure (compression) section from the constant area (6" x 6") expansion section which is kept at atmospheric pressure. The expansion section terminates in a 6 foot long exponential horn having a 4 ft x 4 ft exit. The nearly instantaneous release of the high pressure volume of air generates a series of compression waves which propagate into the expansion section and rapidly coalesce into a shock front a few diameters downstream of the diaphragm. The horn exit is mounted in an anechoic enclosure. By varying the pressure in the compression section and the configuration of the horn throat, various blast wave profiles can be achieved (Hamernik et al., 1973). The SPL of the blast wave can be controlled by systematically adjusting the pressure in the compression section. The blast wave was measured using a transducer located on the center line and 36 inches from the outlet of the shock tube. The experimental animal was mounted next to the microphone.

(2) The Lamont Drivers (Sources II and III): A schematic representation of the blast wave exposure test facility using the 3-inch "Lamont" source is illustrated in Figure 4. The configuration of the 5-inch source is identical except for its overall dimensions. A cross-sectional view of the "Lamont" driver is shown in Figure 5. The Lamont source uses a relatively simple rapid acting valve to quickly establish a high pressure discontinuity in the expansion section in order to "drive" the shock front. A force differential generated over the area of the low pressure chamber relative to the high pressure chamber, on the rear plate, maintains the seal of the high pressure chamber. As the low pressure is gradually reduced a point is reached where the net force acting on the value reverses direction and the valve rapidly thrusts forward releasing the " lug" of high pressure gas into the expansion section. Nitogen is used as the operating gas and the pressure in the high pressure chamber varies from approximately 100 psig to 1000 psig to achieve peak sound pressure levels of the blast wave of from 150 dB to 160 dE at the exposure location. The SPL of the blast wave can be controlled by systematically adjusting the pressure in the compression section. The pressure-time history of the blast wave was recorded using a transducer located on the center line at a variable distance from the outlet of the shock tube. The experimental animal was mounted next to the transducer.

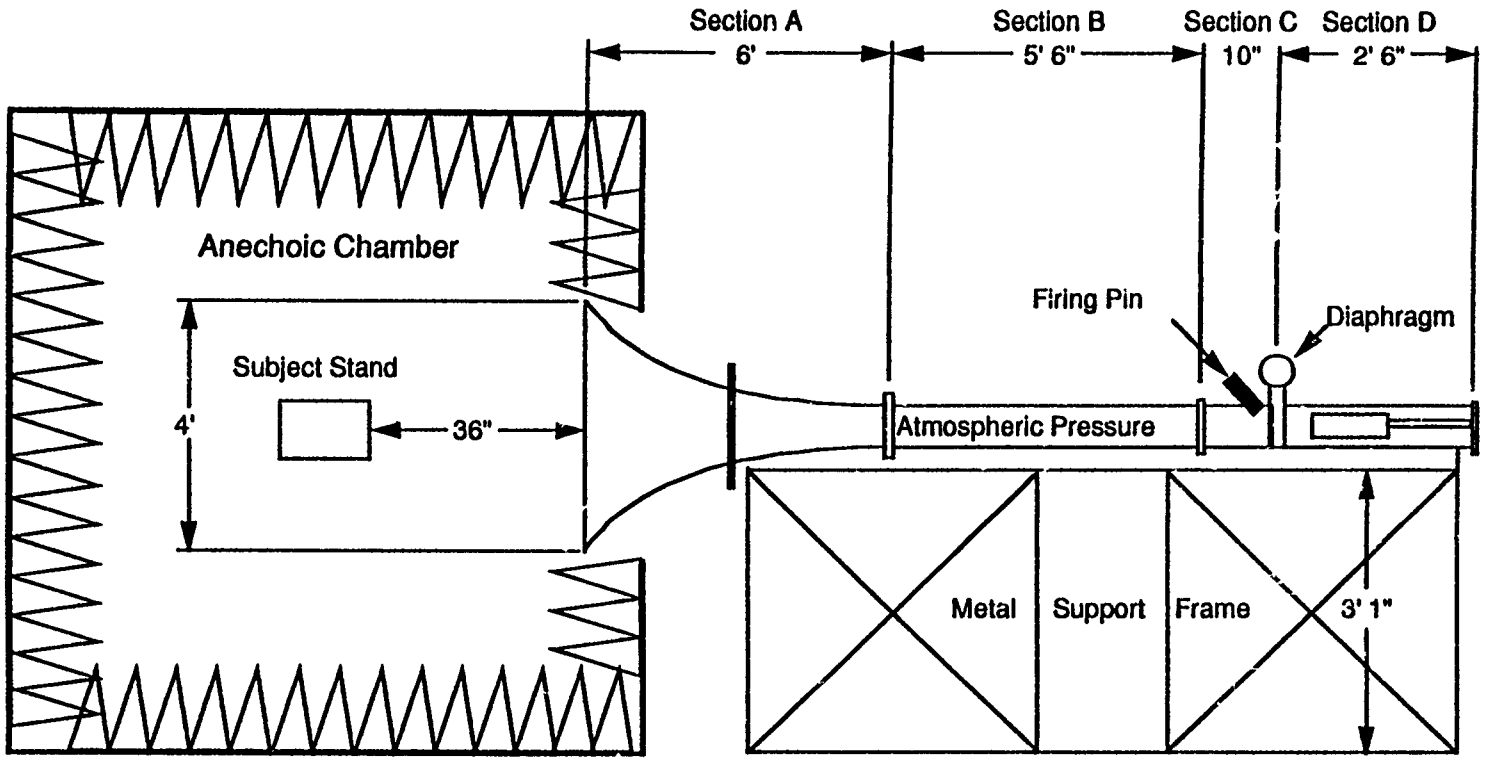

Section A: Exponential Horn (Throat - 6" x 6", Exit - 4' x 4')
Section B: Expansion Tube (6" x 6")
Section C: Transition Section
Section D: Compression Section (Diameter - 5")

Figure 3. Schematic side view of the conventional shock tube.

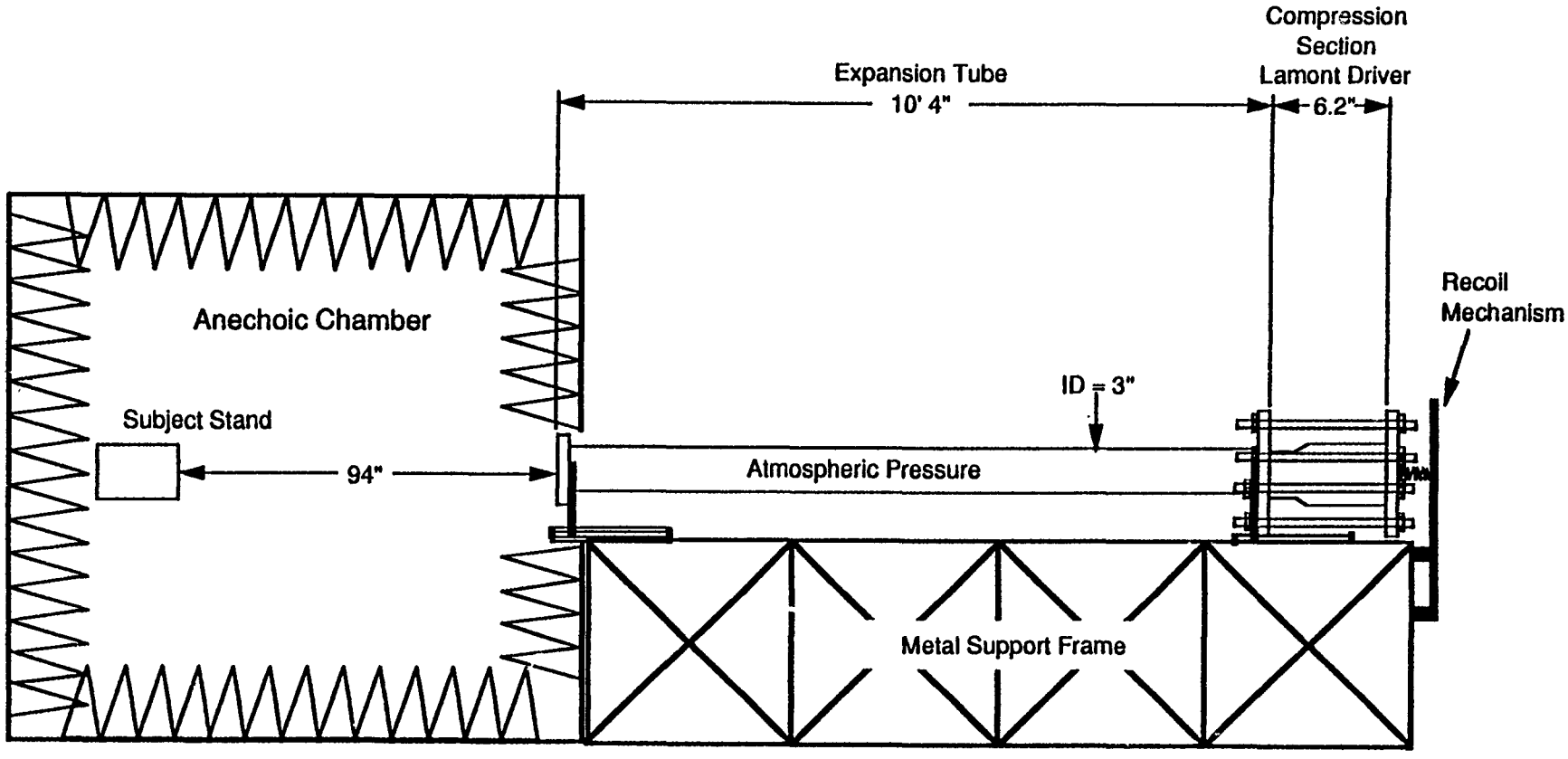

Figure 4. Schematic side view of the 3" Lamont shock tube.

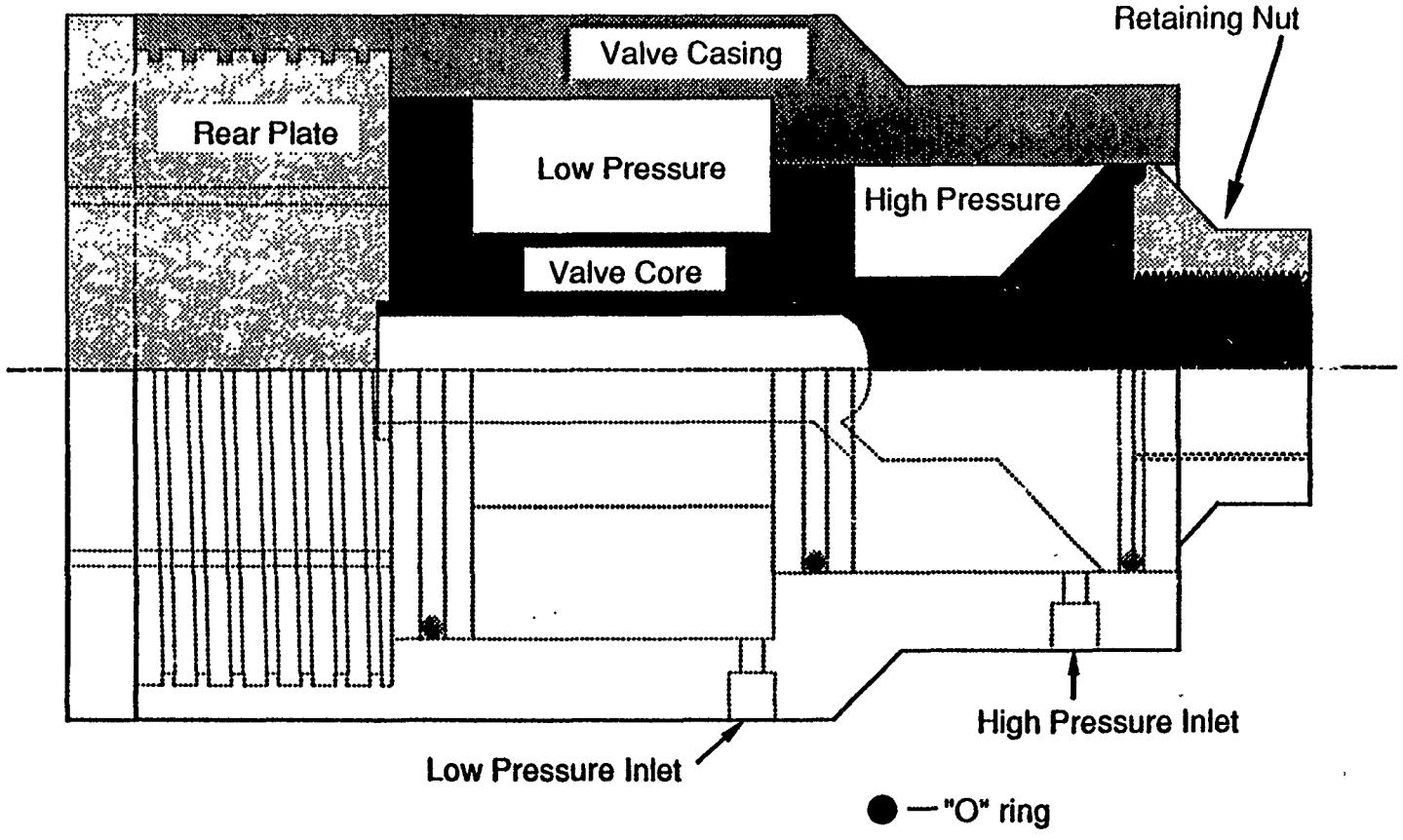

Figure 5. Schematic of the Lamont quick-acting valve.

(3) The Electrical Spark Discharge (Source IV): One of the more straightforward ways of generating an intense and repeatable blast wave is by discharging a high energy capacitor across a pair of electrodes. The electrical circuit is a standard RLC arrangement (Figure 6) in which a high capacitance, low inductance capacitor is charged through a high voltage source. Triggering of the spark gap is controlled through an independent circuit which activates a hydrogen trigger gap switch. The sudden release of energy from the capacitor breaks down the air gap and the subsequent rapid heating of the air produces the characteristic sharp resound. By changing the length of the gap or circuit characteristics, some control over the duration of the blast wave can be achieved. Repetition rates of up to 1/sec can be achieved at intensities that are variable from 130 dB or less to as much as 180 dB peak SPL. Control of intensity is easily achieved by either changing the discharge energy or increasing the distance to the source. Further control of the A-duration can be obtained by varying the angular position of the animal relative to the source. In the past this type of source has proven very unreliable, however with the EG&G components the design shown in Figure 6 is very stable, and with an external oscillator the interstimulus interval is easily controlled from 1/sec to virtually any slower repetition rate.

F. Blastwave Measurement and Analysis: A principal requirement for this study was the precise measurement and recording of the blast wave. The computer system used for this purpose was a Compaq 286 Deskpro personal computer using the ASYST™ application package (ASYST™ Software Technologies, Inc., Rochester, NY). The blast wave was first digitized and then recorded in storage devices (e.g., hard disk or magnetic tape). By using the customized software developed in our laboratory, each digitized blast wave was analyzed to extract characteristics such as the total acoustic energy, energy spectrum, peak and root-mean-square (RMS) sound pressure level (SPL) etc. Figure 7 illustrates the instrumentation used in the blast wave measurement system. Two different types of transducers were used to convert the dynamic acoustic pressure into an analog signal. The B&K 1/8 inch microphone (Type 4138) and the PCB crystal microphone (Model 112A22) were selected because of their ability to record high peak levels and their relatively fast rise times. A B&K microphone preamplifier (Type 2639), a B&K measuring amplifier (Type 2606), and a PCB six-channel amplifying power unit (Model 483A08) were used to amplify the analog signals from the B&K and PCB microphones respectively. Both transducers yielded identical results. The amplified analog signals were monitored on an oscilloscope. The output signal from the transducers was amplified and, in order to avoid aliasing problems that can occur in analog-to-digital (A/D) conversion, the amplified signals were filtered using an anti-aliasing filter prior to digitizing. The sampling rate of the A/D convertor (12-bit) was set at 500 kHz and the cut off frequency of the anti-aliasing filter was set at 150 kHz (approximately 1/3 of the sampling rate). For each blast wave, 16,384 samples were recorded for later analysis. Software was written using a PC-based system to perform the following computations: total sound exposure and sound exposure level calculations (Young, 1970); energy flux calculations; and spectral analysis using a 4096-point FFT; A-weighted analysis, etc.

Thus, for each impact the total sound exposure or sound exposure level (SEL) could be calculated (i.e., the time integrated, squared sound pressure).

$$SEL = 10 \log_{10} \left[\frac{\int p^2(t)\,dt}{p_{ref}^2 \, \Delta t_{ref}} \right] \qquad p_{ref} = 20\mu Pa \text{ and } \Delta t_{ref} = 1s.$$

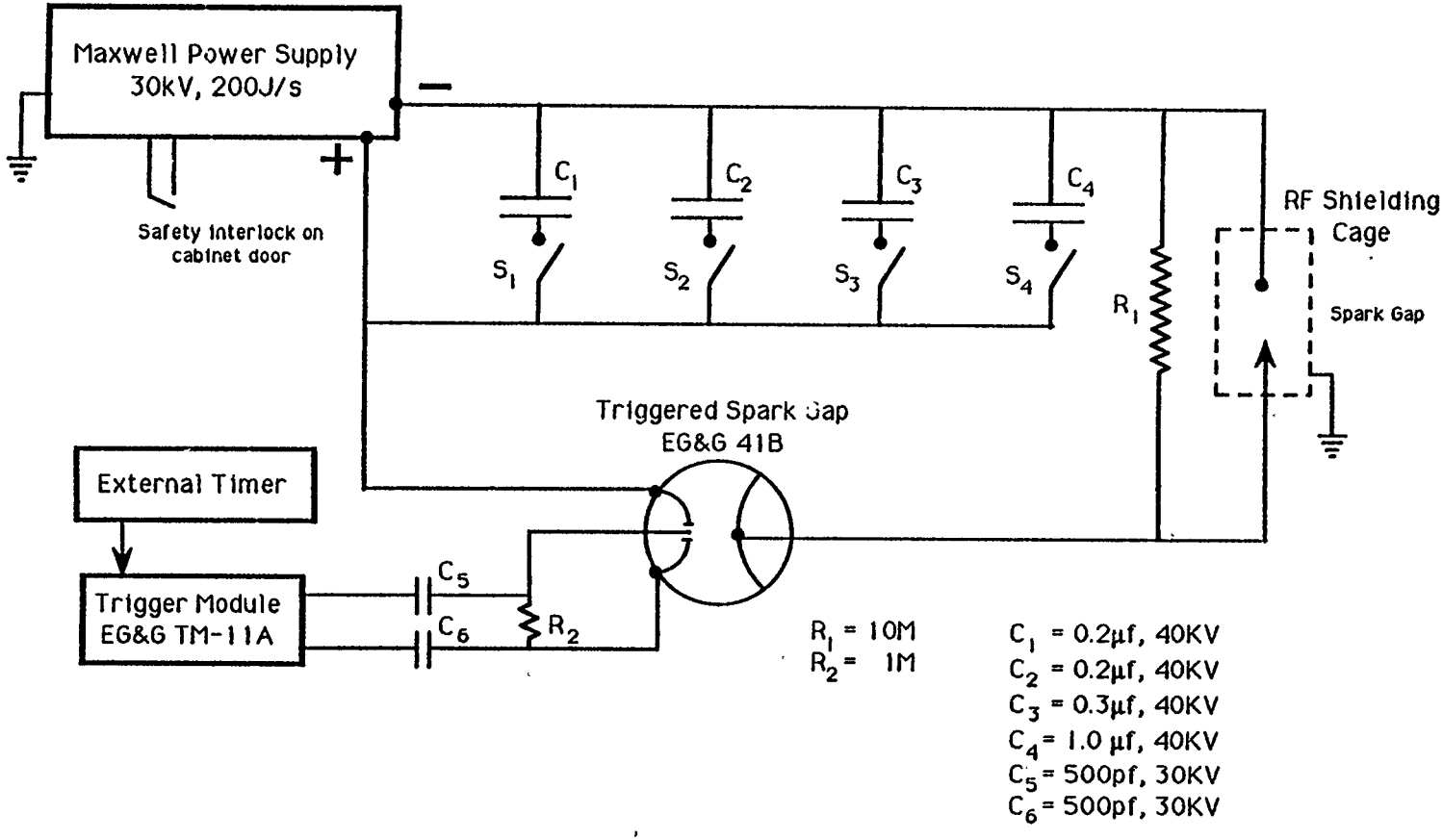

Figure 6. Schematic of the spark discharge impulse noise source.

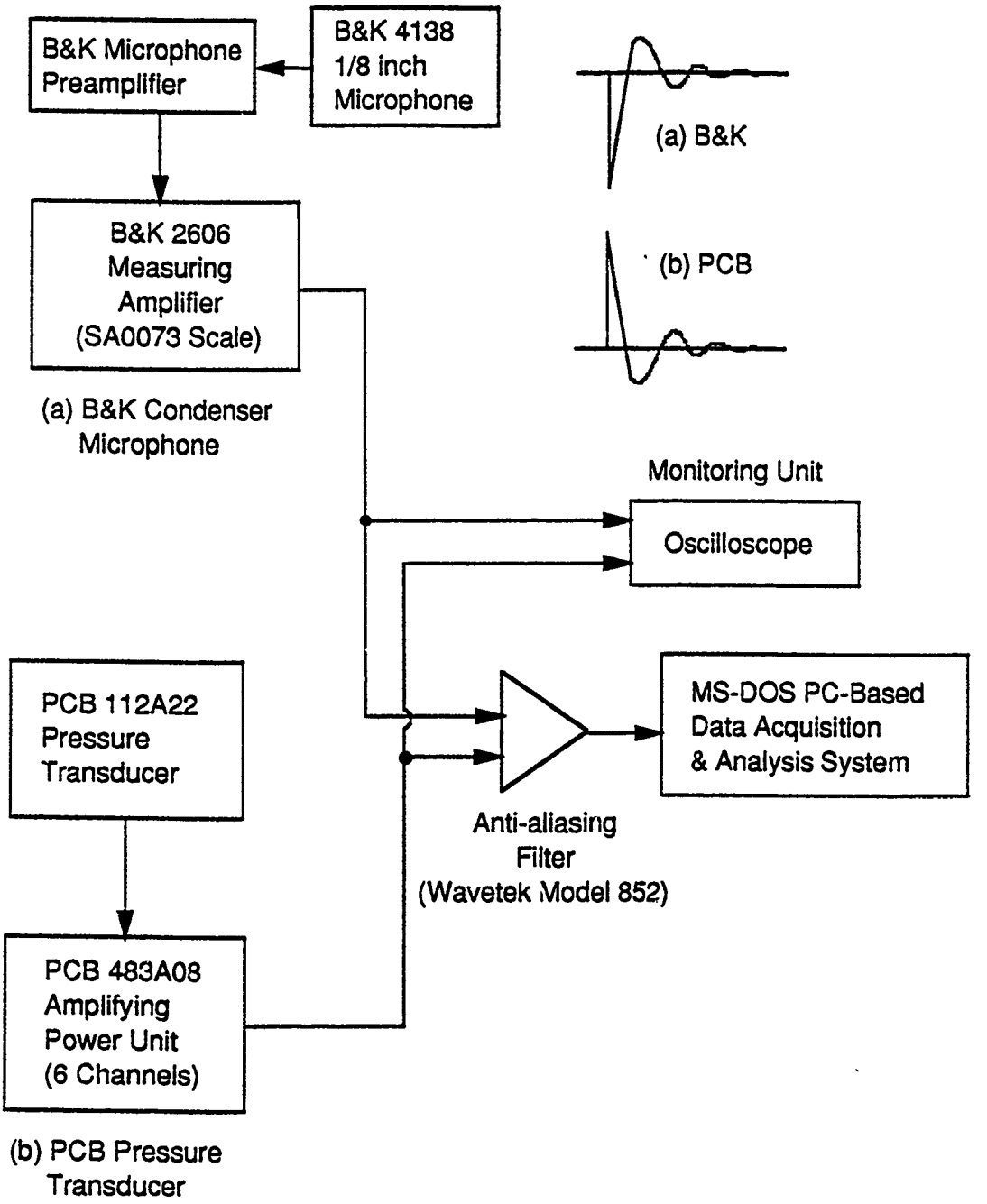

Figure 7. Schematic of the instrumentation used in the blast wave measurement system.

The total sound exposure was also divided by the standard characteristic impedance of air, $\rho c = 406$ mks rayls, to produce a quantity with units of energy flux (i.e., J/m^2). Similarly, all spectral quantities $|P(\omega)|^2$ were converted to units of energy flux spectral density, and for each impulse exposure, the total "energy flux" in the octave bands having center frequencies at the audiometric test frequencies was also calculated. [Since only p(t) was measured, the true energy flux cannot be obtained except in the special case of a plane wave.]

The schematic diagram of the PC-based data acquisition and analysis system is illustrated in Figure 8. A COMPAQ 286 Deskpro PC is configured with 1.2 MB random access memory (RAM), 30 MB winchester disk drive, 10 MB tape drive and EGA graphics adaptor. A 12-bit, 16-channel A/D converter subsystem (RC Electronics ISC-16) allowed rapid digitization of the blast wave at a maximum of one million samples/second (1.0 MHz or 1 μsec sampling period). The fast sampling rate helps in the accurate detection of the peak of the blast wave, one of the primary parameters in this study. The 12-bit resolution of A/D converter provides a reasonably accurate digitization of the analog signals. The acoustics laboratory data acquisition and analysis system was chosen and configured using standard commercial hardware (PC compatible) and software ASYST™ to allow easy replication and exchange of data.

The programs for performing the data acquisition and analysis were written using the ASYST™ application package. This package not only incorporates many features of standard computer languages such as APL and FORTRAN but also contains many pre-written software tools such as interactive graphics, Fast Fourier Transform (FFT), numerical integration and statistical computations. These features greatly simplify the task of performing the signal acquisition and processing.

The flowchart for these ASYST™ programs is illustrated in Figure 9. The programming of the data acquisition part shown in Figure 9(a) is briefly outlined below.

a. Set up the data acquisition parameters for the ISC-16 board such as the sampling time, total number of samples, trigger channel, trigger slope, trigger threshold, pre-trigger delay, etc.

b. Perform A/D conversions using the 12-bit A/D convertor mounted on the ISC-16 board.

c. Move the digitized data from ISC-16 data buffer to PC RAM.

d. Plot the acquired acoustical waveform and compute the peak and RMS SPL.

e. Save the digitized waveform in a data file for analysis.

The programming of the data analysis part of the setup is shown in Figure 9 (b) and is briefly described below.

a. Read the digitized waveform from the data file.

b. Set up the parameters needed for the data analysis window such as the sampling time, starting time and number of data points of the analysis window, and the number of data points to be skipped.

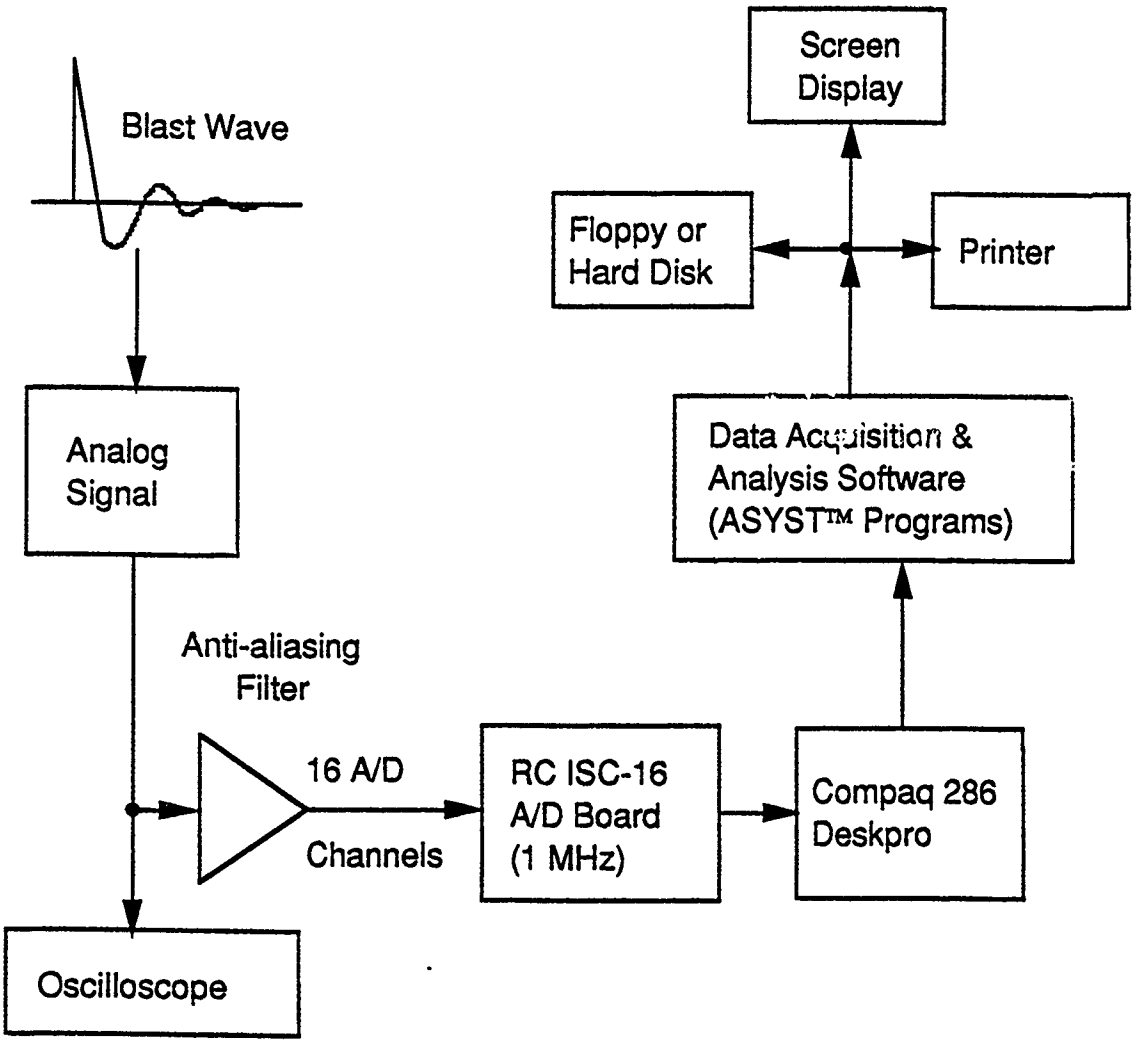

Figure 8. Configuration of the MS-DOS PC-based data acquisition and analysis system.

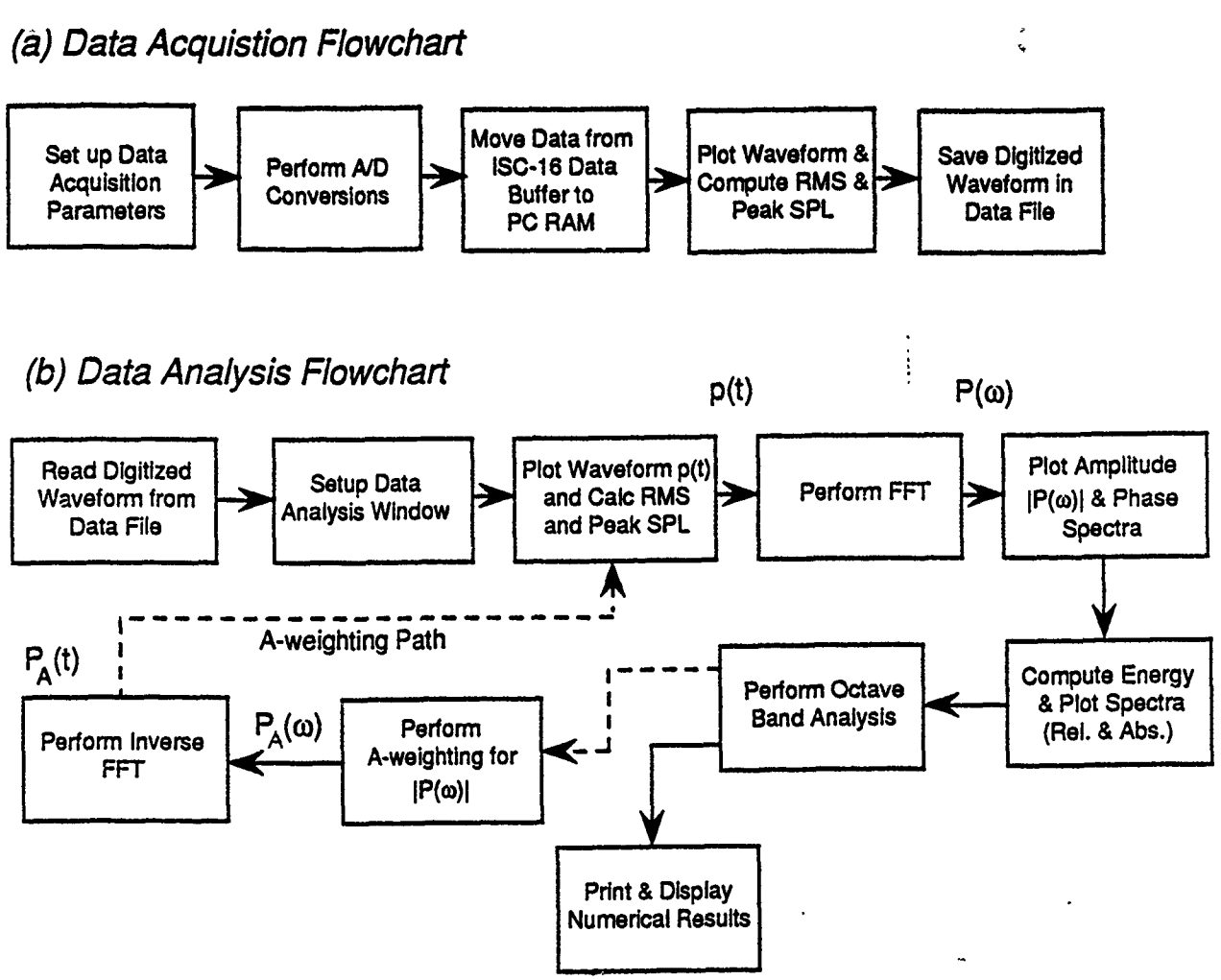

Figure 9. Flowchart of (a) data acquisition and (b) data analysis programs using the ASYST™ application package.

c. Plot the pressure-time waveform, $p(t)$, and compute the peak and RMS SPL.

d. Perform the FFT of $p(t)$ to obtain the spectral components, $P(\omega)$.

e. Plot the amplitude and phase spectra using $P(\omega)$.

f. Compute the total acoustic energy and plot the energy spectrum in both relative units (dB) and absolute units (J/m^2).

g. Perform an octave band analysis on the computed energy.

h. Print and display the computed results such as the data window size, SPL, energy, etc.

i. Perform A-weighting computations for $|P(\omega)|$ based on the standard A-weighting curve.

G. Exposure of Animals: For a given exposure condition, each chinchilla was exposed at the same fixed location relative to the shock tube expansion section outlet or the spark electrodes. During exposure the animal was unanesthetized but immobilized in a leather harness (Patterson et al., 1986). The right pinna was folded back and fixed in place to insure that the entrance of the external meatus was not obstructed and the position of the entire animal was adjusted so that the cross-sectional plane of the meatus was oriented parallel to the advancing shock front (i.e., a normal incidence).

Each experimental group of animals consisted of five animals. Each animal was individually exposed to one of the exposure conditions shown in Table 2. A total of 109 animals were used to complete the experimental paradigm for Source I; 105 for Source II and III and 104 for Source IV. [It should be noted that 70 animals were exposed to Source I stimuli under contract DAMD 17-83-G-9555 and the remaining 39 animals under the present contract. For the sake of completeness, all 109 animals will be integrated into the results of this report.]

H. Postexposure Testing: After the exposure was complete, threshold recovery functions were measured at 0.5, 2.0 and 8.0 kHz at 0, 2, 8, 24 and 240 hours after removal from the noise (using the same method as described for preexposure testing). After at least 30 days, final audiograms were constructed using the average of three separate threshold determinations at each of the seven preexposure frequencies. Permanent threshold shift (PTS) was defined as the difference between the postexposure and preexposure thresholds at each individual test frequency. Postexposure AEP tuning curves were collected at the six preexposure probe tones presented at 15 dB above the postexposure threshold.

I. Cochlear Histology: Following postexposure audiometric testing, animals were euthanatized by decapitation and the cochleas were immediately removed and fixed. The cochleas were dissected and the status of the sensory cell population was evaluated using conventional surface preparation histology (Engstrom et al., 1966). Briefly, the stapes was removed and the round window membrane opened to allow transcochlear perfusion, via the scala tympani/scala vestibuli with cold 2.5% glutaraldehyde in vernonal acetate buffer at 7.3 pH (605 mOsm). Postfixation was performed on the following day with one percent osmium tetroxide in veronal acetate buffer (pH 7.3) for 30 minutes. The

TABLE 2

A definition of the experimental groups

Group	Intensity	Number	Rate
1	150 dB Peak SPL	1	
2	150 dB Peak SPL	10	10 per minute
3	150 dB Peak SPL	10	1 per minute
4	150 dB Peak SPL	10	1 per 10 minutes
5	150 dB Peak SPL	100	10 per minute
6	150 dB Peak SPL	100	1 per minute
7	150 dB Peak SPL	100	1 per 10 minutes
8	155 dB Peak SPL	1	
9	155 dB Peak SPL	10	10 per minute
10	155 dB Peak SPL	10	1 per minute
11	155 dB Peak SPL	10	1 per 10 minutes
12	155 dB Peak SPL	100	10 per minute
13	155 dB Peak SPL	100	1 per minute
14	155 dB Peak SPL	100	1 per 10 minutes
15	160 dB Peak SPL	1	
16	160 dB Peak SPL	10	10 per minute
17	160 dB Peak SPL	10	1 per minute
18	160 dB Peak SPL	10	1 per 10 minutes
19	160 dB Peak SPL	100	10 per minute
20	160 dB Peak SPL	100	1 per minute
21	160 dB Peak SPL	100	1 per 10 minutes

cochleas were dissected and the entire sensory epithelium along with the lateral wall structures was mounted in glycerin on glass slides. [See Hamernik et al., (1987) for a more complete description.] The status of sensory and supporting cells were evaluated with Nomarski Differential Interference Contrast microscopy and entered into a data-base on a laboratory computer (DEC MicroPDP-11/73 and Macintosh II). Standard cochleograms were then constructed by computing the percent outer hair cell (OHC) loss and inner hair cell (IHC) loss across the length of the cochlea in 0.24 mm steps. These cell loss figures were then converted into percent loss over octave bands centered at the audiometric test frequencies along the length of the cochlea and correlated with the frequency-place map constructed by Eldredge et al. (1981). The morphometric system is shown schematically in Figure 10.

J. Inferential Statistics and Data Archive:

(1) Data Management: All audiometric and histological data from individual animals and exposure stimuli were entered into a comprehensive data base on the ARL Host Computer System. The data base contains: (a) subject information (e.g., identification, group designation, etc.); (b) audiometric measurements (e.g., preexposure thresholds, recovery thresholds, tuning curves, and postexposure thresholds); and (c) stimulus variables (e.g., total energy, octave band energies, A-weighted energies, etc.); and (d) cell morphometric data received from the anatomy laboratory. The data were archived daily to prevent loss by equipment or power failures.

(2) Data Reduction: The above-mentioned data base is maintained using custom-written computer software which serves as the basis for the data appendices submitted to the contract officer's representative (COR) with each annual report. Additional custom and commercial software packages are used to tabulate group summaries and to produce graphic representation of the group summaries. Custom-written routines are used to extract data from the data base for further analysis using commercial statistical packages (e.g., SPSS release 4, SAS, etc.). This data base management scheme was used successfully for the past five years to manage and control the large amount of data collected on 423 chinchillas.

(3) Statistical Analysis: The descriptive analysis of the data from these experiments consists of: (a) a complete description of raw data and group means and standard deviations; (b) a graphical representation of all audiometric data; (c) tabular and graphical representation of individual histological summaries; and (d) group summaries of the histological analysis. Further examination of the data employed mixed model analysis of variance with repeated measures on one factor (frequency) using the SPSS statistical package ($SPSS^X$ and SPSS release 4). Multiple contrasts and analysis of trend were employed where appropriate.

K. Tuning Curve Analysis: The evoked potential tuning curves were analyzed in two different ways. First, each of the twelve tuning curves (six pre-exposure and six post-exposure) for each animal was analyzed individually and values computed for $Q_{10\ dB}$, high-frequency slope (S_{HF}) and low-frequency slope (S_{LF}) for each TC. Second, animals were divided into groups based upon the amount of PTS the animal had at a given frequency and a mean tuning curve was computed by averaging the masking functions for all the animals in that particular group at that frequency. If the AEP could not be masked at the maximum output of the acoustic system, the maximum value was used in the analysis. The $Q_{10\ dB}$, S_{HF} and S_{LF} were then computed for each set of mean TCs.

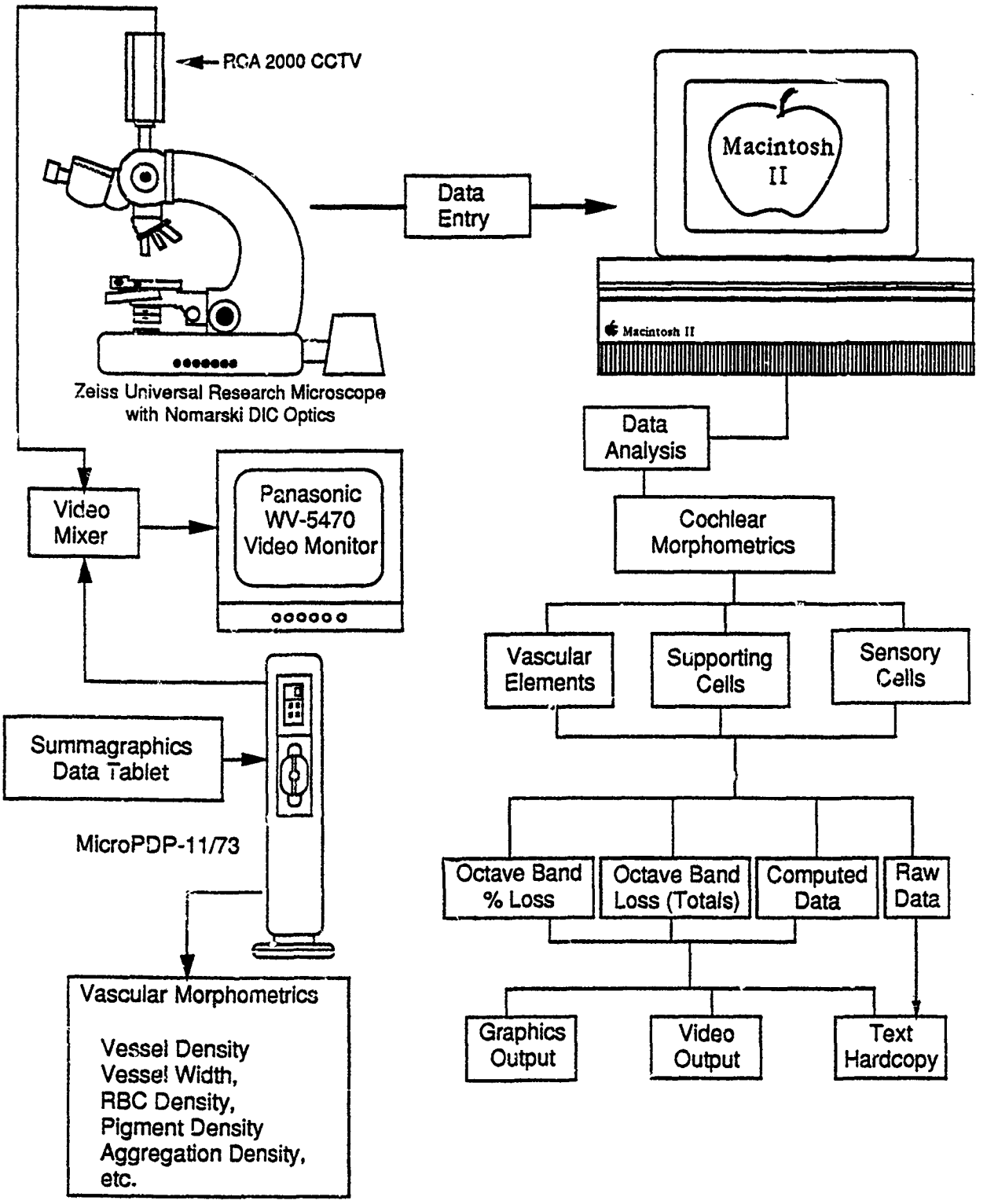

Figure 10. Anatomy laboratory temporal bone morphometric analysis systems.

(1) Individual Tuning Curves: Three parameters were computed for each individual TC: $Q_{10\ dB}$, S_{HF} and S_{LF}. The first statistic $Q_{10\ dB}$, was defined as the characteristic frequency divided by the bandwidth of the tuning curve 10 dB higher than the threshold at that characteristic frequency, i.e.,

$$Q_{10\ dB} = \frac{CF}{f_2 - f_1}$$

where CF is the characteristic frequency, (traditionally considered to be the frequency in Hz of the lowest masked threshold on the tuning curve); and f_2 and f_1 represent the frequencies at which the masking function crosses a line 10 dB higher than the threshold at CF. The high- and low-frequency slopes (dB per octave) represent the slope of the tuning curve function taken from CF toward the higher or lower frequency maskers. These three variables are often computed because the tuning curve is considered analogous to an electrical filter. However, the response of an electrical filter can be measured with a high degree of resolution. Similarly, single-unit tuning curves obtained from VIII nerve fibers are measured with a resolution of up to 50 frequencies or more per octave. However, because of time limitations, evoked potential or psychophysical tuning curves are typically measured using only approximately 10 masking frequencies. Of those 10 frequencies, not all are always able to mask the response to the probe, particularly following an exposure that produces a large PTS. Therefore, in computing the individual tuning curve statistics, it was necessary to institute a number of rules that would allow us to describe as accurately as possible the frequency selectivity of the auditory system as measured by the evoked potential in animals with normal thresholds as well as in those with varying amounts of PTS.

For each TC the characteristic frequency was chosen as the frequency of the masker closest to the probe tone on the high-frequency side (see Table 1). The use of only 10 masker frequencies results in several problems when trying to calculate tuning curve statistics especially in noise-damaged ears where the TCs can be very atypical. Most of these problems can be resolved by using many more masking frequencies. However, even the use of just 10 masker frequencies is extremely time consuming, typically requiring an hour to obtain a single tuning curve. These problems most often occur when the masking function does not resemble the "typical" tuning curve as might be the case when the subject has a large PTS. This often results in an inability to completely mask the probe with the extreme low- and high-frequency maskers (i.e., masked threshold is beyond the SPL output of the instrumentation).

Figure 11 depicts idealized normal and abnormal evoked potential tuning curves and is used in the following explanation of the rules that were used to compute TC characteristics. For the "normal" tuning curve, the low-frequency slope was computed using the masked thresholds at CF and the two frequencies immediately below CF (i.e., points labeled D, E, and F, where F is defined as CF). Only three points were employed since the low-frequency side of many tuning curves (especially at higher frequencies) appears to consist of two legs of different slopes. The low-frequency slopes reported in this report represent the slope of the low-frequency leg of the TC adjacent to the CF. A simple linear regression of threshold and log frequency using points D, E, and F resulted in a slope and intercept. If, because of measurement error or with atypical (pathologic) tuning curve shapes, the low-frequency slope was positive, the value reported in our analyses was assigned the value of zero. The numerical values for the low-frequency slope (dB/octave), which has a negative value, are presented as absolute values only.

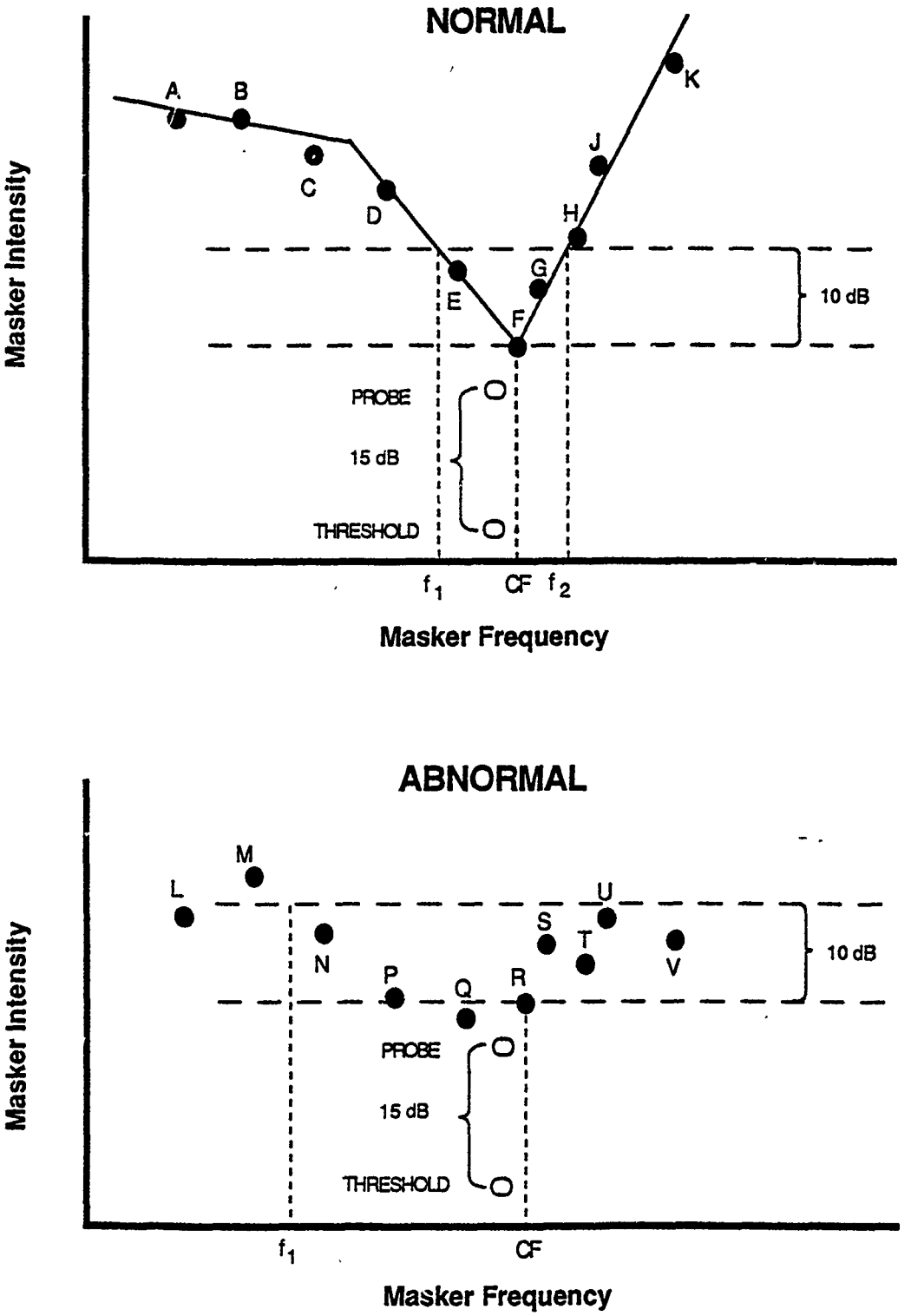

Figure 11. Idealized normal and abnormal tuning curves used to illustrate the calculation of tuning curve statistics.

The high-frequency slope (dB/octave) was computed using all the masker frequencies above the probe frequency for which a masked threshold could be measured (i.e., the points labeled F, G, H, J, and K). Thus, the linear regression coefficients were calculated using two to five or six masked thresholds. As was the rule with the low-frequency slope, a value of zero was reported for any high-frequency leg of the TC with a negative slope.

Values of $Q_{10\ dB}$ may be calculated using the low- and high-frequency slopes as described above. However, in many cases of noise damaged ears, these calculations could result in values of $Q_{10\ dB}$ that are not representative of the tuning exhibited by the TC. (That is, referring to Figure 11, in certain circumstances the calculated low-frequency slope could be positive when using our rules for slope calculations. However, the TC may exhibit some measurable tuning since the low-frequency tail may rise above the 10 dB fence as for example point M). Therefore, the values of $Q_{10\ dB}$ were calculated independently of the slopes in order to provide a more representative estimate of the 'tuning' of the auditory system at the six probe frequencies used in this study. As noted above, the value of CF was taken as the masker frequency immediately above the probe tone frequency. The values of f_2 and f_1 were calculated using the regression coefficients obtained by using the two adjacent points which represented the crossing of a fence 10 dB above the masked threshold of the probe in the presence of the CF masker (e.g., points labeled D and E were used to compute f_1 and points G and H to compute f_2).

Under some circumstances, particularly when a subject had large amounts of PTS, values of f_2 or f_1 could not be estimated accurately. An example of this problem is the case where the masker frequency immediately above CF is unable to mask the probe tone. Therefore, one of the two points needed for the analysis to compute f_2 does not exist. In this case $Q_{10\ dB}$ is not calculated and is defined as 'missing data' in subsequent inferential statistical analyses. The lower portion of Figure 11 gives an example of a tuning curve for which some of the variables cannot be computed. The low-frequency slope, computed using a regression line through the points P, Q, and R, is positive and thus a zero slope is assigned. A high-frequency slope, however, can be computed using points R through V. Although f_1 can be computed using points M and N, the masking function above CF (point R) does not go above the 10 dB line (fence). Thus, f_2 and consequently $Q_{10\ dB}$ cannot be computed. In such situations a value of 0.000 was assigned to the $Q_{10\ dB}$.

(2) Mean Tuning Curves: An alternative approach to quantifying changes in tuning following cochlear trauma is to obtain a group mean TC for each probe tone frequency. Mean tuning curves for specified groups of animals were computed by averaging the masker levels required to just mask the response to the probe presented at 15 dB above threshold. The slopes for these mean TCs were computed using the same rules as were applied to individual tuning curves. However, the calculations of $Q_{10\ dB}$ from mean tuning curves differed from those employed for the individual tuning curves. The values f_1 and f_2 for the mean tuning curves were computed using the regression variables calculated when determining the low- and high-frequency slopes of the mean tuning curve (instead of using only the two points adjacent to the 10 dB fence as was done with the individual tuning curves). Mean TC variables were computed on groups of animals that were partitioned into bins based on the amount of PTS that was measured in that particular animal at a particular audiometric test frequency. The following bins were formed: PTS < 10 dB; 10 dB ≤ PTS < 20 dB; 20 dB ≤ PTS < 30 dB; 30 dB ≤ PTS < 40 dB and PTS ≥ 40 dB.

IV. RESULTS AND DISCUSSION

The results presented below are divided into five sections:

A. Documentation of the stimulus: Blast wave p-t profiles, amplitude spectrum and octave band energy levels.
B. Group mean preexposure hearing threshold levels.
C. Effect of the independent stimulus variables: Intensity, number, repetition rate and source.
D. An analysis of the relation between the energy spectrum of an impulse and the measures of auditory pathology.
E. The relation among hearing loss, sensory cell loss and tuning curve characteristics.

There are five independent variables in the experiments reported here: (1) N, the number of impulses (1X, 10X, 100X); (2) impulse peak SPL (150, 155, 160 dB); (3) impulse presentation rate or interstimulus interval (ISI), (10/m, 1/m, 1/10 m); (4) impulse source (I, II, III, IV); and (5) audiometric test frequency. The first four are stimulus related parameters. The independent variables number and peak are proportional to the total energy of the exposure, while variations in the ISI do not change the total energy. Also, as is evident in Table 3, the energy delivered in a fixed level of a single impulse decreases from Source I through Source IV, and the relative distribution of energy across the audible spectrum varies across the four sources used (Table 5). Thus, direct comparisons among the effects of the source and exposure parameters on the dependent variables (PTS, OHC loss and IHC loss) are difficult to interpret unless an approach is developed which considers the different distribution of spectral energy in each of the sources. Such an approach will be presented in Section D of this results section.

A. Documentation of the Stimuli: This section documents the impulsive (blast wave) stimuli that were produced by the four sources. The pressure-time (p-t) wave forms along with their respective amplitude spectra shown in Figures 12 through 15, approximate the basic free-field Friedlander (1946) wave.

Octave band and total energy levels for each source and each exposure condition are presented in Tables 3 through 6. The energy values, both A-weighted and unweighted, are presented in J/m^2, dB re $1J/m^2$, and dB SEL in order that comparisons could be made with other published studies. Bar graphs which summarize the tabulated A-weighted octave band data are shown in Figure 16. As is evident from these data, Source I stimuli contained the most low frequency energy with an A-weighted peak in the 0.250 kHz octave band, while Source IV had a distribution of A-weighted energy which peaked in the 4.0 and 8.0 kHz octave bands. Sources II and III were intermediate with A-weighted energy peaks in the 1 and 2 kHz octave bands respectively.

B. Preexposure Hearing Thresholds: The mean preexposure audiogram for all 423 animals is illustrated in Figure 17 along with the behavioral audibility curve published by Miller (1970). The Miller curve was corrected for the effects of temporal integration using the data of Henderson (1969). The error bars in this figure represent one standard deviation above and below the mean. The mean preexposure thresholds are generally better than Miller's (1970) behavioral data in the mid-frequency region (when corrected for temporal integration). Lower thresholds, which have been found in other published data, probably reflect improvements in audiometric measurement techniques over the past 20 years.

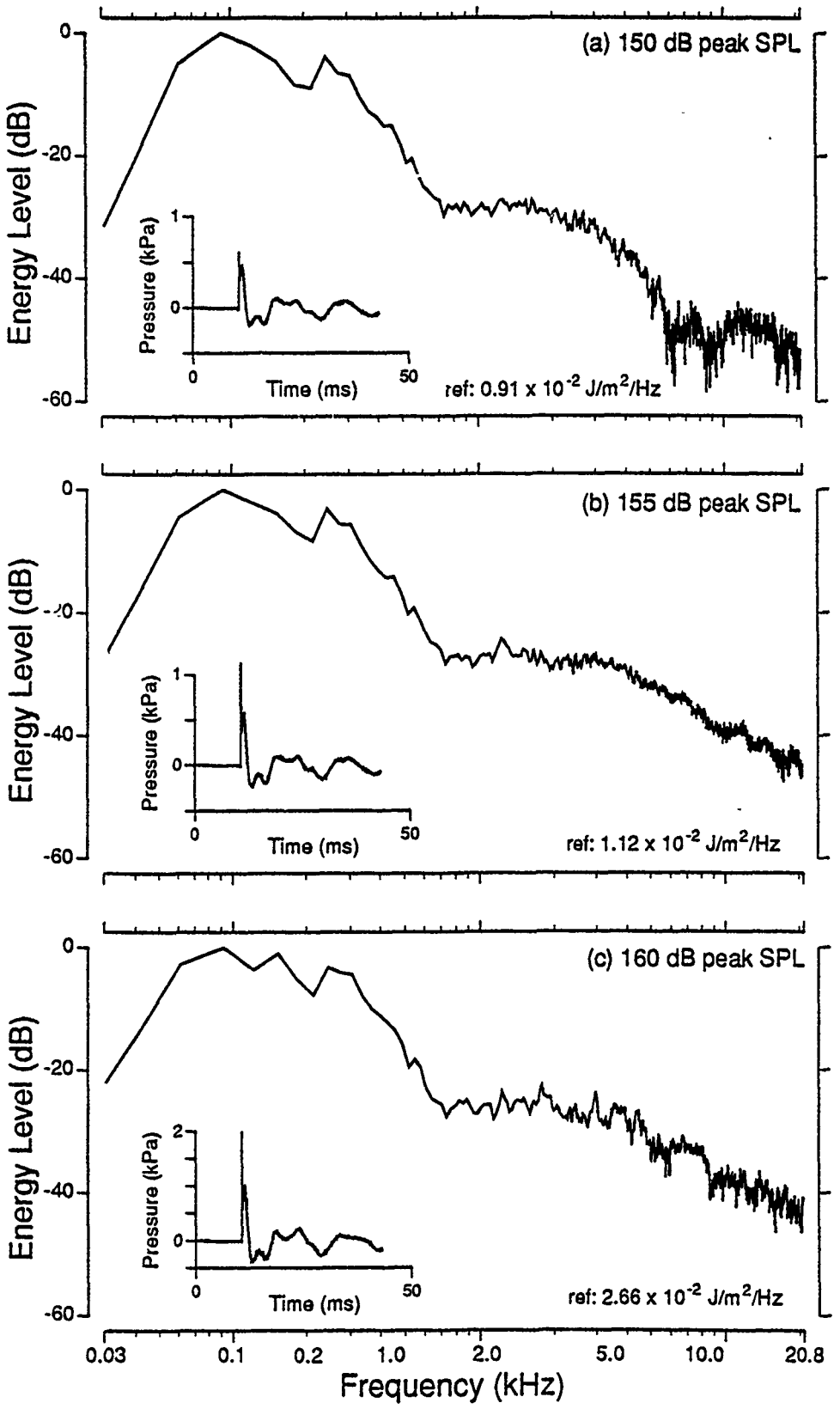

Figure 12. Amplitude spectra and pressure-time waveforms for the blast waves from Source I.

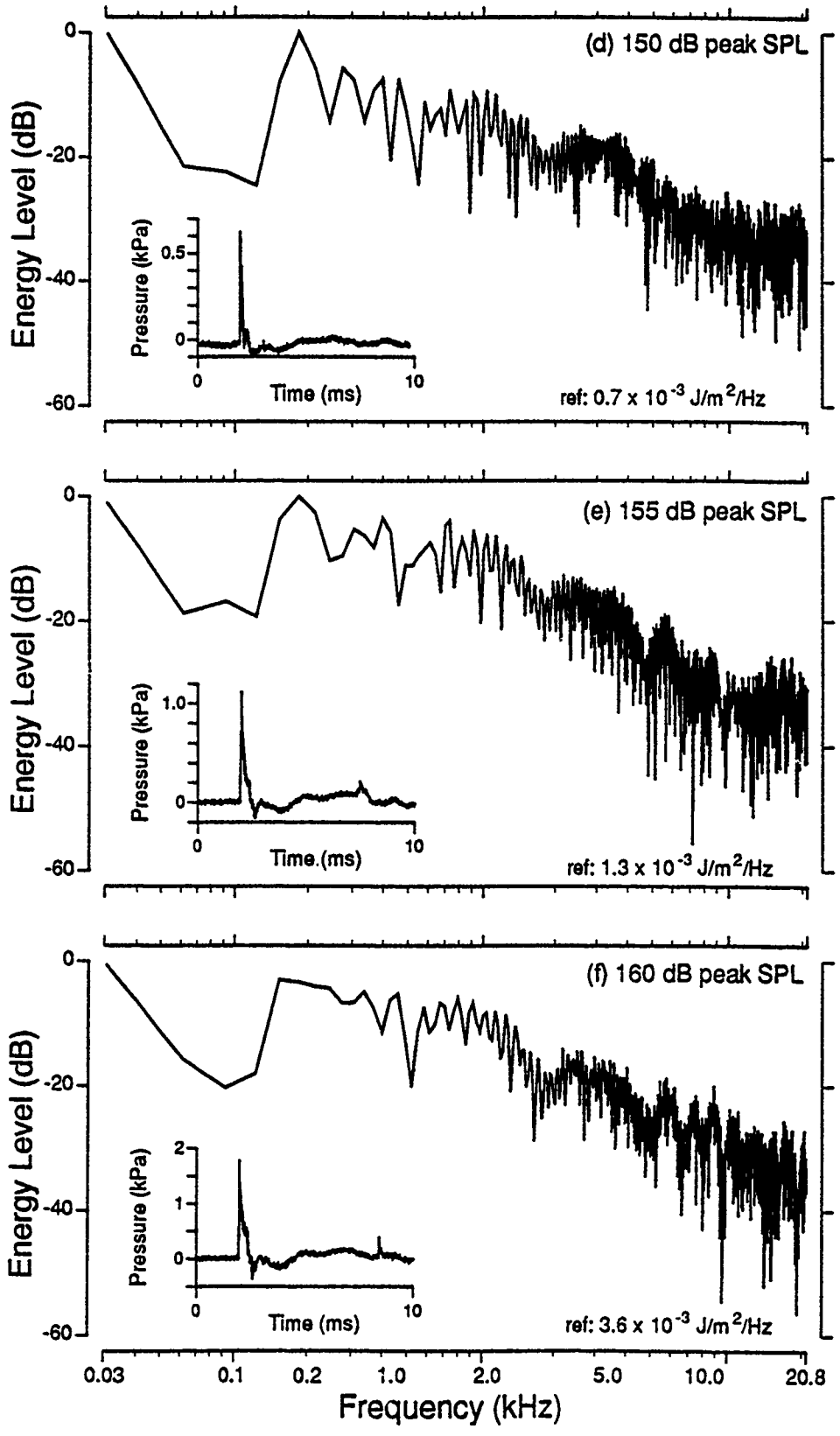

Figure 13. Amplitude spectra and pressure-time waveforms for the blast waves from Source II.

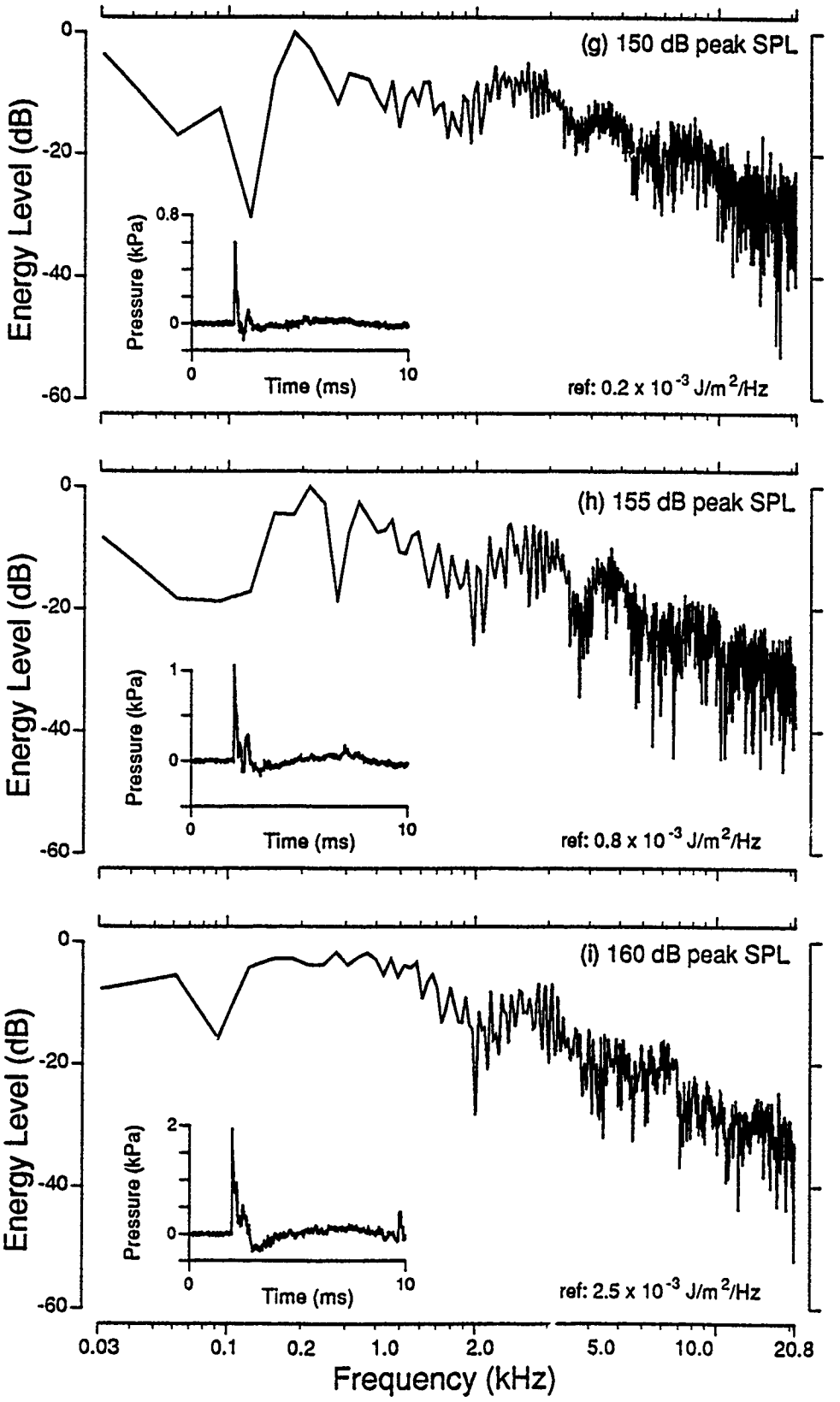

Figure 14. Amplitude spectra and pressure-time waveforms for the blast waves from Source III.

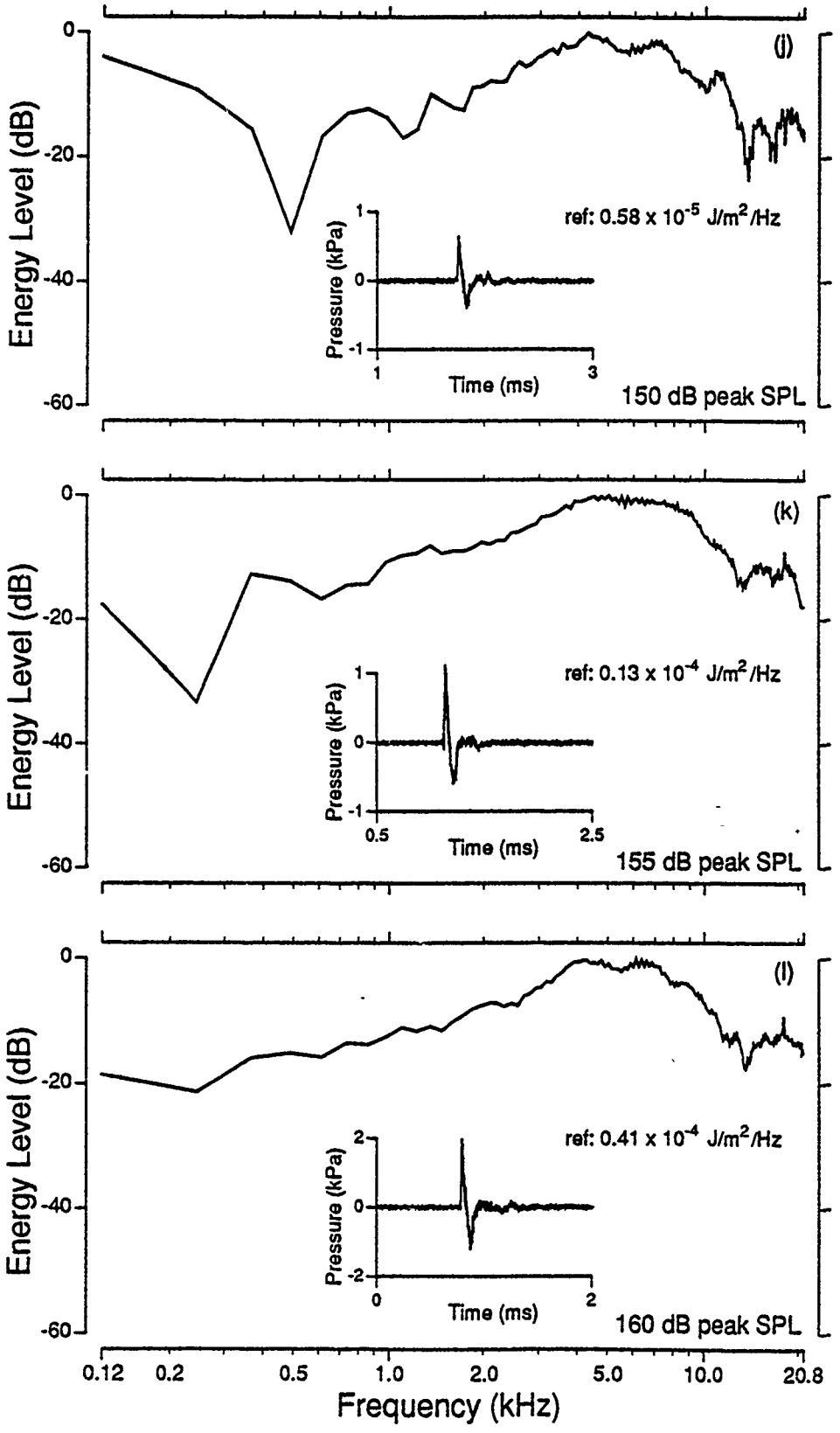

Figure 15. Amplitude spectra and pressure-time waveforms for the blast waves from Source IV.

Table 3

Total weighted and unweighted sound exposure level (dB) for each exposure condition and blast wave source

Peak SPL (dB)	Weight	Sound Exposure Level 1X	10X	100X	Sound Exposure Level 1X	10X	100X
		Source I			Source II		
150 dB	None	120.3	130.3	140.3	111.4	121.4	131.4
	A	111.0	121.0	131.0	108.9	118.9	128.9
155 dB	None	121.8	131.8	141.8	116.5	126.5	136.5
	A	113.8	123.8	133.8	114.7	124.7	134.7
160 dB	None	126.4	136.4	146.4	120.6	130.6	140.6
	A	118.6	128.6	138.6	118.6	128.6	138.6
		Source III			Source IV		
150 dB	None	109.0	119.0	129.0	105.0	115.0	125.0
	A	108.4	118.4	128.4	104.8	114.8	124.8
155 dB	None	115.0	125.0	135.0	109.2	119.2	129.2
	A	113.9	123.9	133.9	108.8	118.8	128.8
160 dB	None	119.1	129.1	139.1	113.8	123.8	133.8
	A	117.8	127.8	137.8	113.6	123.6	133.6

Table 4

Total weighted and unweighted energy flux (J/m^2) values for each exposure condition and blast wave source

Peak SPL (dB)	Weight	Absolute Energy (J/m^2) 1X	10X	100X	Relative Energy (dB) re: $1 J/m^2$ 1X	10X	100X
			Source I				
150	None	1.06	10.64	106.42	0.27	10.27	20.27
	A	0.13	1.25	12.54	-9.02	0.98	10.98
155	None	1.53	15.27	152.69	1.84	11.84	21.84
	A	0.24	2.38	23.83	-6.23	3.77	13.77
160	None	4.37	43.71	437.12	6.40	16.40	26.40
	A	0.72	7.25	72.48	-1.41	8.59	18.59
			Source II				
150	None	0.14	1.39	13.90	-8.54	1.46	11.46
	A	0.08	0.78	7.79	-10.97	-0.97	9.03
155	None	0.45	4.51	45.09	-3.47	6.53	16.53
	A	0.30	2.98	29.77	-5.23	4.77	14.77
160	None	1.14	11.41	114.15	0.57	10.57	20.57
	A	0.72	7.17	71.69	-1.43	8.57	18.57
			Source III				
150	None	0.08	0.79	7.94	-11.00	-1.00	9.00
	A	0.07	0.69	6.93	-11.59	-1.59	8.41
155	None	0.31	3.14	31.36	-5.03	4.97	14.97
	A	0.25	2.47	24.72	-6.07	3.93	13.93
160	None	0.82	8.20	82.04	-0.86	9.14	19.14
	A	0.61	6.07	60.66	-2.17	7.83	17.83
			Source IV				
150	None	0.03	0.31	3.15	-15.02	-5.02	4.98
	A	0.03	0.30	2.99	-15.24	-5.24	4.76
155	None	0.08	0.83	8.28	-10.82	-0.82	9.18
	A	0.08	0.76	7.64	-11.17	-1.17	8.83
160	None	0.24	2.42	24.23	-6.16	3.84	13.84
	A	0.23	2.29	22.95	-6.39	3.61	13.61

Table 5

Octave band unweighted and A-weighted sound exposure levels (dB) for a single impulse generated by each blast wave source

Octave Band CF (kHz)	150 dB Peak SPL Unwtg. SEL	150 dB Peak SPL A-Wtg. SEL	155 dB Peak SPL Unwtg. SEL	155 dB Peak SPL A-Wtg. SEL	160 dB Peak SPL Unwtg. SEL	160 dB Peak SPL A-Wtg. SEL
			Source I			
< 0.125	109.7	98.3	111.2	98.9	116.5	96.2
0.125	117.4	100.1	118.4	101.3	122.6	106.2
0.25	115.3	107.0	117.1	108.9	121.8	113.6
0.5	107.6	103.4	109.5	105.4	114.6	110.4
1.0	99.6	99.7	102.2	102.4	106.9	107.0
2.0	101.4	102.5	104.2	105.4	109.6	110.8
4.0	98.1	99.2	105.0	106.0	110.0	111.0
8.0	88.5	87.0	101.5	100.5	106.7	105.7
16.0	90.4	86.0	98.3	94.0	103.7	99.2
> 16.0	80.0	80.0	84.8	84.8	89.5	89.5
			Source II			
< 0.125	102.9	70.0	106.8	102.0	111.9	107.4
0.125	95.6	80.0	102.5	88.5	107.7	93.8
0.25	105.7	95.9	109.5	100.2	113.4	104.9
0.5	102.3	98.8	108.9	105.8	112.7	109.8
1.0	103.4	103.3	110.3	110.1	114.2	114.0
2.0	101.3	102.5	106.9	108.1	109.3	110.5
4.0	101.5	102.6	105.3	106.3	108.8	109.7
8.0	96.0	94.8	99.8	98.9	106.8	105.7
16.0	95.4	90.8	100.0	96.2	104.4	100.6
> 16.0	97.0	97.0	99.6	99.6	104.1	104.1
			Source III			
< 0.125	93.4	83.0	100.6	98.8	105.7	103.4
0.125	90.8	86.0	99.8	86.0	108.2	93.6
0.25	100.3	90.8	108.0	99.4	111.0	103.0
0.5	97.6	94.6	106.2	102.8	111.4	108.1
1.0	100.5	100.8	105.6	106.0	109.0	109.1
2.0	103.0	104.1	108.5	109.6	111.8	113.0
4.0	100.4	101.4	106.3	107.4	110.2	111.2
8.0	99.4	98.3	102.6	101.3	107.8	106.7
16.0	95.9	92.3	100.5	95.7	104.4	100.3
> 16.0	97.1	97.1	99.2	99.2	104.2	104.2
			Source IV			
< 0.125	92.6	92.6	84.9	84.9	94.1	94.1
0.125	84.6	68.0	74.3	57.8	78.5	62.0
0.25	79.3	70.4	58.5	49.7	75.7	66.9
0.5	75.6	71.9	82.6	78.7	86.3	82.9
1.0	83.4	83.4	89.3	89.5	92.8	92.9
2.0	91.9	93.2	95.6	96.9	100.2	101.4
4.0	100.2	101.0	104.2	105.0	109.1	109.9
8.0	100.8	99.8	105.7	104.8	110.1	109.2
16.0	93.9	89.6	98.7	93.6	103.2	98.6
> 16.0	94.2	94.2	98.1	98.1	103.4	103.4

Table 6

Octave band unweighted and A-weighted energy (J/m^2)
for a single impulse generated by each blast wave source

	150 dB Peak SPL		155 dB Peak SPL		160 dB Peak SPL	
Octave Band CF (kHz)	Unwtg. Energy	A-Wtg. Energy	Unwtg. Energy	A-Wtg. Energy	Unwtg. Energy	A-Wtg. Energy
			Source I			
< 0.125	0.0938	0.0068	0.1311	0.0077	0.4463	0.0042
0.125	0.5468	0.0103	0.6938	0.0136	1.8082	0.0418
0.25	0.3354	0.0497	0.5176	0.0769	1.5187	0.2279
0.5	0.0572	0.0221	0.0885	0.0344	0.2877	0.1099
1.0	0.0091	0.0093	0.0167	0.0172	0.0487	0.0497
2.0	0.0137	0.0179	0.0266	0.0350	0.0905	0.1189
4.0	0.0065	0.0083	0.0317	0.0395	0.1004	0.1259
8.0	0.0007	0.0005	0.0140	0.0112	0.0465	0.0372
16.0	0.0011	0.0004	0.0068	0.0025	0.0233	0.0084
> 16.0	0.0001	0.0001	0.0003	0.0003	0.0009	0.0009
			Source II			
< 0.125	0.0197	0.0000	0.0474	0.0159	0.1553	0.0549
0.125	0.0036	0.0001	0.0177	0.0007	0.0588	0.0024
0.25	0.0369	0.0039	0.0890	0.0105	0.2193	0.0309
0.5	0.0168	0.0075	0.0773	0.0382	0.1876	0.0954
1.0	0.0219	0.0213	0.1073	0.1034	0.2603	0.2530
2.0	0.0136	0.0179	0.0495	0.0650	0.0845	0.1115
4.0	0.0142	0.0180	0.0339	0.0427	0.0751	0.0944
8.0	0.0040	0.0030	0.0096	0.0078	0.0474	0.0370
16.0	0.0035	0.0012	0.0099	0.0042	0.0274	0.0114
> 16.0	0.0050	0.0050	0.0092	0.0092	0.0260	0.0260
			Source III			
< 0.125	0.0022	0.0002	0.0115	0.0075	0.0371	0.0221
0.125	0.0012	0.0004	0.0095	0.0004	0.0662	0.0023
0.25	0.0106	0.0012	0.0631	0.0088	0.1262	0.0200
0.5	0.0057	0.0029	0.0421	0.0191	0.1385	0.0649
1.0	0.0112	0.0120	0.0366	0.0397	0.0797	0.0820
2.0	0.0199	0.0259	0.0700	0.0914	0.1522	0.1980
4.0	0.0110	0.0139	0.0430	0.0546	0.1058	0.1332
8.0	0.0087	0.0067	0.0181	0.0136	0.0605	0.0472
16.0	0.0039	0.0017	0.0113	0.0037	0.0278	0.0107
> 16.0	0.0051	0.0051	0.0084	0.0084	0.0264	0.0264
			Source IV			
< 0.125	0.0018	0.0018	0.0003	0.0003	0.0026	0.0026
0.125	0.0003	0.0000	0.0000	0.0000	0.0001	0.0000
0.25	0.0001	0.0000	0.0000	0.0000	0.0000	0.0000
0.5	0.0000	0.0000	0.0002	0.0001	0.0004	0.0002
1.0	0.0002	0.0002	0.0008	0.0009	0.0019	0.0020
2.0	0.0016	0.0021	0.0036	0.0049	0.0105	0.0140
4.0	0.0105	0.0127	0.0264	0.0315	0.0811	0.0975
8.0	0.0119	0.0095	0.0375	0.0299	0.1030	0.0841
16.0	0.0024	0.0009	0.0073	0.0023	0.0207	0.0073
> 16.0	0.0026	0.0026	0.0065	0.0065	0.0219	0.0219

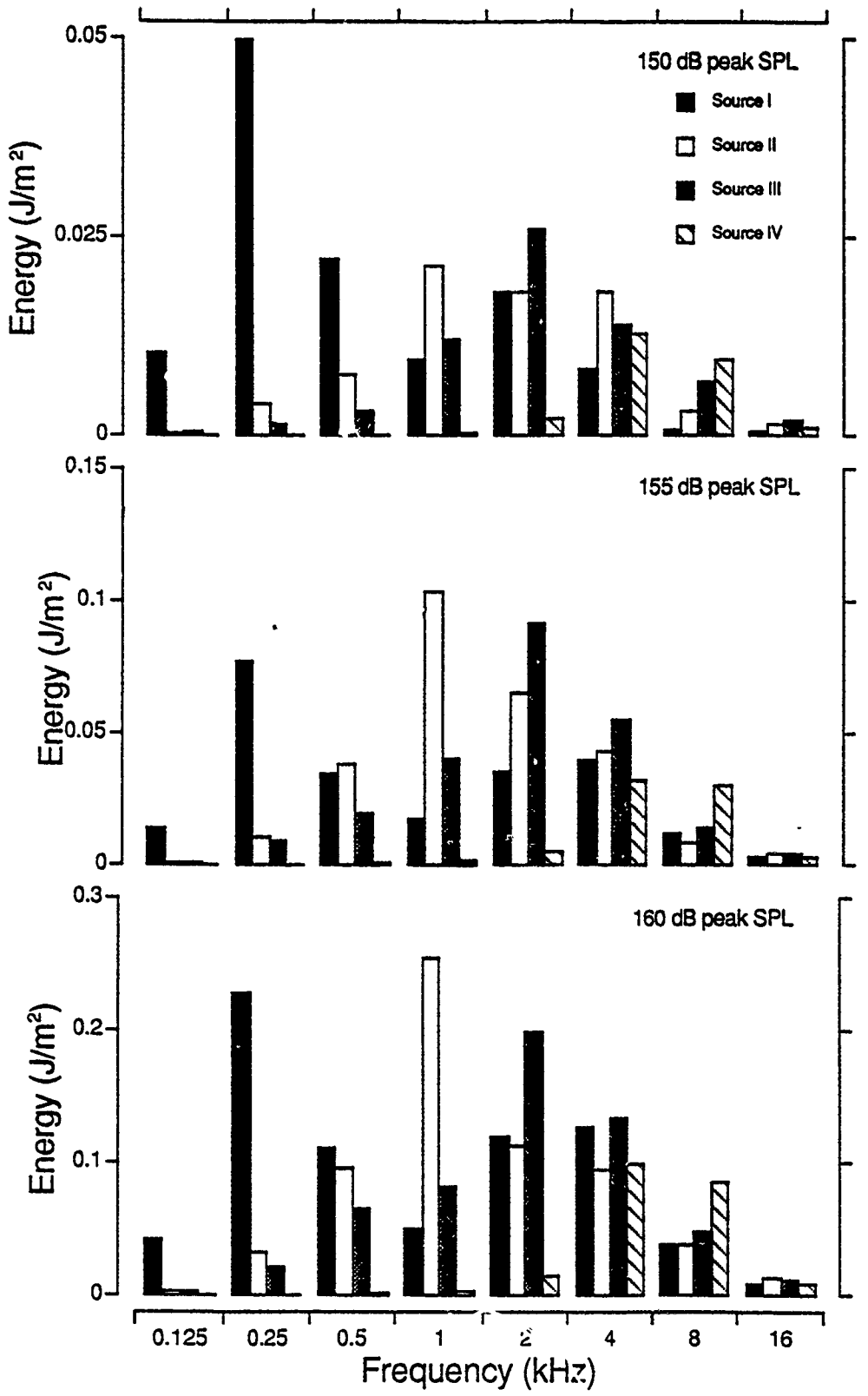

Figure 16. Absolute A-weighted octave band energy for a single impulse from each of the four impulse noise sources.

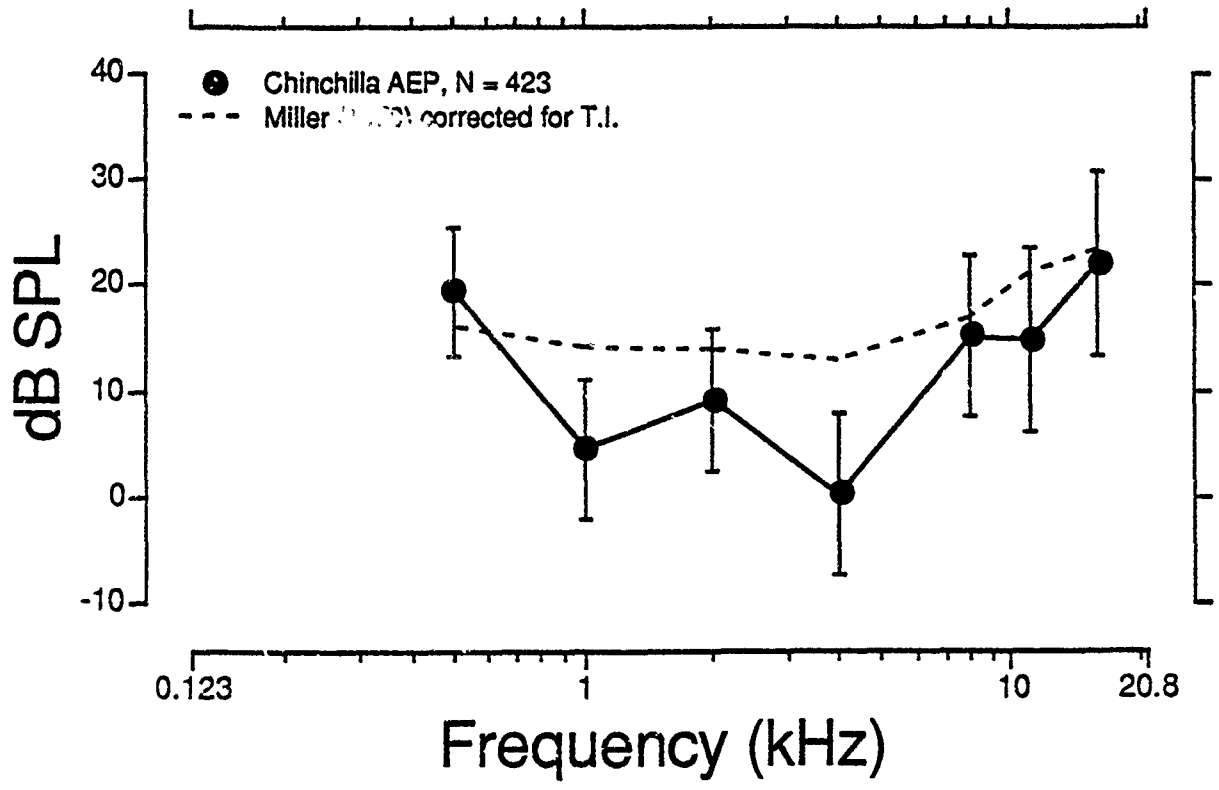

Figure 17. Mean preexposure thresholds for the 423 chinchillas used in this study.

The preexposure thresholds for the animals exposed to each source are presented in Table 7 and illustrated in Figure 18. There was a statistically significant frequency main effect ($F = 754.84$, $df = 5/2095$, $p < .05$) that was anticipated on the basis of our previous knowledge of the chinchilla audiogram (Fay, 1988). Both the main effect of source ($F = 41.96$, $df = 3/419$, $p < .05$) and source by frequency interaction ($F = 8.50$, $df = 15/2095$, $p < .05$) were statistically significant. Since the significant interaction indicated that the preexposure thresholds for some groups differed at some frequency or frequencies, we must be concerned whether differing preexposure thresholds may contribute to differences in the dependent measures. The dependent audiometric variables that are employed in this study are maximum threshold shift (TS_{max}) and permanent threshold shift (PTS). Each of these variables is computed by subtracting the preexposure from the postexposure thresholds. Thus, each animal serves as its own control subject. Since the audiological dependent measures (TS_{max}, PTS) are computed as a difference between an audiological measurement and preexposure threshold, it is unlikely that differences in preexposure thresholds would have any effect on these variables (see also Humes, 1984). As can be seen in Figure 18, animals exposed to the Source I impulses had thresholds that were on average approximately 5 dB poorer than the remaining three groups. The reason for this difference is that since the Source I animals were run, we have initiated stricter criteria for acceptable preexposure thresholds which each animal must meet, in order to continue in the experiment. The reason for this more restrictive screening was to avoid using animals that may have had preexisting lesions or poor electrode placement.

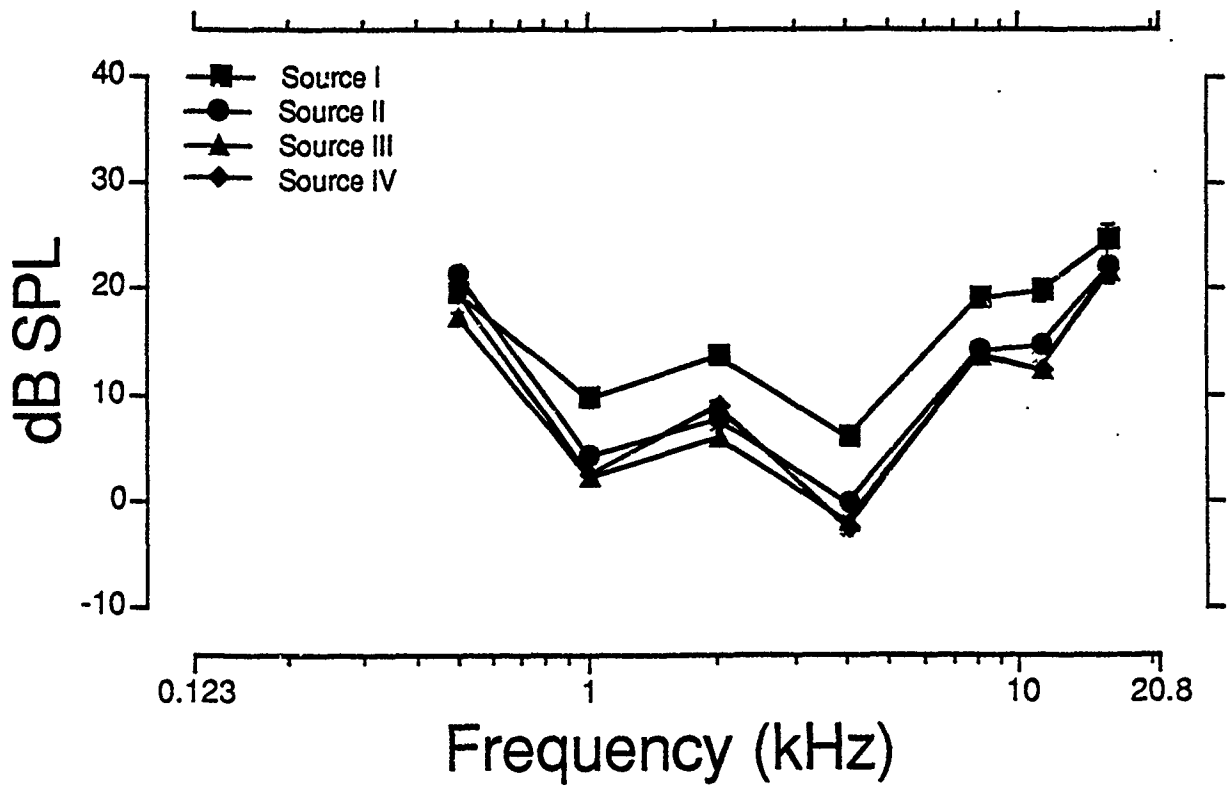

Figure. 18. Mean preexposure audiograms for animals exposed to the four impulse noise sources.

C. The Effect of the Independent Stimulus Variables on Trauma: Intensity, Number, Repetition Rate and Source: A conventional descriptive presentation of the entire data set showing the effects of the independent stimulus variables on TS_{max}, PTS, OHC loss and IHC loss was presented in the following annual reports: ADA 206-180, ADA 203-854, ADA 221-731, ADA 228-368 and the fifth year report for which an ADA number is not yet available. These reports include the descriptive statistics, analysis of variance and a graphical representation of the group mean data. This section is organized into two parts; (1) a summary of the effects of repetition rate which concludes with a rational for why we have chosen to collapse the data across the ISI variable in the subsequent analysis of the effects of number and intensity and (2) an analysis of the number, intensity and source variables in which we have attempted to interrelate and compare auditory effects across these three variables. This section illustrates the reasons why the more appropriate approach to the data analysis is one which focuses on an energy analysis rather than on peak and number separately.

(1) Impulse Presentation Rate: The independent variable of frequency is the only within-subjects variable. For each source, the experimental design did not lend itself to a typical four factor mixed design analysis of variance since there was no rate variable for the three groups exposed to a single impulse. Therefore, several different analyses were performed on each of the four dependent variables. Since the rate variable could not be applied to an analysis which included all groups, the rate variable was analyzed as one variable in a three-factor mixed-design analysis of variance with impulse peak

Table 7

Preexposure threshold means (dB) and standard deviations (dB) for each source

Source	N	Test Frequency (kHz) 0.5	1.0	2.0	4.0	8.0	11.2	16.0	
I	109*	19.6	9.6	13.7	6.0	19.1	19.7	24.6	$\bar{X}$
		6.6	6.1	6.1	6.7	7.8	8.9	9.7	s
II	105	21.4	4.2	7.7	-0.3	14.2	14.6	22.0	$\bar{X}$
		6.0	5.8	6.1	7.6	7.1	8.3	9.6	s
III	105	17.3	2.2	6.0	-2.0	13.5	12.4	21.5	$\bar{X}$
		5.8	6.4	6.1	6.4	6.8	8.0	8.4	s
IV	104	19.6	2.5	8.8	-2.5	14.0	12.4	21.8	$\bar{X}$
		5.2	5.1	5.7	6.6	6.6	7.3	7.3	s
All Animals		19.49	4.68	9.1	0.36	15.24	14.83	22.12	$\bar{X}$
		6.1	6.57	6.65	7.62	7.45	8.66	8.69	s
Miller (1970) (750 ms) signals		5.1	3.0	2.7	1.9	5.8	9.9	12.1	$\bar{X}$
		6.1	4.1	4.7	7.1	5.4	6.7	6.9	s
		36	36	36	36	36	34	36	N
Miller (1970) corrected for temporal integration		16.2	14.1	13.8	13.0	16.9	21.0	23.2	$\bar{X}$

* Measurement at 16.0 is based on data from 45 animals.

and frequency as the other two factors. In other words, two separate three-factor analyses were performed, the first on the groups exposed to 10 impulses, and the second on the groups exposed to 100 impulses. Thus, each of the analysis was performed only upon those groups that were exposed to an equal number of impulses. The following represents a summary of the results of the analyses:

(a) Source I: There were no statistically significant main effects of rate in the 10X exposures. However, there was a statistically significant interaction between rate and frequency for the OHC and IHC losses and a three way interaction between level, frequency and rate for the OHC losses in the 100X exposures. An examination of the mean cell loss data for the 100X exposures suggested that the 10/m rate was most hazardous for the 155 and 160 dB exposures but that the 1/m rate was most hazardous for the 150 dB exposures. As indicated by the interactions these results are dependent upon audiometric test frequency.

(b) Source II: There were no statistically significant main effects of impulse presentation rate in any of the analyses. However, there were significant interactions between presentation rate and frequency. A significant interaction between rate and frequency in the percent outer hair cell losses in groups exposed to 100 impulses suggested that the faster rates (10/m) were more hazardous than the slower rates. However, a parallel analyses of the groups exposed to 10 impulses showed a different pattern of interactions. When examining these groups, it was apparent that the groups

exposed to the intermediate rate of one impulse per minute showed the greatest amount of damage at 155 dB but the least damage overall at 160 dB. Thus, in general a systematic or consistent effect of impulse presentation rate could not be extracted from the data from Source II.

(c) Source III: The main effect of impulse presentation rate was statistically significant for only the percent outer hair cell losses for those groups exposed to 100 impulses. In these groups, the faster impulse presentation rate caused the greatest amount of damage. There were significant interactions between presentation rate and frequency. A significant interaction between rate and frequency in the percent outer hair cell losses in groups exposed to 100 impulses showed a different pattern of interactions. When examining these groups, it was apparent that the groups exposed to the intermediate rate of one impulse per minute either caused the greatest damage or was almost as damaging as the faster rate. The statistically significant interaction of rate and frequency for PTS in groups exposed to 100 impulses shows that the fastest rate caused the most hearing loss at the middle and upper frequency regions.

(d) Source IV: The main effect of impulse presentation rate was not statistically significant for any of the analyses for subjects exposed to 10 impulses, but was statistically significant for all audiometric and histological variables for groups exposed to 100 impulses. In these groups, the faster impulse presentation rate caused the greatest amount of damage. There were also significant interactions between presentation rate and frequency for the groups exposed to 100 impulses. A significant interaction between rate and frequency for PTS and both histological variables suggested that the faster rates (10/m) were more hazardous that the slower rates. There were no statistically significant interactions involving rate in any of the analyses of groups exposed to 10 impulses.

Thus, based upon an analysis of variance, there was not a clear and consistent effect of impulse presentation rate on PTS and sensory cell losses across the four impulse sources used. This lack of a clear relation is probably the result of the highly variable effects of the exposures on PTS and cell loss which may have masked the effects of the rate variable.

An alternate objective approach to determining the effect of impulse rate was obtained by computing the mean PTS evaluated at 1, 2 and 4 kHz ($PTS_{1,2,4}$) and comparing the means across the various groups exposed to the different impulse rates. Table 8 presents the summary of such an evaluation.

In addition to the above quantitative evaluation of the effect of the rate variable, a subjective evaluation was also made based upon a decision of which of the three rates caused the most hearing loss or cell loss. The results are shown in Table 9. The term "mixed" indicates an exposure for which no clear determination of the most hazardous exposure could be made. Multiple contrasts may be performed on individual means to determine which groups showed the greatest losses at individual frequencies. However, visual inspection of the mean data also provides an indication of which groups are most severely damaged by the impulse noise exposures. The conclusions made from the visual inspection are unlikely to be appreciably different than those made using a large number of multiple contrasts.

The results shown in Tables 8 and 9 differ for some exposure conditions because the sensory cell losses did not necessarily correlate perfectly with the PTS measure. It appears that the effects of ISI over the range of

Table 8

Summary evaluation of the exposure producing the largest mean PTS evaluated at 1, 2 and 4 kHz, based upon repetition rate of the impulse

	Source I	Source II	Source III	Source IV
150 dB 10X	1/m	1/10m	10/m	1/10m
150 dB 100X	1/m	10/m	1/m	10/m
155 dB 10X	1/m	1/m	1/m	1/m
155 dB 100X	10/m	10/m	10/m	10/m
160 dB 10X	10/m	1/10m	1/m	1/m
160 dB 100X	10/m	10/m	10/m	10/m

Table 9

Summary evaluation of the exposure producing the greatest degree of trauma based upon the repetition rate of the impulse. Trauma is estimated on the basis of PTS or sensory cell loss.

	Source I	Source II	Source III	Source IV
150 dB 10X	mixed	mixed	mixed	1/10m
150 dB 100X	1/m	mixed	mixed	mixed
155 dB 10X	1/m	1/m	mixed	1/m
155 dB 100X	mixed	10/m	10/m	10/m
160 dB 10X	10/m	mixed	mixed	mixed
160 dB 100X	10/m	10/m	mixed	10/m

variables used in these studies tend to be "masked" by the variability in the dependent measures. However, despite some inconsistencies in the above analyses there is a general trend for the fastest rate (10/m) to cause the greatest amount of trauma; especially for the most severe exposure conditions.

On the basis of the analysis of variance presented in the earlier reports, it was apparent that the effects of the different impulse presentation rates was, at best, a marginal statistical effect. Thus, a decision was made to evaluate the data on peak, number and source by collapsing the data across the rate variable. This effectively increased the number of animals at each sound exposure level to 15 except for the 1X exposure conditions.

(2) A Comparison Between the Effects of Number and Intensity Across the Four Sources: In order to summarize the large body of data acquired in these experiments in a manner that illustrates as clearly as possible the effects of intensity, number and source, the following approach was taken: For each audiometric test frequency (0.5, 1.0, 2.0, 4.0, 8.0 and 16.0 kHz) a "scatter

graph" of each individual animal's PTS, OHC loss* and IHC loss* at that frequency was plotted for each source as a function of the peak SPL of the impulse for each N and as a function of the number of impulses for each peak SPL. This exercise resulted in 432 separate scatter plots [i.e., 4 sources x 6 frequencies x 3 dependent variables (PTS, OHC, IHC) x 6 (2 independent variables, N and Peak, taken at 3 values each)]. A sample of a few of these plots is shown in Figures 19 through 22. One of the most obvious features of this presentation of the data is the very large variability in the dependent measures across animals exposed to the same stimuli. The variability increases as the severity of the exposure increases. In order to analyze these data in a manner that would be appropriate for developing relationships for use in establishing exposure criteria, it was decided to establish a 90th percentile point (PTS_{90}; OHC_{90}; IHC_{90}) for each of the three dependent data sets in each set of scatter plots. For example, the 90th percentile, PTS_{90} at any frequency was computed from:

$$PTS_{90} = \bar{X} + st_{.10}$$

where, $\bar{X}$ is the group mean PTS; $t_{.10}$ is the value of t below which 90% of the PTS data lies; s is the group standard deviation. A similar calculation was performed to compute OHC_{90} and IHC_{90}. A linear regression line was then drawn through each of these sets of three 90th percentile points. These linear regression lines clearly show that the severity of trauma increases as the energy of the exposure increases either as a result of increasing the peak SPL or N. For each of the linear regression lines a slope was computed as well as the dependent variable coordinate (y-intercept) for the exposure condition having the least energy based upon either N or peak. A listing of the slopes and intercepts that were computed for each of the regression lines in each of the "scatter" graphs is presented in Tables 10 through 15, and the results are shown plotted as a function of audiometric test frequency for each source in Figures 23 through 34. These twelve figures summarize, in a highly reduced manner, all the audiometric and histological data that were acquired from all the exposure conditions. Figures 23 through 34 need to be "read" in slope-intercept pairs (i.e., Figure 23 together with 24; Figure 25 with 26, etc.) in order to properly interpret the data and to make comparisons across exposure conditions. For example, the slopes for the higher energy exposures can be very low while the intercepts can be relatively high indicating that the dependent variable is reaching an upper bound typically on the order of 40-50 dB for PTS measures and 100% for cell loss measures, while the low energy exposures tend to be coupled with high slope values but low intercepts. Also, it should be noted that for some exposure conditions (especially at lower total SEL's) or some test frequencies the regression line could have a negative slope which was indicative of a set of three exposure conditions which produced no significant trauma. In these situations the negative slope was the result of sampling error, and a value of zero was accepted as the slope.

In analyzing these figures it is also important to note that the dynamic range of the impulse peaks is only 10 dB while there is a two decade (i.e., 20 dB) range in N over which slopes were computed from the regression lines. Although as previously explained, even though the data were collapsed across the ISI variable, we are still faced with trying to interrelate measures of trauma with N, peak and source at different audiometric test frequencies, i.e., a 5-dimensional data space. Because of the number of variables

---

* Cell losses were computed as a percent loss over an octave band "length" of the cochlea centered at that audiometric test frequency.

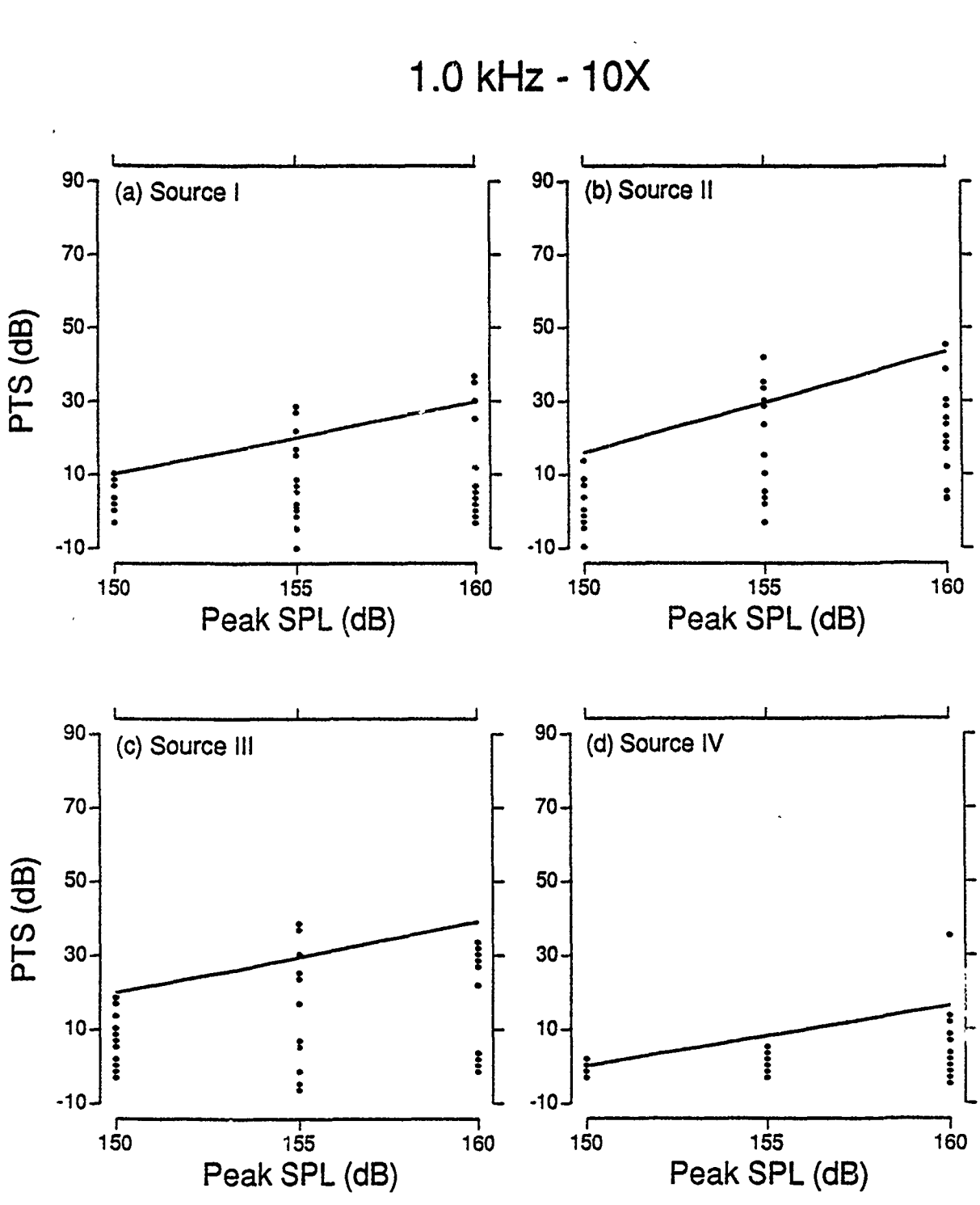

Figure 19. The PTS measured at 1.0 kHz in individual animals exposed to 10 impulses at one of the three levels shown (150, 155 or 160 dB peak SPL) for each of the four impulse noise sources. The solid line represents the linear regression through the 90th percentile points in the PTS distribution for each of the three exposure energy levels.

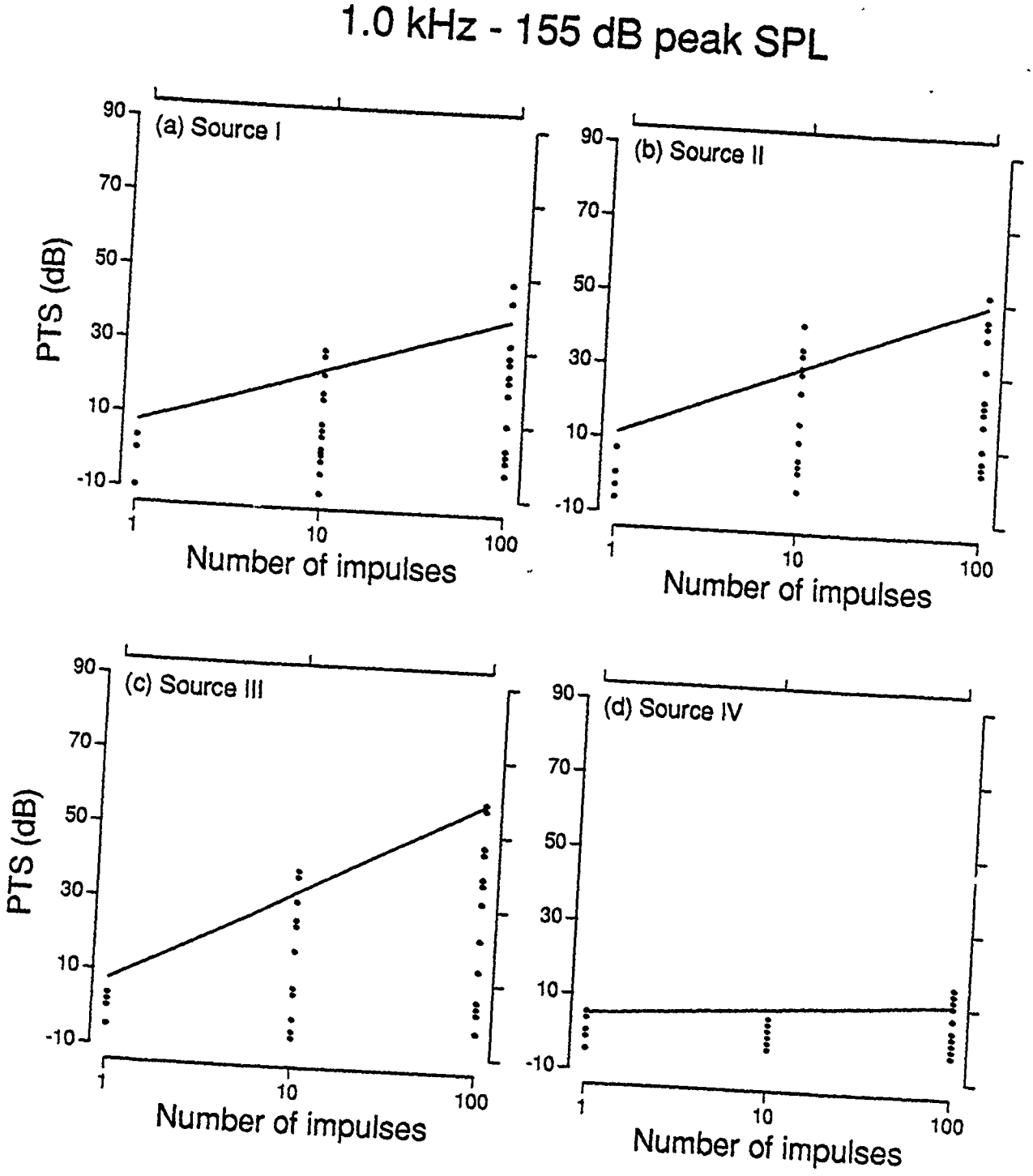

Figure 20. *The PTS measured at 1.0 kHz in individual animals exposed to 1, 10 or 100 impulses at 155 dB peak SPL for each of the four impulse noise sources. The solid line represents the linear regression through the 90th percentile points in the PTS distribution for each of the three exposure energy levels.*

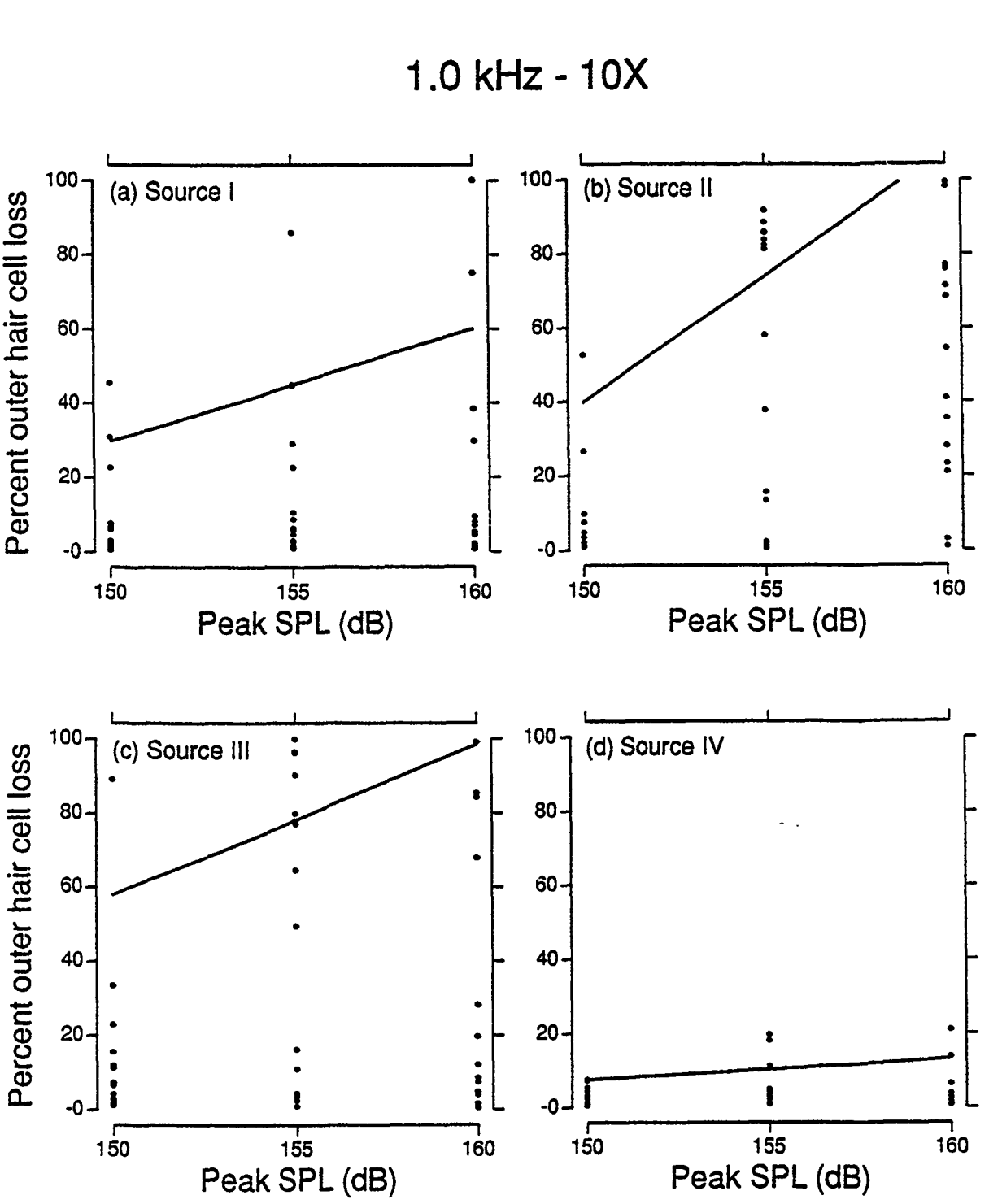

Figure 21. The percent outer hair cell loss (OHC) computed over the octave band length of the cochlea centered at 1.0 kHz for individual animals exposed to 10 impulses at one of the three levels shown (150, 155 or 160 dB peak SPL) for each of the four impulse noise sources. The solid line represents the linear regression through the 90th percentile points in the OHC distribution for each of the three exposure energy levels.

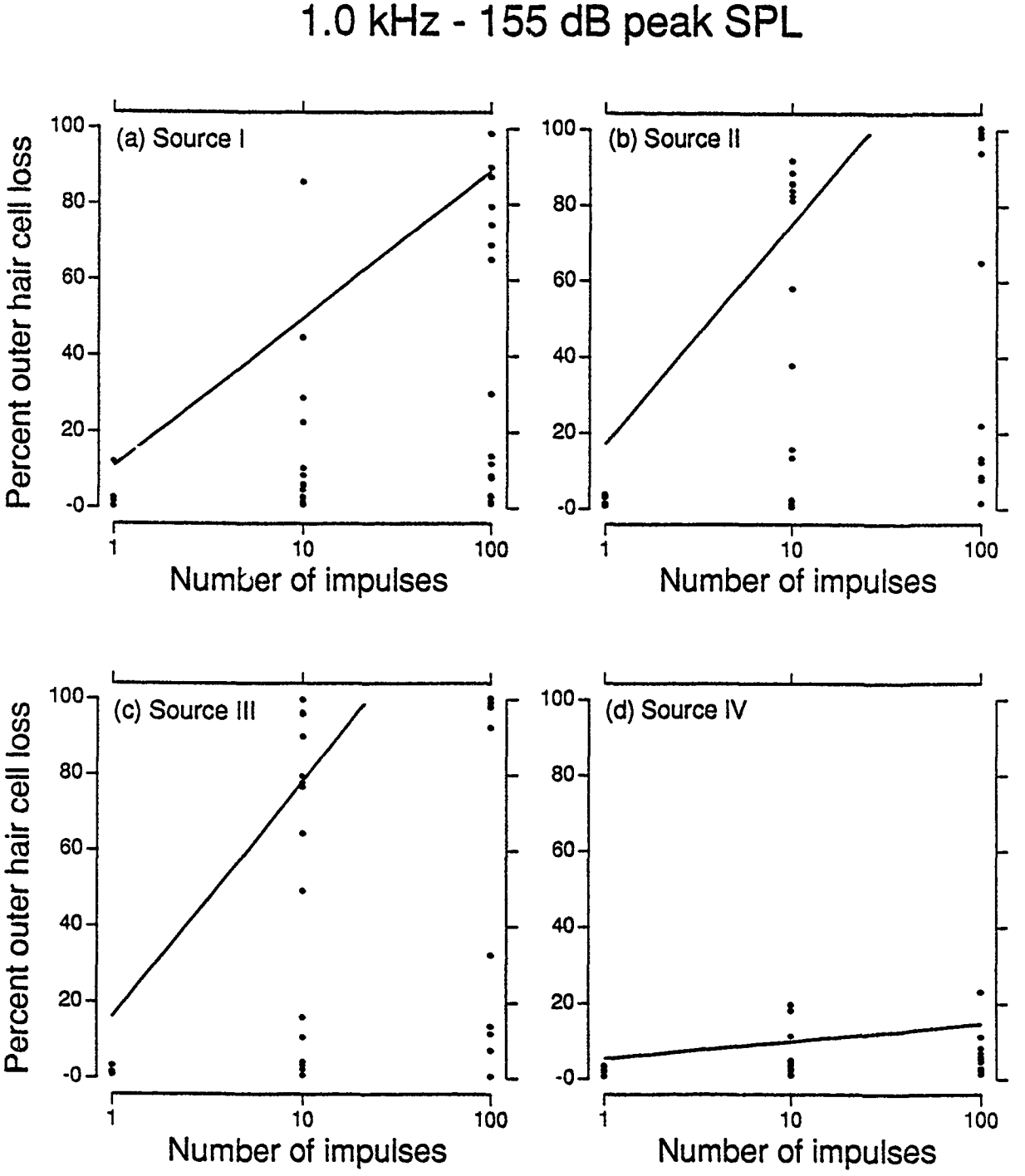

Figure 22. The percent outer hair cell loss (OHC) computed over the octave band length of the cochlea centered at 1.0 kHz for individual animals exposed to 1, 10 or 100 impulses presented at 155 dB peak SPL for each of the four impulse noise sources. The solid line represents the linear regression through the 90th percentile points in the OHC distribution for each of the three exposure energy levels.

Table 10

Slope (dB PTS / dB peak SPL) and intercept (dB PTS at 150 dB peak SPL) of the regression line drawn through the 90th percentile points for PTS at each audiometric test frequency for all animals exposed to 150, 155 or 160 dB peak SPL for N's of 1, 10 and 100 impulses for each source.

		Source I		Source II		Source III		Source IV	
N	kHz	Slope	Intercept	Slope	Intercept	Slope	Intercept	Slope	Intercept
1	0.5	0.0	8.2	0.0	8.0	0.1	4.6	0.2	5.4
	1.0	0.5	1.7	0.3	5.6	0.0	8.7	0.7	2.4
	2.0	0.4	1.5	0.0	5.9	0.5	5.3	0.0	6.0
	4.0	0.9	1.0	0.0	9.0	0.3	5.3	0.0	7.7
	8.0	0.7	7.6	0.0	14.9	0.0	11.3	0.1	11.6
	16.0	0.0	5.8	0.0	16.1	0.0	15.2	0.5	11.4
10	0.5	0.5	10.9	1.5	10.3	0.8	12.9	0.5	3.7
	1.0	2.0	10.2	2.8	15.7	1.9	20.0	1.6	0.1
	2.0	1.8	8.9	2.7	16.2	2.5	20.5	1.1	10.8
	4.0	0.7	9.2	1.3	18.0	1.6	15.6	0.3	24.8
	8.0	0.0	12.9	0.0	18.1	2.1	10.7	2.6	5.7
	16.0	1.1	5.9	1.4	12.2	1.0	13.6	2.0	7.8
100	0.5	1.6	20.6	1.7	17.7	3.0	17.1	0.2	10.3
	1.0	2.8	20.4	2.3	26.0	3.1	30.3	0.6	14.5
	2.0	3.1	20.2	3.5	25.8	3.3	36.8	2.1	30.2
	4.0	3.2	15.7	4.4	20.6	2.7	38.1	1.6	43.2
	8.0	3.8	13.6	4.5	20.1	3.6	33.2	0.6	42.8
	16.0	4.9	-2.8	5.0	19.1	3.2	31.6	2.3	27.6

Table 11

Slope (%OHC loss / dB peak SPL) and intercept (%OHC loss at 150 dB peak SPL) of the regression line drawn through the 90th percentile points for percent outer hair cell loss at each octave band length along the cochlea for all animals exposed to 150, 155 or 160 dB peak SPL for N's of 1, 10 and 100 impulses for each source.

		Source I		Source II		Source III		Source IV	
N	kHz	Slope	Intercept	Slope	Intercept	Slope	Intercept	Slope	Intercept
1	0.5	0.0	23.2	0.0	7.9	0.0	5.5	0.5	2.2
	1.0	0.0	12.4	0.0	6.8	0.0	7.3	0.1	5.4
	2.0	0.0	12.8	0.1	5.0	0.0	4.9	0.5	1.8
	4.0	0.0	12.5	0.0	5.2	0.0	8.9	0.0	7.7
	8.0	0.0	7.6	0.2	2.1	0.3	3.2	0.0	2.5
	16.0	0.1	2.6	0.0	3.9	0.0	7.1	0.0	3.8
10	0.5	0.5	12.6	2.0	20.4	2.5	18.9	0.0	6.4
	1.0	3.1	29.6	6.8	39.7	4.1	57.8	0.6	7.4
	2.0	5.9	14.3	8.8	29.9	5.7	48.1	1.9	14.2
	4.0	4.3	5.4	7.4	18.5	6.2	26.0	2.8	15.3
	8.0	0.7	2.6	2.0	13.8	2.9	15.2	6.1	-6.4
	16.0	1.6	1.2	1.2	13.3	0.8	7.0	3.7	2.3
100	0.5	5.7	18.0	6.5	33.9	5.8	39.7	0.0	13.0
	1.0	5.9	50.6	4.4	77.3	7.2	65.6	3.1	7.3
	2.0	5.6	52.8	5.6	69.6	7.4	68.5	2.6	48.7
	4.0	7.9	24.3	6.6	57.8	8.4	54.3	1.3	79.5
	8.0	8.0	11.0	9.3	28.6	7.9	51.7	1.8	79.0
	16.0	7.2	10.6	8.4	22.4	6.4	48.5	4.5	44.7

Table 12

Slope (%IHC loss / dB peak SPL) and intercept (%IHC loss at 150 dB peak SPL) of the regression line drawn through the 90th percentile points for percent inner hair cell loss at each octave band length along the cochlea for all animals exposed to 150, 155 or 160 dB peak SPL for N's of 1, 10 and 100 impulses for each source.

		Source I		Source II		Source III		Source IV	
N	kHz	Slope	Intercept	Slope	Intercept	Slope	Intercept	Slope	Intercept
1	0.5	0.0	4.1	0.0	2.4	0.0	0.5	0.0	0.7
	1.0	0.3	1.2	0.0	3.1	0.0	1.1	0.0	0.8
	2.0	0.0	2.5	0.0	2.0	0.0	3.8	0.0	1.0
	4.0	0.0	8.0	0.0	4.3	0.0	7.4	0.0	3.3
	8.0	0.0	3.4	0.0	1.2	0.2	1.2	0.0	1.5
	16.0	0.1	0.5	0.2	0.0	0.0	6.1	0.0	0.7
10	0.5	0.0	5.0	0.0	5.0	0.1	5.7	0.0	6.0
	1.0	1.1	2.1	2.7	7.3	0.3	11.3	0.0	3.0
	2.0	3.5	-4.0	1.8	7.7	1.0	10.5	0.0	6.7
	4.0	1.6	3.5	4.0	3.1	0.7	8.3	0.4	4.0
	8.0	0.5	0.6	0.3	10.3	0.0	8.4	3.5	-3.6
	16.0	0.6	1.0	0.0	2.5	0.0	2.8	1.9	0.8
100	0.5	0.8	1.1	1.1	6.1	2.4	18.5	0.0	2.2
	1.0	2.0	7.3	2.1	15.9	3.3	32.7	0.2	1.5
	2.0	1.5	7.9	2.4	20.6	4.0	26.7	0.1	19.6
	4.0	1.0	9.7	1.2	9.2	7.0	8.2	1.0	40.0
	8.0	1.9	11.1	3.2	6.0	5.1	14.6	1.3	44.9
	16.0	4.4	-5.4	5.1	9.4	6.0	10.8	3.8	22.3

Table 13

Slope (dB PTS / 10X ΔN) and intercept (dB PTS at a single impulse) of the regression line drawn through the 90th percentile points for PTS at each audiometric test frequency for all animals exposed to 1, 10 or 100 impulses at 150, 155 and 160 dB peak SPL for each source.

		Source I		Source II		Source III		Source IV	
Peak	kHz	Slope	Intercept	Slope	Intercept	Slope	Intercept	Slope	Intercept
150	0.5	6.2	6.5	2.3	6.7	5.0	4.4	2.0	5.1
	1.0	9.2	-0.2	8.2	4.9	8.1	8.6	7.6	-0.6
	2.0	8.9	0.9	8.3	4.4	11.8	5.5	12.8	2.5
	4.0	6.2	0.2	3.6	9.2	14.9	-0.1	19.1	6.8
	8.0	0.5	10.3	0.0	13.4	8.7	5.0	15.1	4.6
	16.0	1.6	6.7	0.0	11.9	5.1	11.4	7.4	6.2
155	0.5	11.2	5.9	15.7	6.9	16.2	6.1	3.5	3.3
	1.0	15.3	7.9	18.9	11.2	25.3	7.6	2.8	4.9
	2.0	17.2	2.6	22.4	10.4	30.8	7.8	16.1	5.4
	4.0	15.4	5.7	23.4	6.7	25.3	11.8	18.9	8.3
	8.0	16.0	3.9	22.9	8.9	24.8	12.2	18.0	8.3
	16.0			22.5	13.8	23.5	10.0	13.9	13.6
160	0.5	16.1	2.2	13.7	4.2	19.8	2.4	2.1	7.9
	1.0	20.6	6.1	17.9	13.2	26.4	5.0	7.4	9.5
	2.0	22.9	4.5	26.6	6.5	25.9	12.3	23.7	1.8
	4.0	17.8	4.7	30.0	-0.9	26.9	3.2	26.7	5.5
	8.0	16.4	9.3	29.0	-5.9	27.4	4.6	17.5	13.2
	16.0	33.8	-10.5	27.4	1.6	23.4	5.3	16.2	13.6

Table 14

Slope (%OHC loss / 10X ΔN) and intercept (%OHC loss at a single impulse) of the regression line drawn through the 90th percentile points for percent outer hair cell loss at each octave band length along the cochlea for all animals exposed to 1, 10 or 100 impulses at 150, 155 and 160 dB peak SPL for each source.

		Source I		Source II		Source III		Source IV	
Peak	kHz	Slope	Intercept	Slope	Intercept	Slope	Intercept	Slope	Intercept
150	0.5	0.0	23.3	9.6	6.9	8.6	5.6	6.5	1.2
	1.0	16.9	11.7	29.6	3.9	22.2	13.1	2.8	5.5
	2.0	18.8	8.9	26.7	-0.7	25.8	5.4	27.1	-5.1
	4.0	4.2	11.9	20.8	-1.3	16.9	1.1	39.2	-5.3
	8.0	0.0	7.7	4.4	0.7	17.8	-1.3	38.5	-10.5
	16.0	0.5	2.5	0.0	8.1	13.5	2.8	19.2	-3.2
155	0.5	20.1	2.0	36.8	5.9	49.1	0.1	1.4	5.2
	1.0	38.8	11.1	57.9	17.0	62.0	16.2	4.6	5.2
	2.0	39.3	2.4	57.2	19.3	62.9	17.7	21.7	7.3
	4.0	31.1	-2.2	53.8	11.9	56.9	19.6	32.9	8.2
	8.0	32.9	-7.4	53.8	-0.4	56.2	-0.5	42.4	-10.2
	16.0	28.9	-5.6	51.4	-9.6	52.9	-12.1	34.4	-2.2
160	0.5	35.4	-2.6	43.7	-0.1	38.4	2.7	3.1	5.5
	1.0	47.6	10.1	52.5	17.7	59.9	11.7	17.6	3.1
	2.0	52.8	9.3	54.0	20.2	63.9	10.3	37.9	0.6
	4.0	47.7	6.0	53.5	12.5	62.2	2.6	46.4	0.4
	8.0	40.1	-8.6	49.8	-6.4	56.1	-2.4	47.7	6.6
	16.0	36.4	-3.7	41.2	-2.5	48.9	-11.0	42.0	1.1

Table 15

Slope (%IHC loss / 10X ΔN) and intercept (%IHC loss at a single impulse) of the regression line drawn through the 90th percentile points for percent inner hair cell loss at each octave band length along the cochlea for all animals exposed to 1, 10 or 100 impulses at 150, 155 and 160 dB peak SPL for each source.

		Source I		Source II		Source III		Source IV	
Peak	kHz	Slope	Intercept	Slope	Intercept	Slope	Intercept	Slope	Intercept
150	0.5	0.0	5.6	0.6	2.4	9.8	-1.9	0.7	2.2
	1.0	1.1	1.6	0.0	4.1	14.3	-2.1	0.6	1.3
	2.0	1.6	2.0	6.7	0.1	9.5	0.9	12.3	-2.6
	4.0	0.0	8.2	3.5	0.4	0.0	4.8	16.7	-2.9
	8.0	2.9	2.0	1.3	0.5	8.7	1.0	19.6	-4.8
	16.0	0.0	1.4	1.2	0.7	0.0	5.2	10.9	-3.0
155	0.5	1.5	0.9	7.4	1.6	13.1	0.0	0.6	1.7
	1.0	11.2	-0.2	25.8	0.1	27.1	-0.5	0.3	1.3
	2.0	9.1	-1.9	21.0	2.5	26.3	1.3	3.6	4.4
	4.0	7.8	1.0	3.4	14.1	19.9	6.5	24.6	-2.7
	8.0	11.1	-2.3	12.4	7.2	15.0	-1.2	29.4	-8.2
	16.0	1.9	-0.1	23.9	-6.8	24.0	-5.3	20.2	-3.0
160	0.5	4.1	0.4	6.5	-0.8	21.6	-5.4	0.4	1.2
	1.0	9.5	4.5	11.8	6.9	31.0	-7.0	1.5	0.6
	2.0	10.2	9.1	19.3	1.1	31.5	-5.7	12.7	-3.1
	4.0	8.1	5.7	9.8	11.6	37.6	-8.7	22.3	-4.1
	8.0	13.8	-1.6	17.0	-3.7	33.2	-5.8	26.3	4.2
	16.0	21.4	-3.2	25.6	-6.0	32.8	-9.8	30.1	-3.5

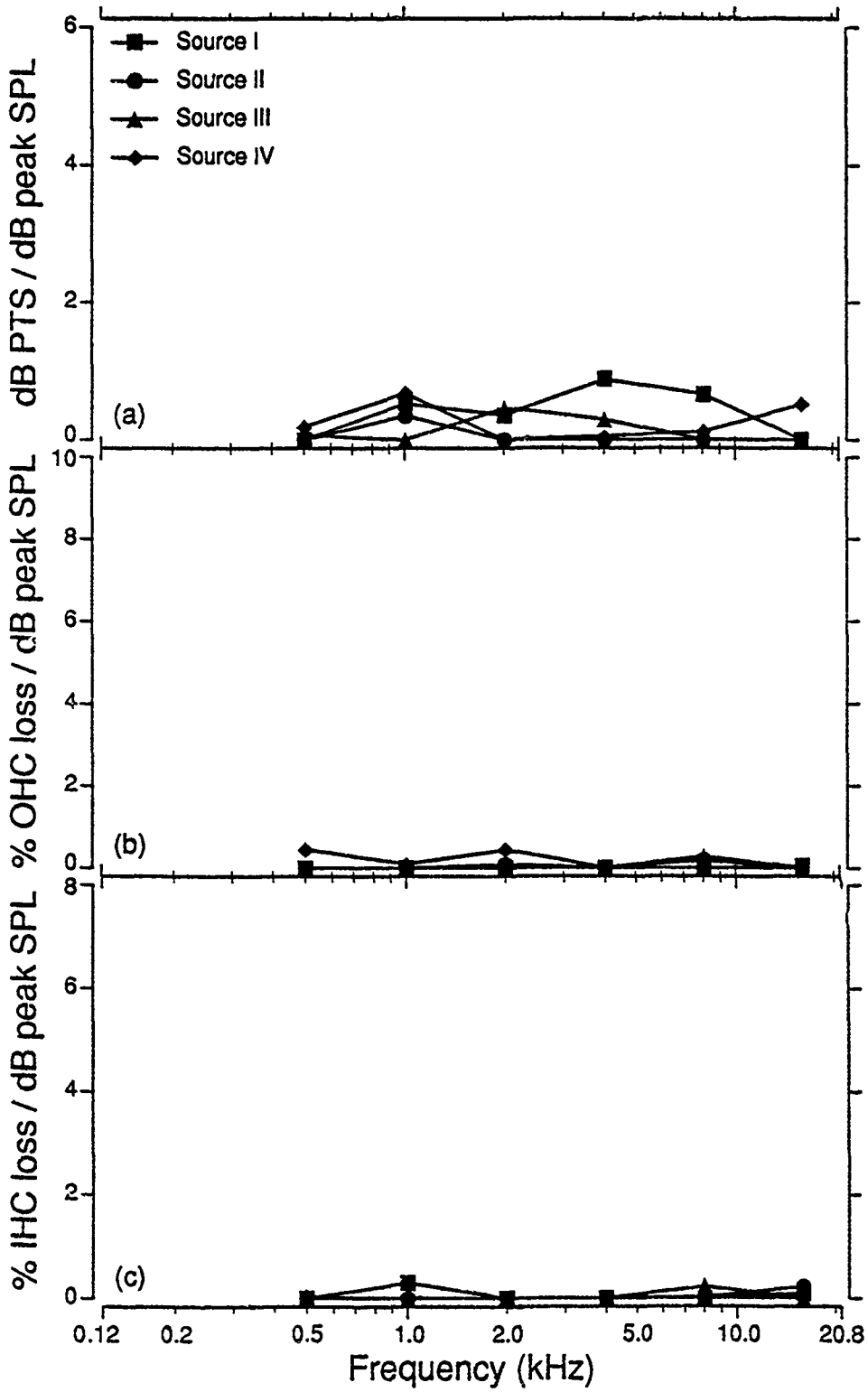

Figure 23. The slope of the regression line drawn through the 90th percentile points at each audiometric test frequency for all animals exposed to a single (1X) impulse at 150, 155 or 160 dB peak SPL showing for each source the increase in (a) PTS, (b) percent outer hair cell loss and (c) percent inner hair cell loss for each dB increase in the peak SPL of the impulse.

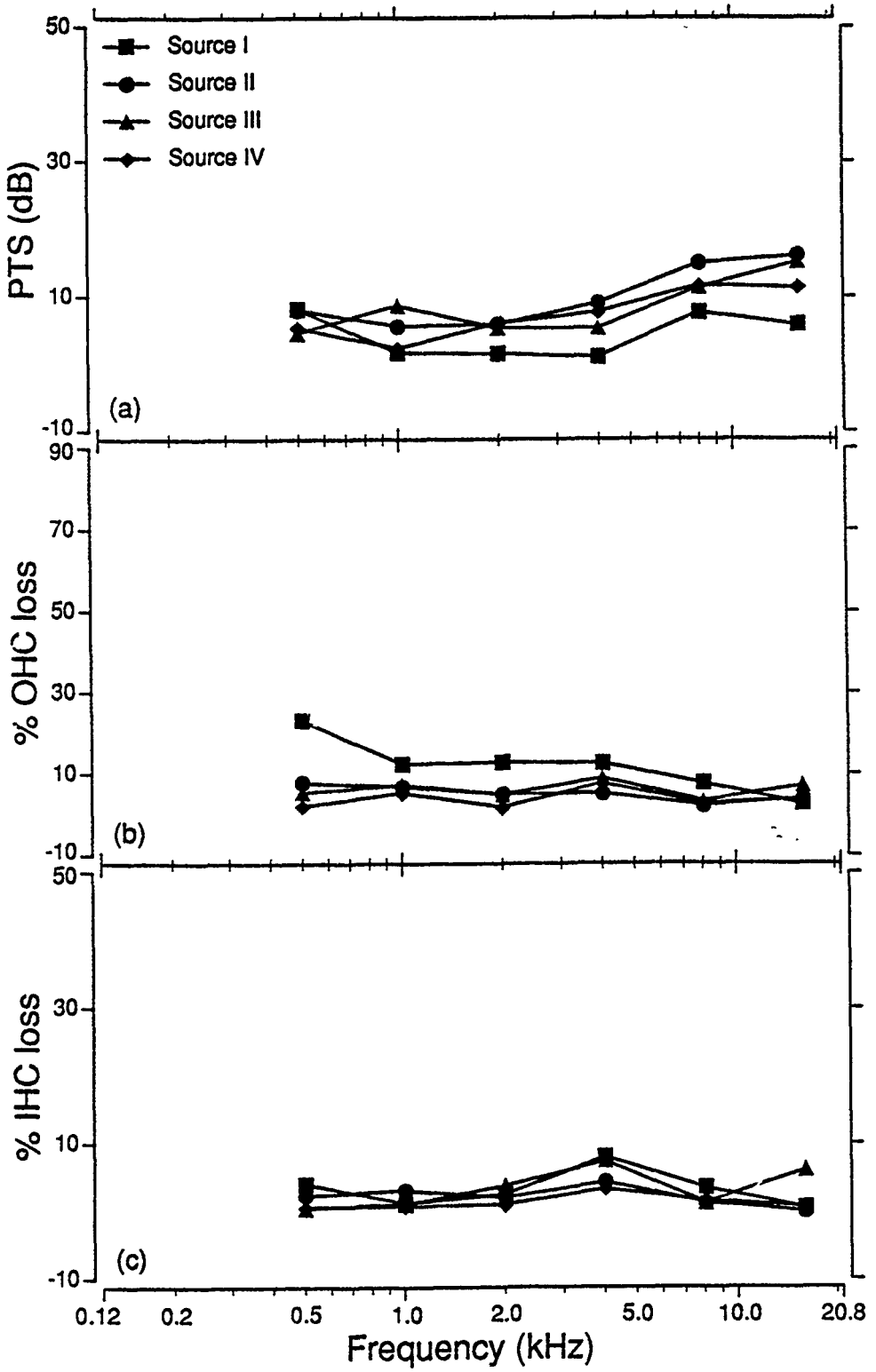

Figure 24. The predicted (a) PTS, (b) percent outer hair cell loss and (c) percent inner hair cell loss at each audiometric test frequency following exposure to a single (1X) impulse at 150 dB peak SPL for each source. The value of each dependent variable is taken from the regression line drawn through the 90th percentile points relating that dependent variable to the peak SPL for an exposure to a single impulse.

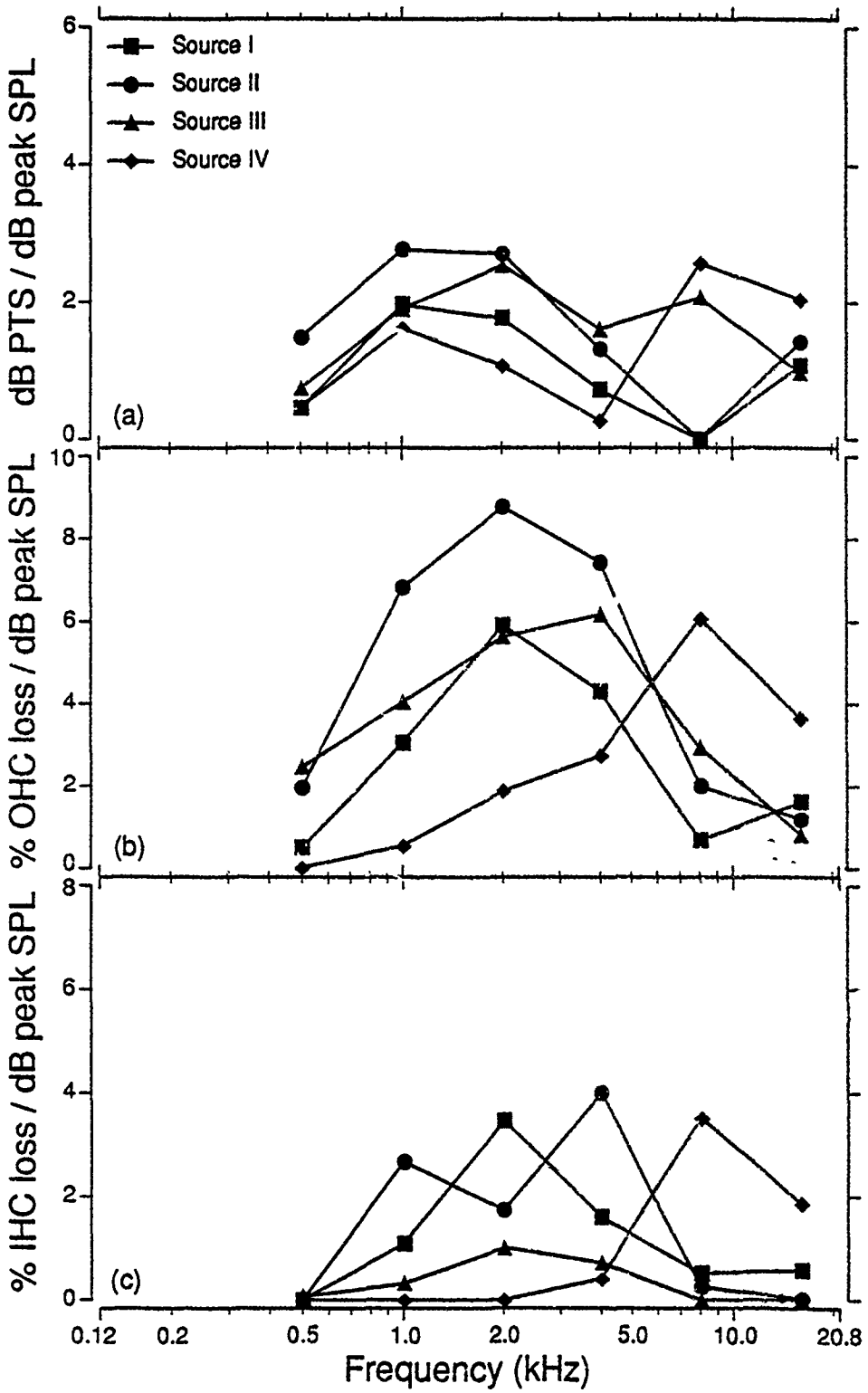

Figure 25. The slope of the regression line drawn through the 90th percentile points at each audiometric test frequency for all animals exposed to 10 impulses at 150, 155 or 160 dB peak SPL showing for each source the increase in (a) PTS, (b) percent outer hair cell loss and (c) percent inner hair cell loss for each dB increase in the peak SPL of the impulse.

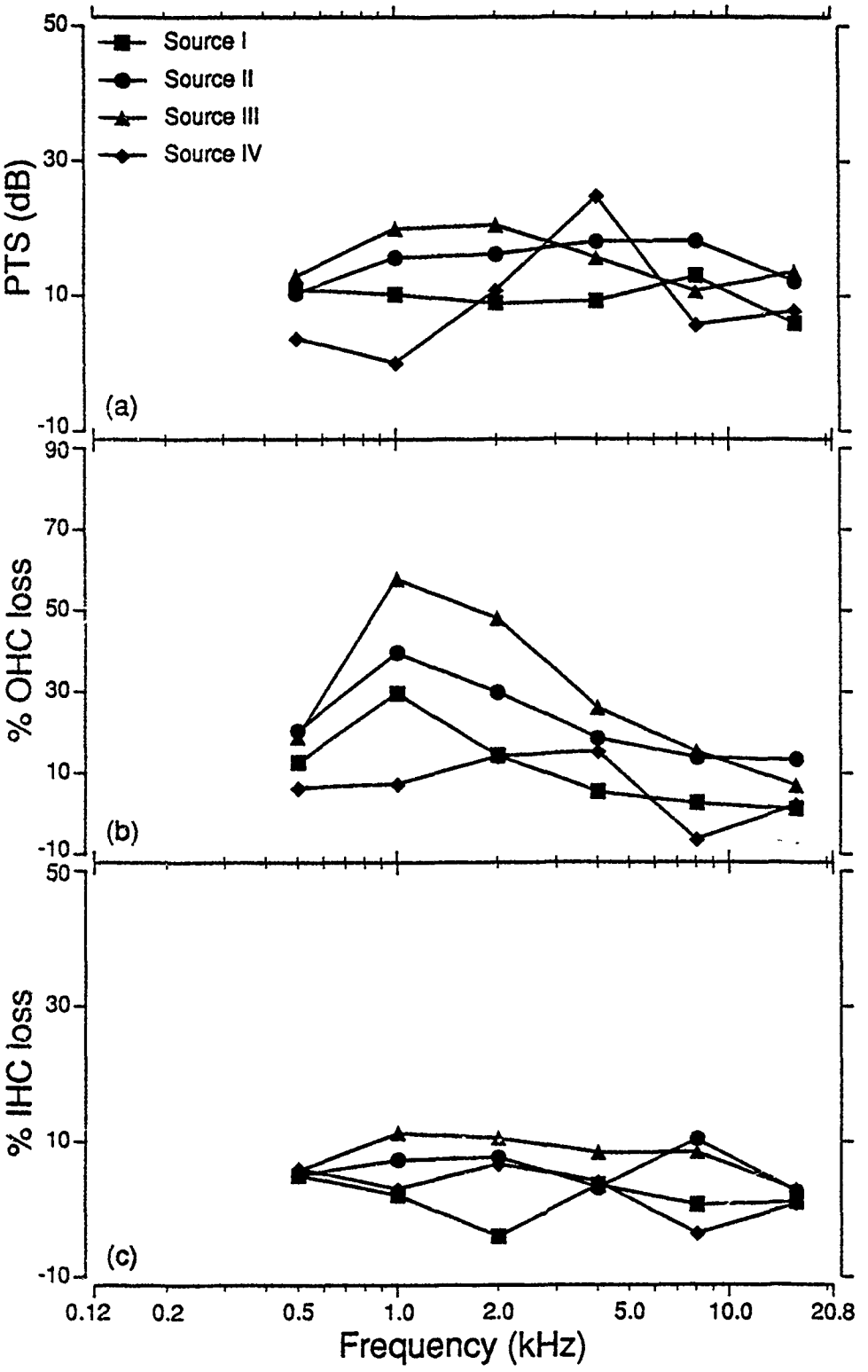

Figure 26. The predicted (a) PTS, (b) percent outer hair cell loss and (c) percent inner hair cell loss at each audiometric test frequency following exposure to 10 impulses at 150 dB peak SPL for each source. The value of each dependent variable is taken from the regression line drawn through the 90th percentile points relating that dependent variable to the peak SPL for an exposure of 10 impulses.

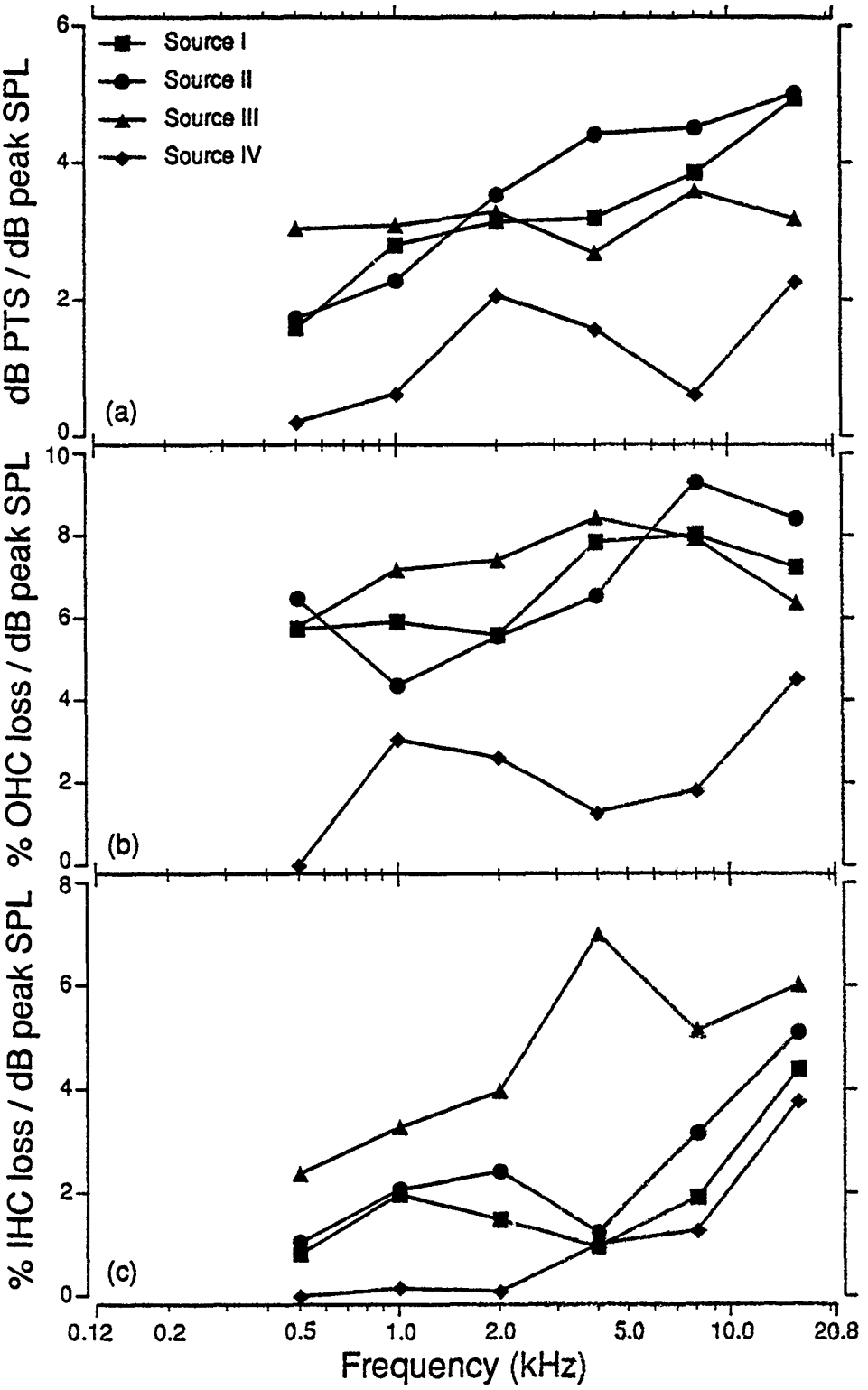

Figure 27. The slope of the regression line drawn through the 90th percentile points at each audiometric test frequency for all animals exposed to 100 impulses at 150, 155 or 160 dB peak SPL showing for each source the increase in (a) PTS, (b) percent outer hair cell loss and (c) percent inner hair cell loss for each dB increase in the peak SPL of the impulse.

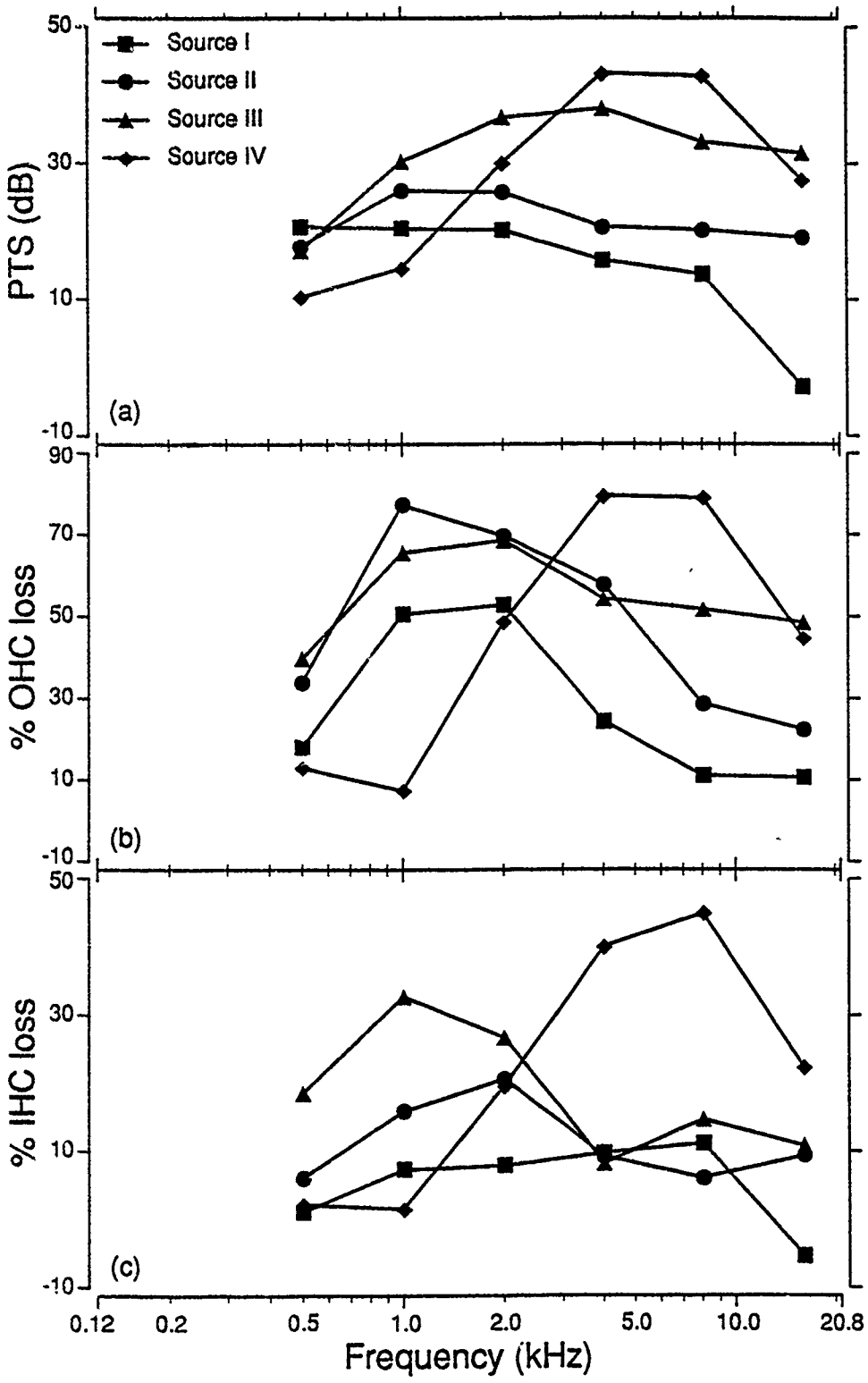

Figure 28. The predicted (a) PTS, (b) percent outer hair cell loss and (c) percent inner hair cell loss at each audiometric test frequency following exposure to 100 impulses at 150 dB peak SPL for each source. The value of each dependent variable is taken from the regression line drawn through the 90th percentile points relating that dependent variable to the peak SPL for an exposure of 100 impulses.

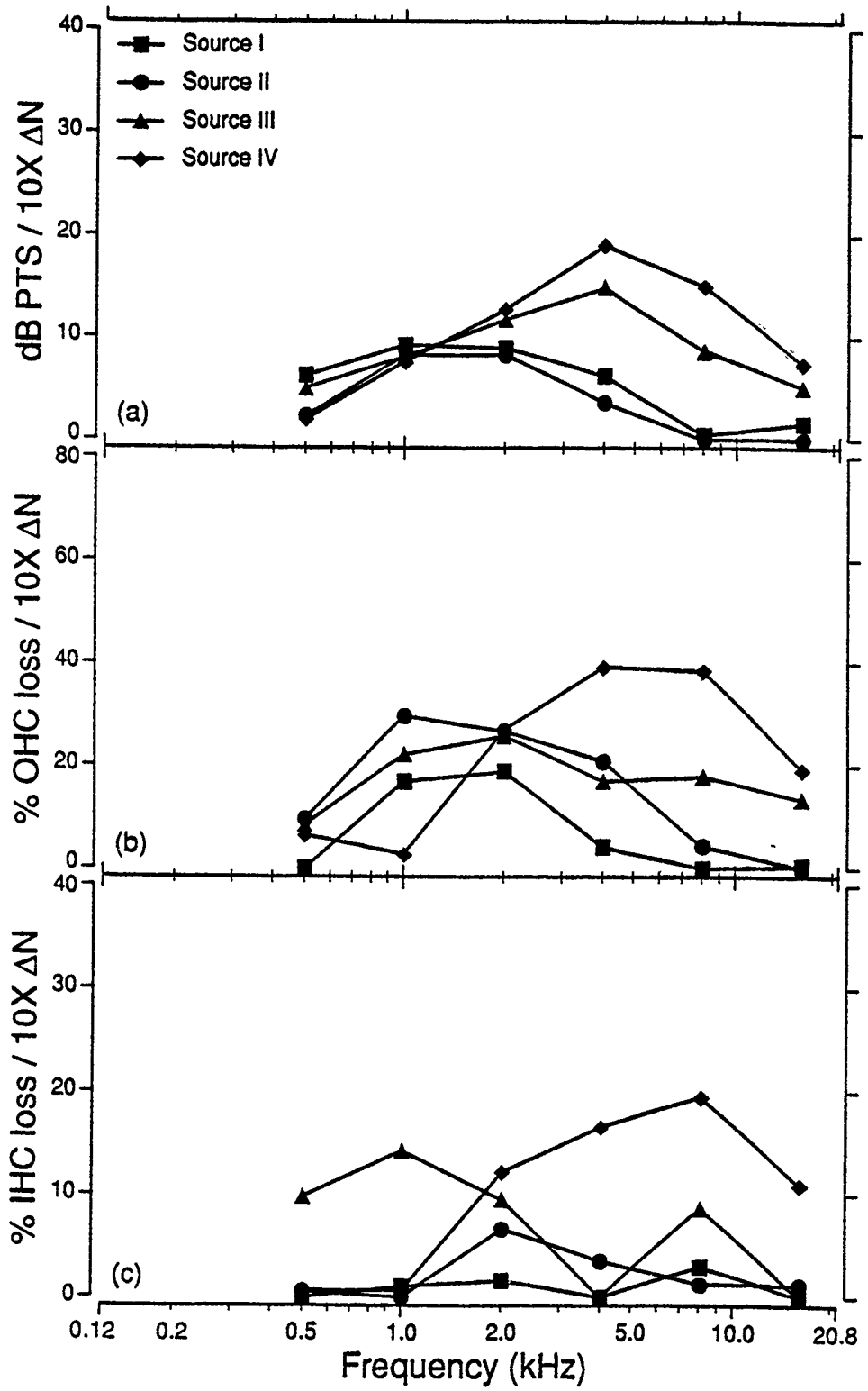

Figure 29. The slope of the regression line drawn through the 90th percentile points at each audiometric test frequency for all animals exposed to 1, 10 or 100 impulses at 150 dB peak SPL showing for each source the increase in (a) PTS, (b) percent outer hair cell loss and (c) percent inner hair cell loss for each decade increase in the number of impulses.

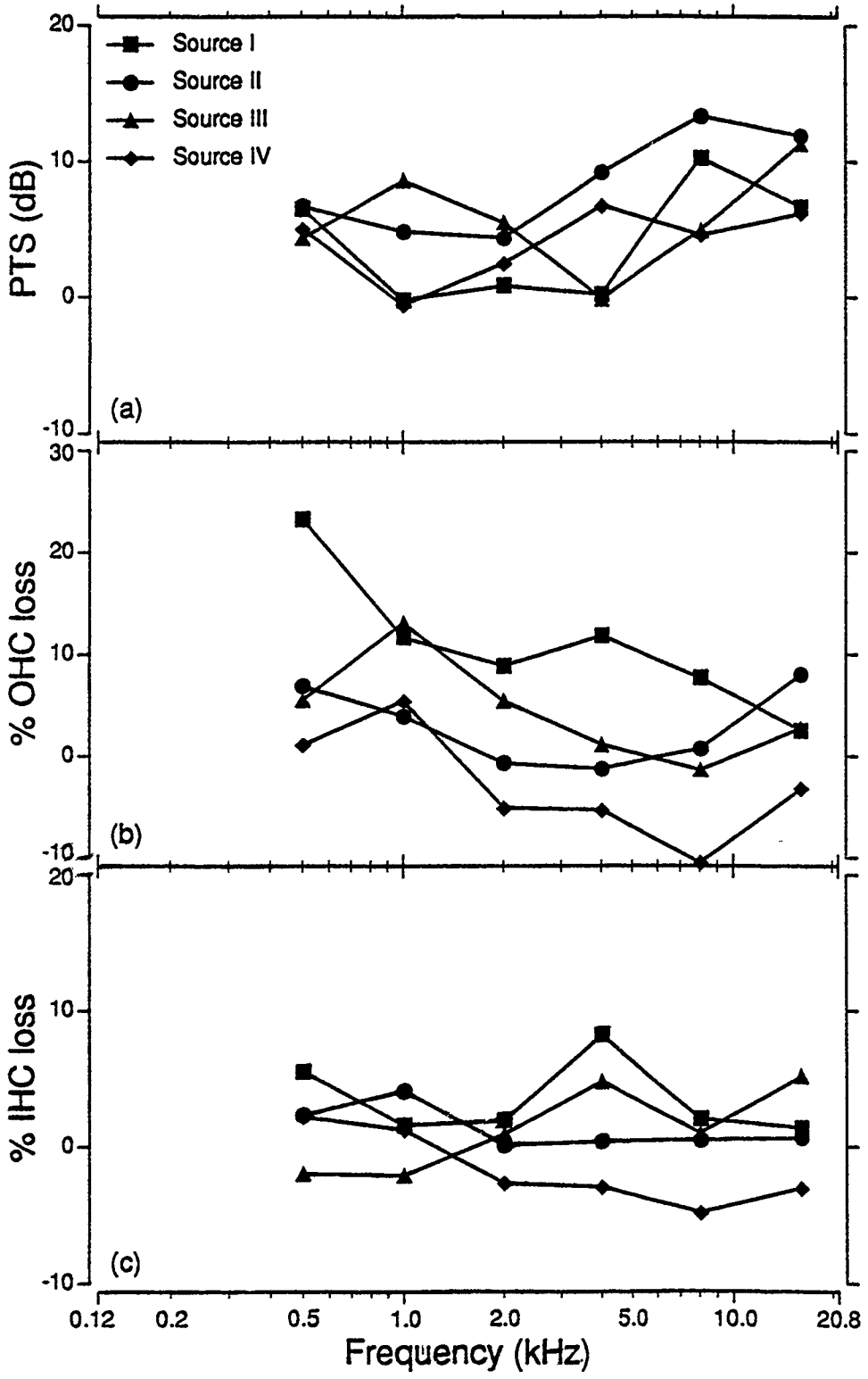

Figure 30. The predicted (a) PTS, (b) percent outer hair cell loss and (c) percent inner hair cell loss at each audiometric test frequency following exposure to a single impulse at 150 dB peak SPL for each source. The value of each dependent variable is taken from the regression line drawn through the 90th percentile points relating that dependent variable to the number of impulses presented at 150 dB peak SPL.

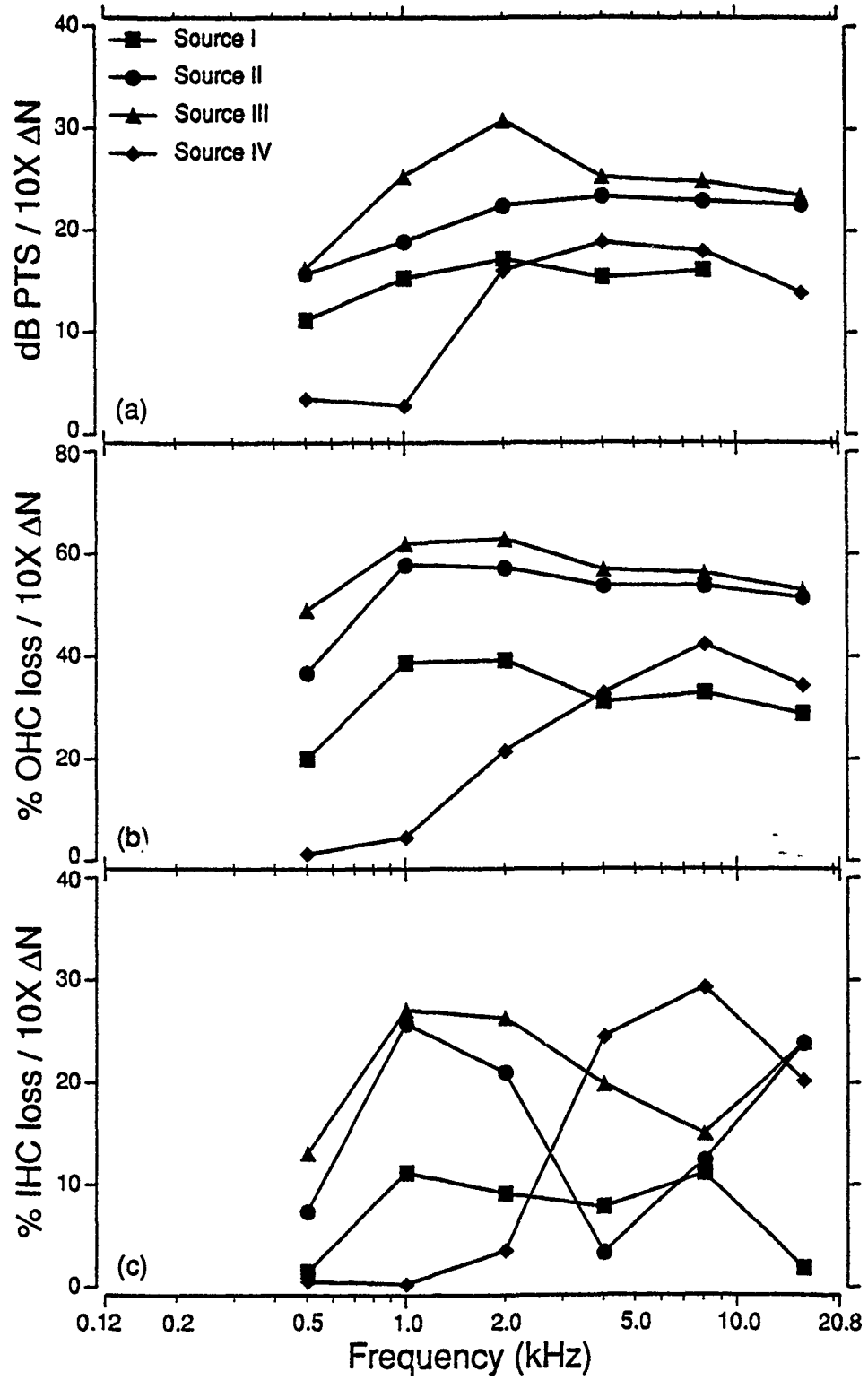

Figure 31. The slope of the regression line drawn through the 90th percentile points at each audiometric test frequency for all animals exposed to 1, 10 or 100 impulses at 155 dB peak SPL showing for each source the increase in (a) PTS, (b) percent outer hair cell loss and (c) percent inner hair cell loss for each decade increase in the number of impulses.

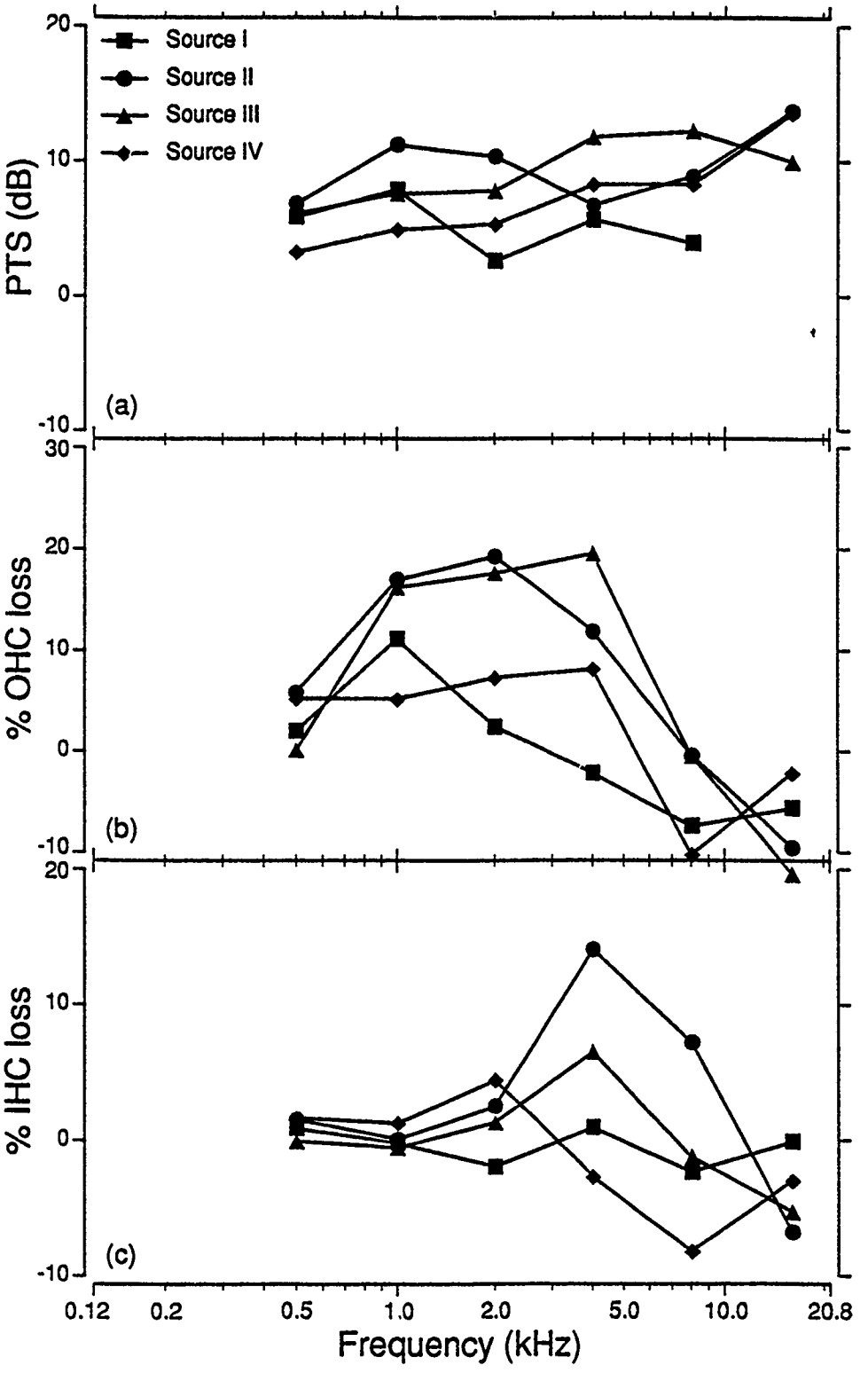

Figure 32. The predicted (a) PTS, (b) percent outer hair cell loss and (c) percent inner hair cell loss at each audiometric test frequency following exposure to a single impulse at 155 dB peak SPL for each source. The value of each dependent variable is taken from the regression line drawn through the 90th percentile points relating that dependent variable to the number of impulses presented at 155 dB peak SPL.

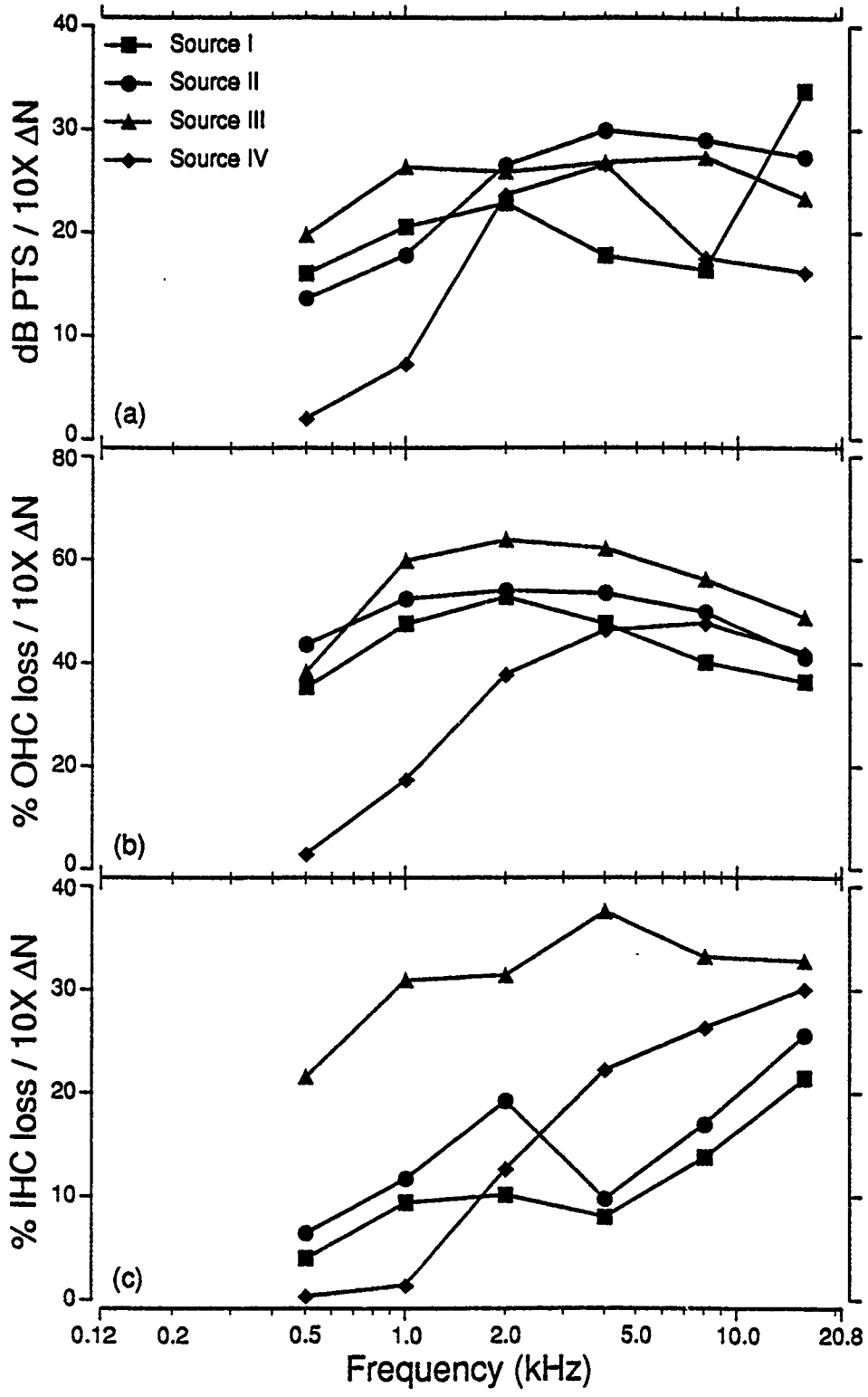

Figure 33. The slope of the regression line drawn through the 90th percentile points at each audiometric test frequency for all animals exposed to 1, 10 or 100 impulses at 160 dB peak SPL showing for each source the increase in (a) PTS, (b) percent outer hair cell loss and (c) percent inner hair cell loss for each decade increase in the number of impulses.

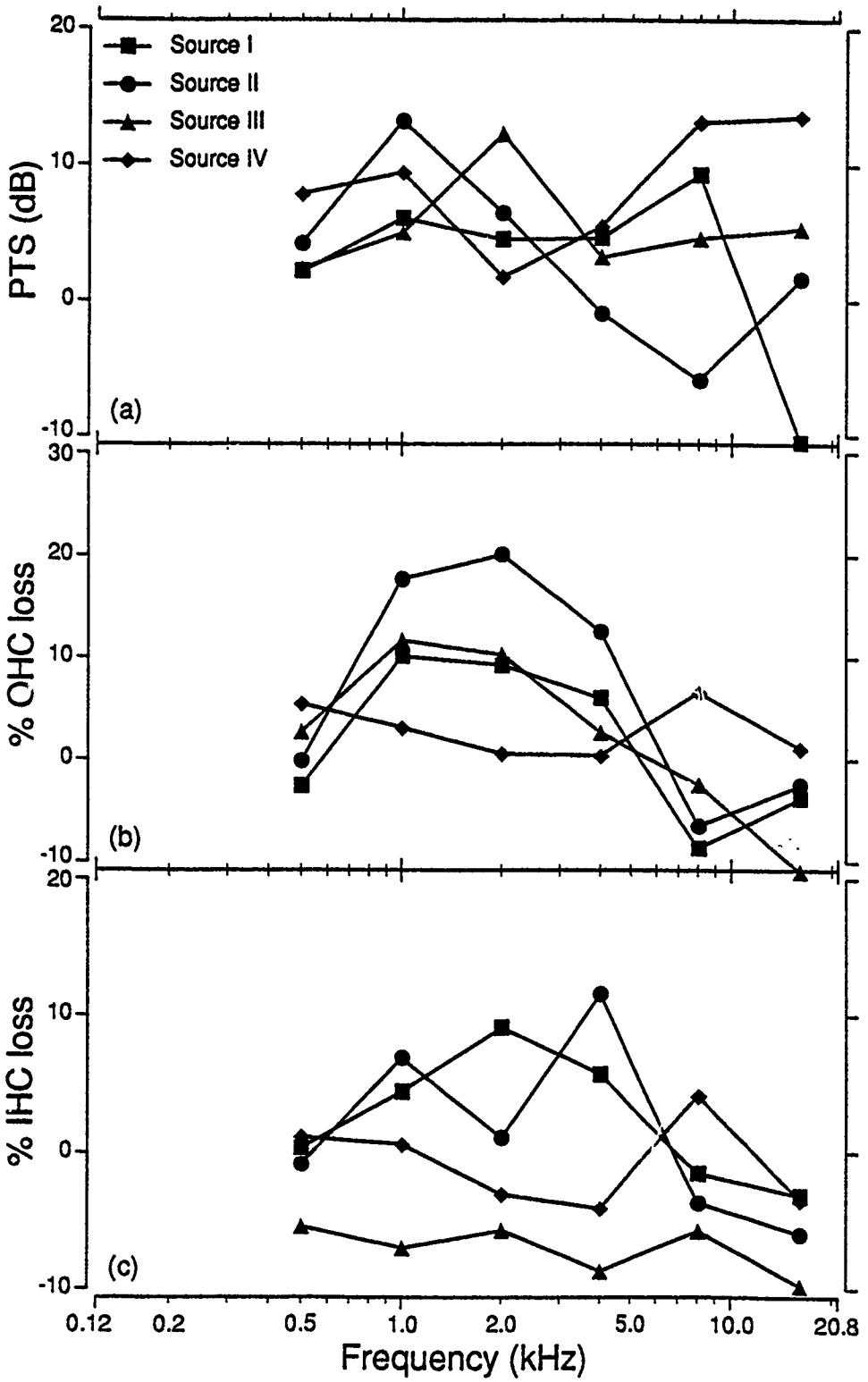

Figure 34. The predicted (a) PTS, (b) percent outer hair cell loss and (c) percent inner hair cell loss at each audiometric test frequency following exposure to a single impulse at 160 dB peak SPL for each source. The value of each dependent variable is taken from the regression line drawn through the 90th percentile points relating that dependent variable to the number of impulses presented at 160 dB peak SPL.

involved, it is difficult to make generalizations regarding the effects of any single variable, however, the following points can be deduced from Figures 23 through 34: (a) There are clear frequency effects resulting from the distribution of energy in a given impulse as well as from the different spectral distribution of energy in the impulses generated by the four different sources. (b) Trauma to the auditory system clearly increases as either N or peak levels of the impulse are increased. Over the range of parameters used, there is no clear indication that either peak or N is the more important variable in producing trauma. However, at some audiometric test frequencies and for large N, increases of the peak level over a 10 dB range produce more severe trauma than does a 10 dB increase in N. This effect is most noticeable for the 160 dB peak SPL exposures. The implication is that in a cochlea that is "stressed" by a large number of impulses, an increase in the peak of the impulse will produce disproportionate increases in trauma. Part of the reason for this effect lies in the fact that all the 1X exposures were relatively non-traumatic and a 10 dB increase in N did not produce a similar growth in trauma that a 10 dB increase in peak does for the 100X exposures. Such comparisons are, however, tenuous since the total energies of the exposures that are being compared are not equal. (c) When the slopes are compared for exposure conditions that vary from lower to higher energy exposures at a fixed frequency, the slopes vary from low to near zero values through a maximum and then at the highest energy exposures the slopes return to zero values again. The corresponding trend for the intercepts is to monotonically increase. Thus, there is the indication that trauma develops, not surprisingly, in a "ogive-like" manner, i.e., follows a function of the approximate form

$$y\ (\text{trauma}) = [1 + e^{(b-x)/c}]^{-1}$$

where x is proportional to the energy of the exposure and b and c are constants (probably frequency dependent). There is also the suggestion that the maximum slope of the above function may occur at the stimulus frequency having the greatest (weighed?) energy. Depending upon the value of the variables b and c, such a relation between trauma and exposure energy can be related to the idea of the "critical level" discussed in the Background Section.

In order to affect a further simplification and reduce the number of variables, audiometric test frequency was eliminated by using as measures of trauma, the mean PTS evaluated at 1, 2 and 4 kHz and the total OHC and total IHC loss. A set of 72 scatter graphs was generated and slopes and intercepts again plotted. Four typical examples of the scatter graphs are shown in Figures 35 through 38, while slopes and intercepts are shown in Tables 16 and 17. The data in these tables is shown plotted in Figures 39 through 50. Reduced in this manner, the data show (1) strong source effects, (2) clear increases in trauma as N and peak increase and (3) for large N, increasing the peak level over a 10 dB range produces more severe trauma than does a 10 dB increase in N for the 160 dB peak exposures.

As a result of the foregoing analyses, it became evident that within the range of parameters studied that the effects on trauma of increasing N or the peak SPL were not clearly decipherable and that the most advantageous approach to the analysis of this data would be an energy based approach where the contributions of N and peak to the total energy of the exposure were clear. Furthermore, an energy based analysis reduces the number of variables. This is the approach followed in the following section.

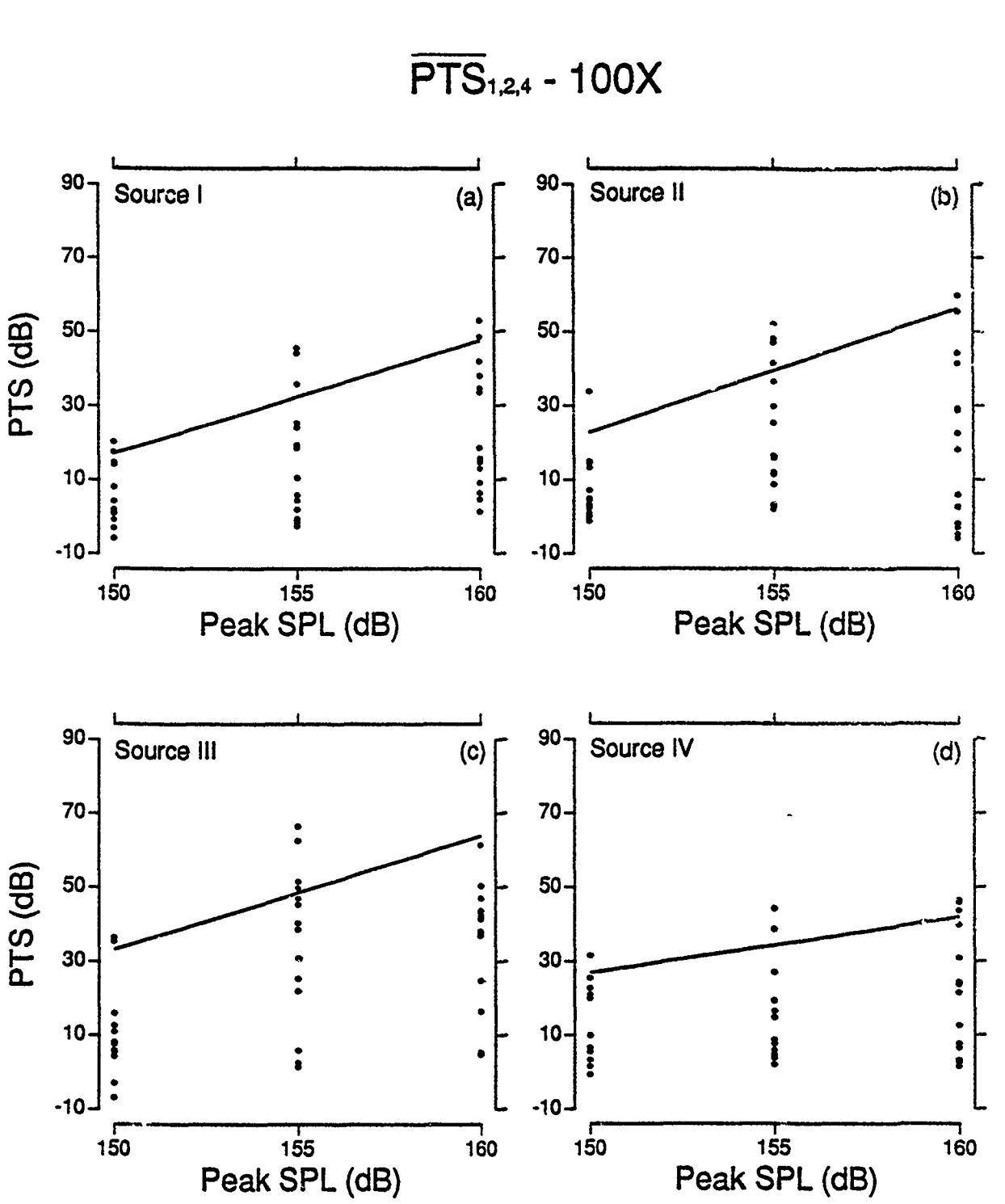

Figure 35. The mean PTS measured at 1, 2 and 4 kHz for each animal exposed to 100 impulses at one of the three levels shown (150, 155 or 160 dB peak SPL) for each of the four impulse noise sources. The solid line represents the linear regression through the 90th percentile points in the PTS distribution for each of the three exposure energy levels.

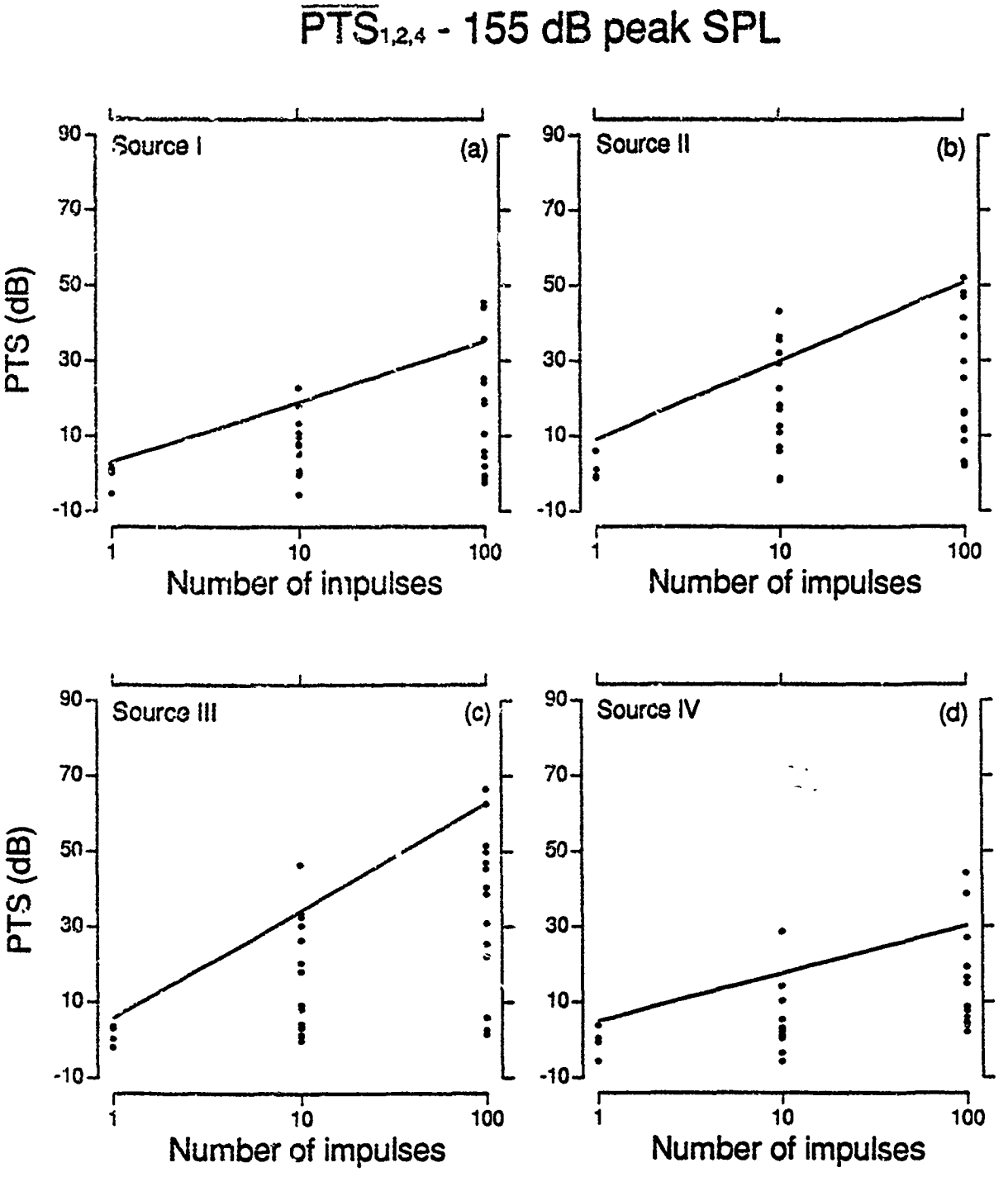

Figure 36. The mean PTS measured at 1, 2 and 4 kHz for each animal exposed to 1, 10 or 100 impulses at 155 dB peak SPL for each of the four impulse noise sources. The solid line represents the linear regression through the 90th percentile points in the mean PTS distribution for each of the three exposure energy levels.

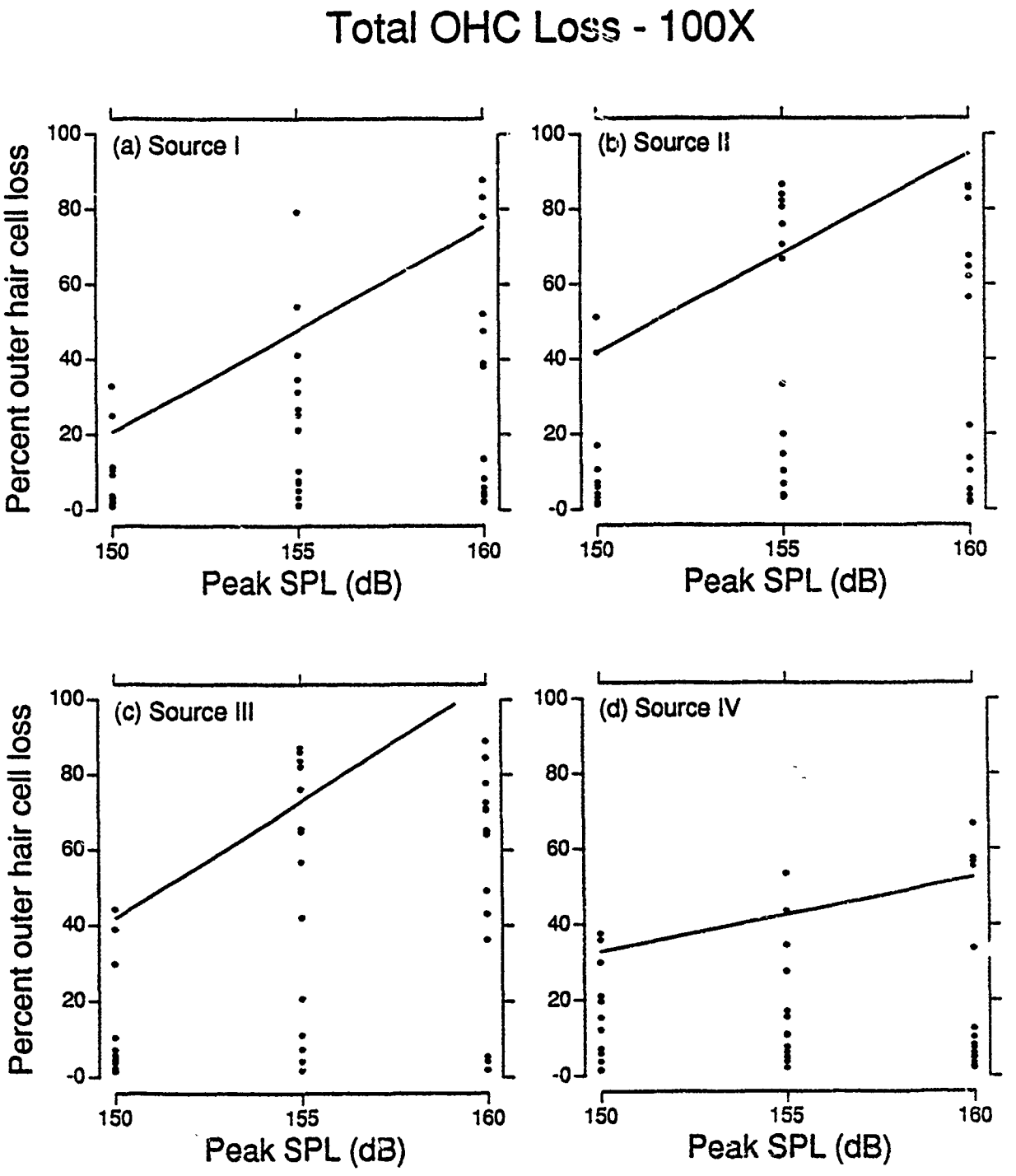

Figure 37. The percent total outer hair cell loss (OHC) for individual animals exposed to 100 impulses at one of the three levels shown (150, 155 or 160 dB peak SPL) for each of the four impulse noise sources. The solid line represents the linear regression through the 90th percentile points in the OHC distribution for each of the three exposure energy levels.

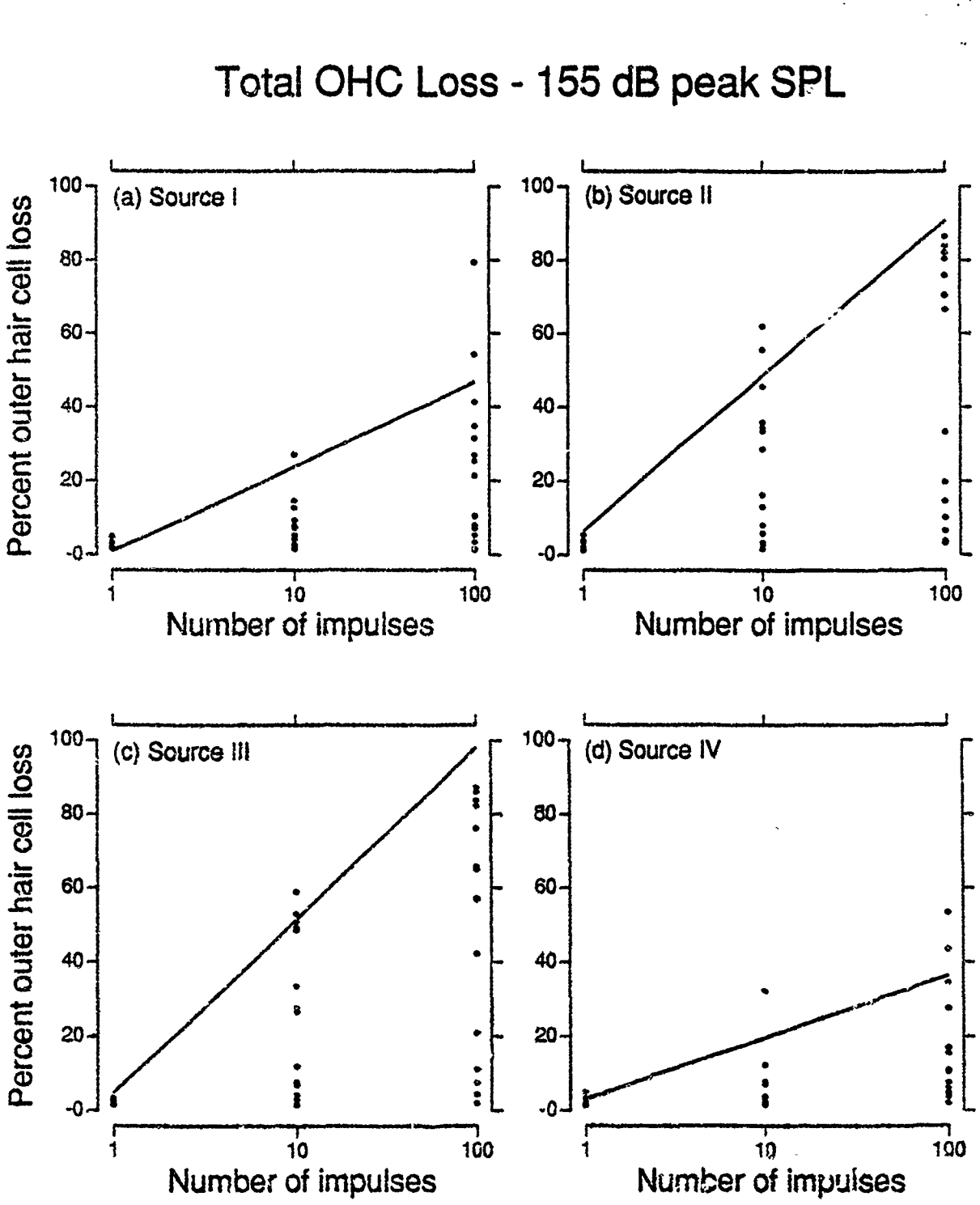

Figure 38. The percent total outer hair cell loss (OHC) for each animal exposed to 1, 10 or 100 impulses at 155 dB peak SPL for each of the four impulse noise sources. The solid line represents the linear regression through the 90th percentile points in the OHC distribution for each of the three exposure energy levels.

Table 16

Slope (per decade increase in N) and the y-intercept (at a single impulse) of the regression line drawn through the 90th percentile points for all animals exposed to 1, 10 or 100 impulses at 150, 155 and 160 dB peak SPL for each source.

	Source I		Source II		Source III		Source IV	
Peak	Slope	Intercept	Slope	Intercept	Slope	Intercept	Slope	Intercept
			Mean Permanent Threshold Shift at 1, 2 and 4 kHz					
150	8.0	-0.6	6.3	4.8	12.7	0.6	12.3	1.6
155	16.0	3.0	21.0	8.8	28.5	5.7	12.7	4.7
160	20.7	3.4	26.5	1.3	26.0	5.7	19.7	2.2
			Total Percent Outer Hair Cell Loss					
150	3.4	10.7	12.3	4.2	11.1	6.1	15.4	0.0
155	22.9	1.0	42.3	6.2	46.6	4.8	16.6	3.0
160	35.1	0.4	39.4	4.0	44.5	0.9	24.8	2.2
			Total Percent Inner Hair Cell Loss					
150	0.3	2.7	1.4	1.3	4.9	1.2	6.8	0.0
155	3.4	0.7	10.2	3.1	16.4	0.0	9.9	0.0
160	9.3	0.8	10.0	0.9	21.7	0.0	11.8	0.0

Table 17

Slope (per dB peak SPL) and the y-intercept (at 150 dB peak SPL) of the regression line drawn through the 90th percentile points for all animals exposed to 150, 155 or 160 dB peak SPL for N's of 1, 10 and 100 impulses for each source.

	Source I		Source II		Source III		Source IV	
Number	Slope	Intercept	Slope	Intercept	Slope	Intercept	Slope	Intercept
			Mean Permanent Threshold Shift at 1, 2 and 4 kHz					
1	0.5	0.0	0.0	6.8	0.4	1.6	0.0	4.3
10	1.5	7.9	2.3	14.4	2.0	16.9	0.9	10.2
100	3.6	17.1	3.4	22.5	3.1	33.1	1.5	26.7
			Total Percent Outer Hair Cell Loss					
1	0.0	11.4	0.0	6.2	0.0	7.2	0.1	4.1
10	1.8	9.5	2.9	20.1	2.7	22.7	1.6	6.3
100	5.5	20.7	5.3	41.7	6.2	41.8	2.0	32.6
			Total Percent Inner Hair Cell Loss					
1	0.0	2.6	0.0	1.7	0.0	2.6	0.0	1.3
10	0.6	1.6	0.8	5.5	0.1	5.6	0.6	2.5
100	1.6	2.4	1.7	7.4	3.2	14.5	0.9	15.3

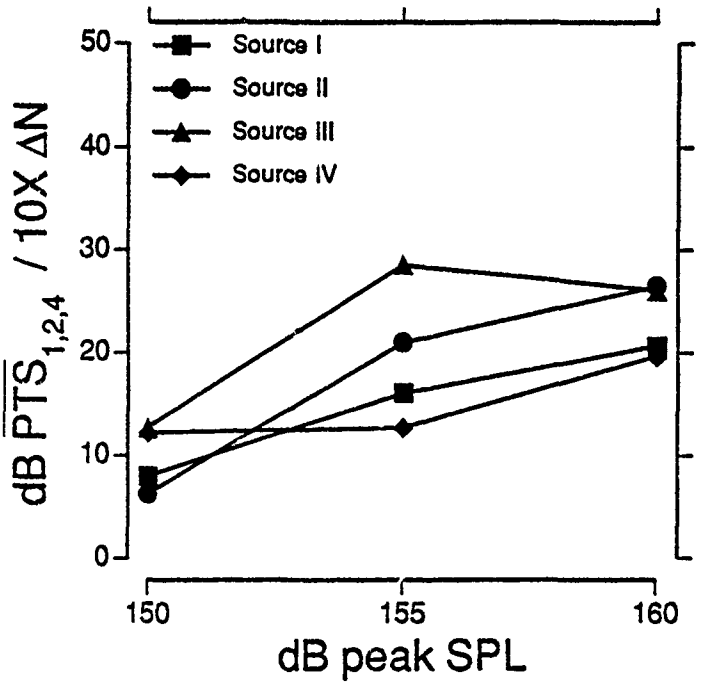

Figure 39. The slope of the regression line drawn through the 90th percentile points of the mean PTS measured at 1, 2 and 4 kHz for animals exposed to 1, 10 or 100 impulses at 150, 155 and 160 dB peak SPL for each source.

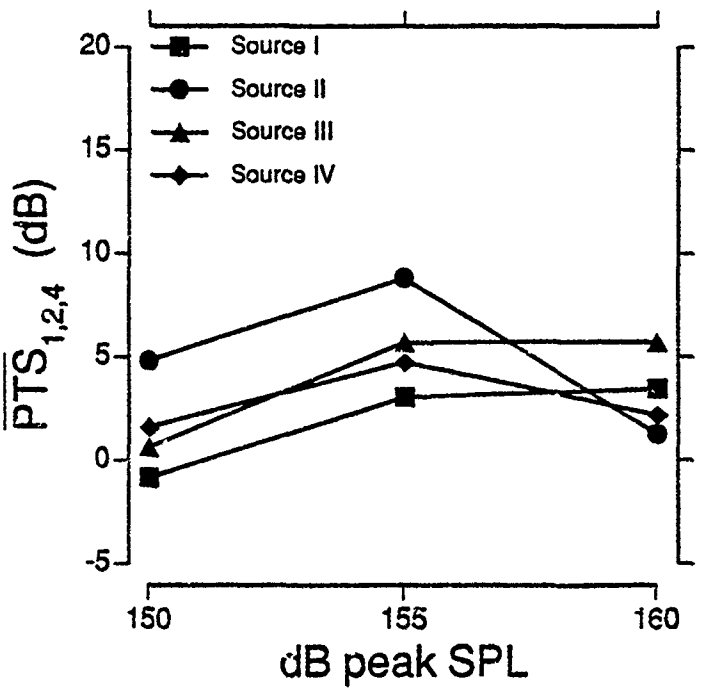

Figure 40. The predicted $\overline{PTS}_{1,2,4}$ following exposure to a single impulse at the indicated peak SPL. The value of $\overline{PTS}_{1,2,4}$ was obtained from the regression line through the 90th percentile points relating the measured $\overline{PTS}_{1,2,4}$ to the number of impulses presented at 150, 155 or 160 dB peak SPL.

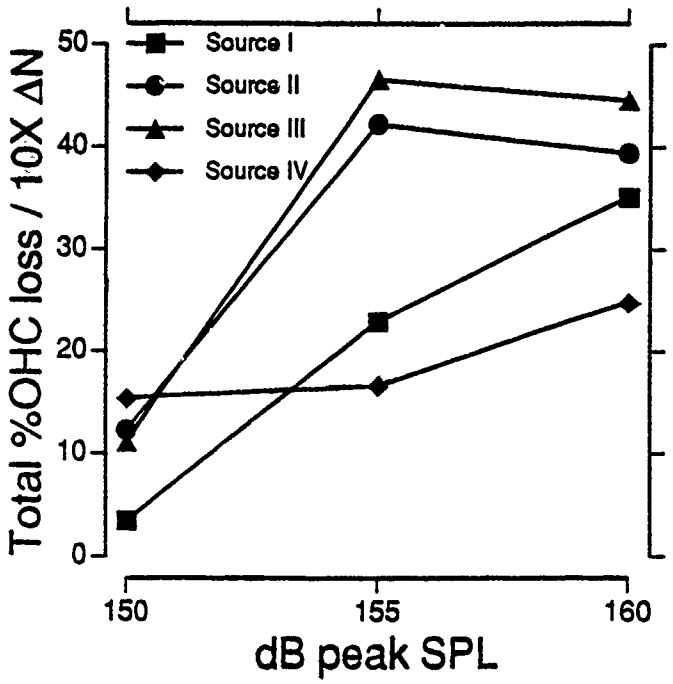

Figure 41. The slope of the regression line drawn through the 90th percentile points of the total percent outer hair cell loss for animals exposed to 1, 10 or 100 impulses at 150, 155 and 160 dB peak SPL for each source.

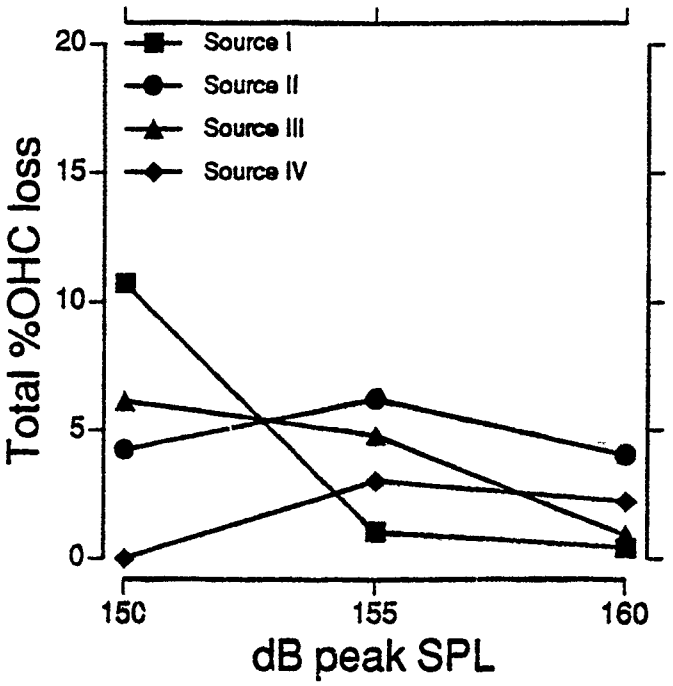

Figure 42. The predicted total percent outer hair cell loss following exposure to a single impulse at the indicated peak SPL. The values plotted were obtained from the regression line through the 90th percentile points relating the measured %OHC loss to the number of impulses presented at 150, 155 or 160 dB peak SPL.

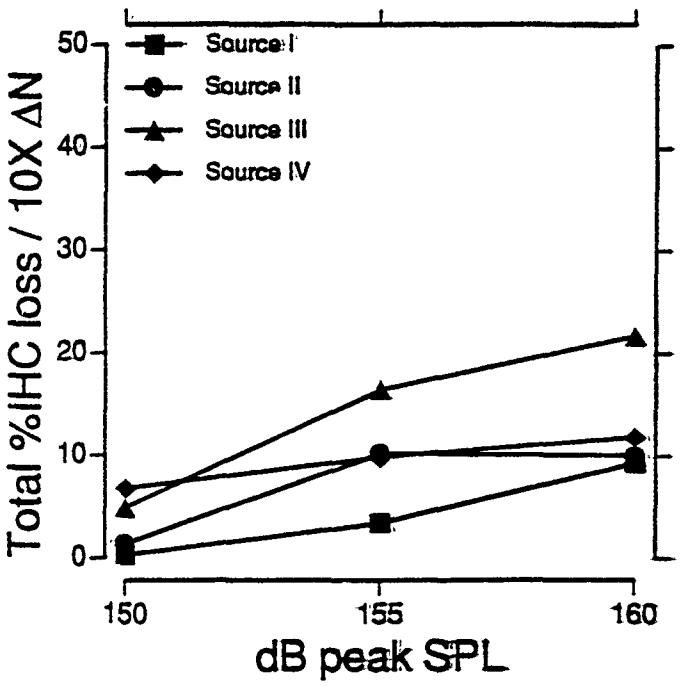

Figure 43. The slope of the regression line drawn through the 90th percentile points of the total percent inner hair cell loss for animals exposed to 1, 10 or 100 impulses at 150, 155 and 160 dB peak SPL for each source.

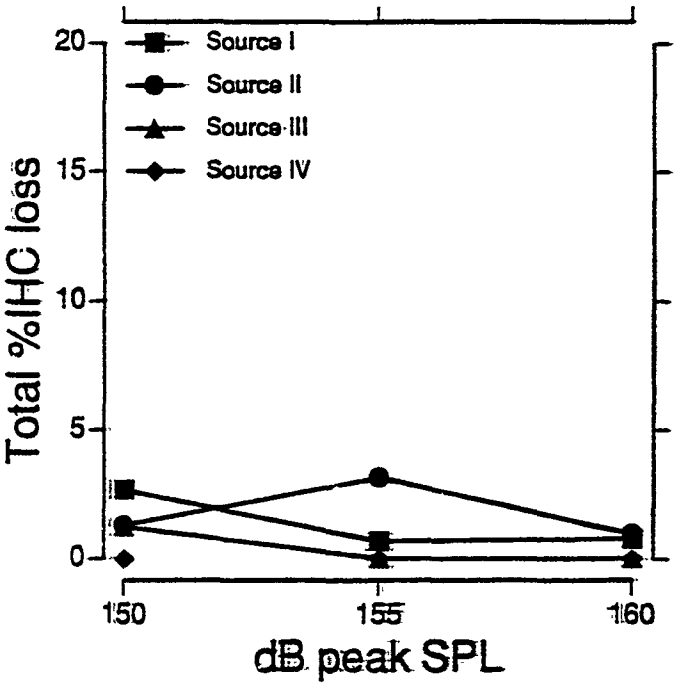

Figure 44. The predicted total percent inner hair cell loss following exposure to a single impulse at the indicated peak SPL. The values plotted were obtained from the regression line through the 90th percentile points relating the measured %IHC loss to the number of impulses presented at 150, 155 or 160 dB peak SPL.

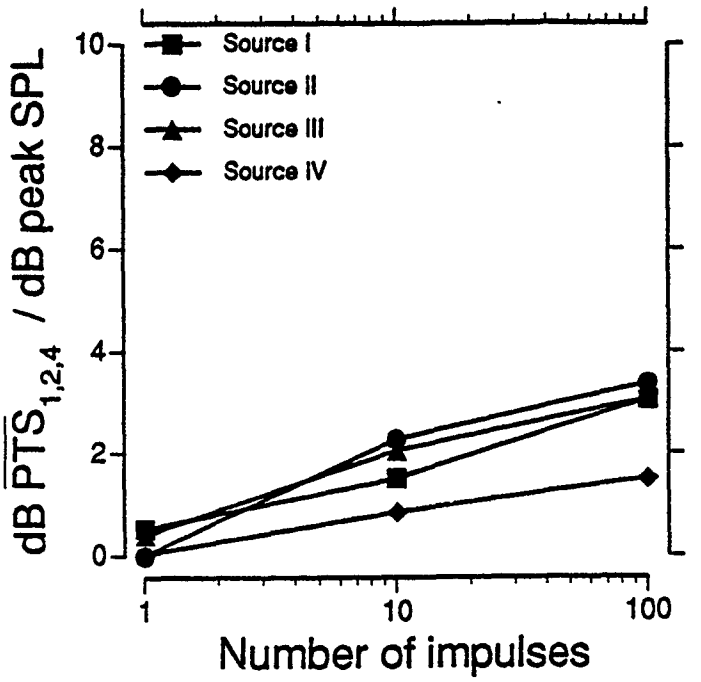

Figure 45. The slope of the regression line drawn through the 90th percentile points of the mean PTS measured at 1, 2 and 4 kHz for animals exposed to 150, 155 or 160 dB peak SPL impulses for N's of 1, 10 and 100 impulses for each source.

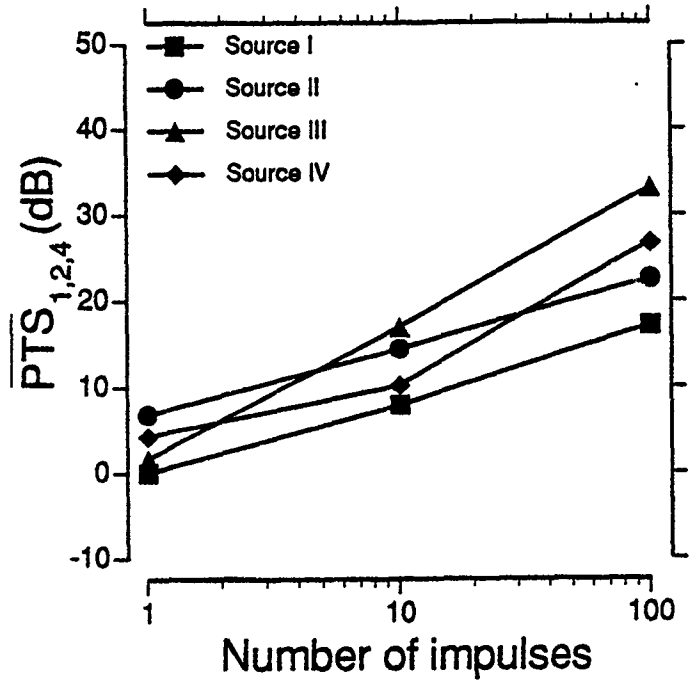

Figure 46. The predicted $\overline{PTS}_{1,2,4}$ following exposure to 150 dB impulses. The value of $\overline{PTS}_{1,2,4}$ was obtained from the regression line through the 90th percentile points relating the measured $\overline{PTS}_{1,2,4}$ to the peak SPL of the impulse for 1, 10 or 100 impulses.

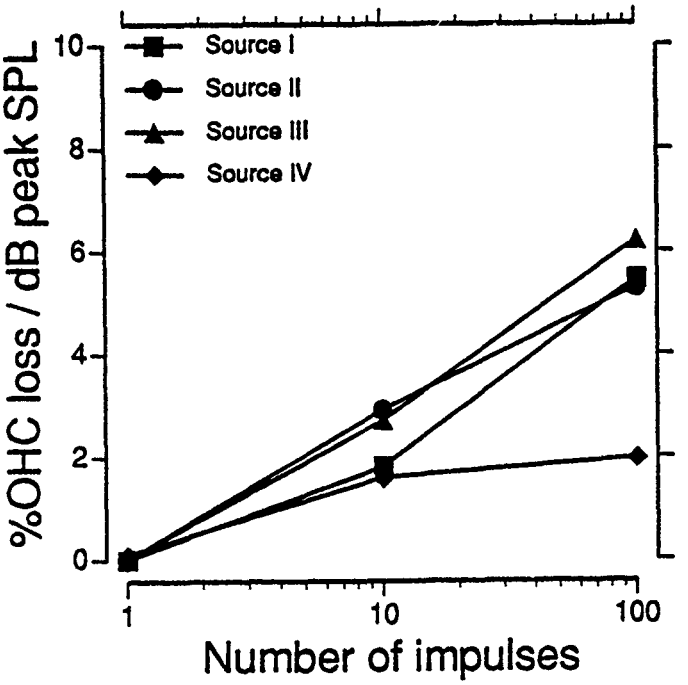

Figure 47. The slope of the regression line drawn through the 90th percentile points of the total percent outer hair cell loss for animals exposed to 150, 155 or 160 dB peak SPL impulses for N's of 1, 10 or 100 impulses for each source.

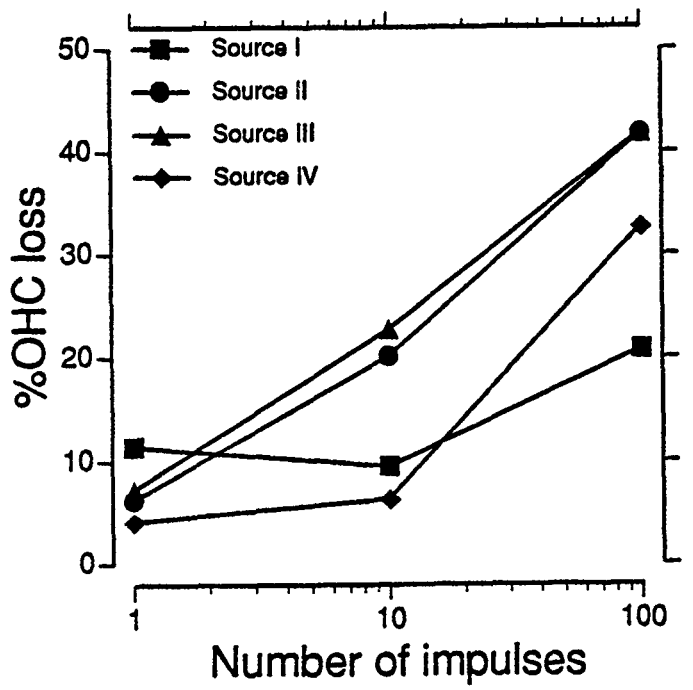

Figure 48. The predicted total percent outer hair cell loss following exposure to 150 dB impulses. The values plotted were obtained from the regression line through the 90th percentile points relating the measured %OHC loss to the peak SPL of the impulse for 1, 10 or 100 impulses.

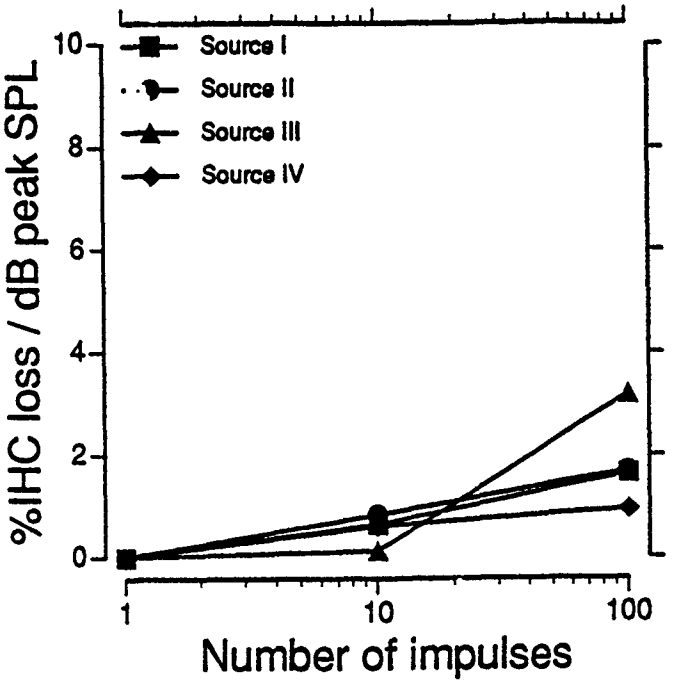

Figure 49. The slope of the regression line drawn through the 90th percentile points of the total percent inner hair cell loss for animals exposed to 150, 155 or 160 dB peak SPL impulses for N's of 1, 10 or 100 impulses for each source.

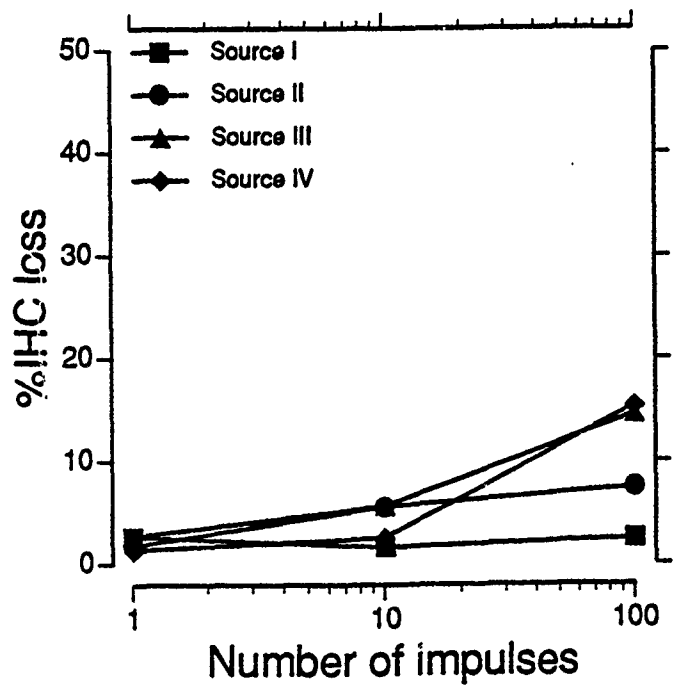

Figure 50. The predicted total percent inner hair cell loss following exposure to 150 dB impulses. The values plotted were obtained from the regression line through the 90th percentile points relating the measured %IHC loss to the peak SPL of the impulse for 1, 10 or 100 impulses.

D. The Relation Between the Energy Spectrum of an Impulse and Auditory Trauma: The following analysis illustrates an approach to the reduction of the previously discussed data that is somewhat different from that which has been attempted in the past. It is an approach that develops a direct relation between frequency specific measures of PTS and sensory cell loss and the frequency-domain representation of the impulse. The results of this approach can be directly related to the Price (1983) model and can also be used to estimate the permanent effects of traumatic impulse noise exposure in a manner similar to that proposed by Kryter (1970) for estimating TTS after an impulse noise exposure.

As in the previous section all the data has been collapsed across the ISI variable for the reasons specified. This effectively increased the number of animals at each sound exposure level to 15 except for the 1X exposure conditions. ISI does not affect the total SEL of the exposure which, for each source, is directly related only to the peak SPL and to the number of impulses.

The following procedure was used for the analysis of the PTS, OHC loss and IHC loss data: For each audiometric test frequency, a plot of the individual animal PTS, OHC loss or IHC loss at that frequency as a function of the total unweighted sound exposure level in the octave band centered on that test frequency was prepared for each source. Some typical examples of this display of the data at 1 kHz for each source are shown in Figures 51 and 52. The actual number of data points in Figures 51 and 52 is less than the actual number of animals used since a number of animals had the same data coordinate. Using data sets such as those shown in Figures 51 and 52 the 90th percentile hearing loss (PTS_{90}) or cell loss (OHC_{90}, IHC_{90}) was computed as previously described for each sound exposure level at each octave frequency from 0.5 to 16 kHz.

This procedure yields a maximum of nine percentile points; one for each of the nine distributions of data along the SEL axis of Figures 51 and 52, (i.e. three peak levels x three numbers of impacts). A linear regression line using these nine points was then computed. In many cases, the animals in the groups exposed to only a single impulse did not show a PTS (or OHC, IHC loss) statistically different from zero at some frequency, and including these points in the least squares regression would artifactually decrease the slope of the regression line. In these cases, only the highest energy exposure for which a PTS (or OHC, IHC loss) was not significantly greater than zero was used in computing the regression line. Most often this "zero anchor" point was the 1X, 160 dB peak SPL group, since in general all the 1X exposures proved to be relatively non-traumatic and the 160 dB exposure had the highest SEL of the 1X exposures. Thus the regression line could be computed on a minimum of seven or a maximum of nine points. This exercise was repeated for each of the six octave test frequencies and for each of the four sources. The entire procedure was repeated for OHC percent loss and IHC percent loss. From this set of 72 regression lines, the following relations could be obtained: (1) the threshold sound exposure level, $E_o(f)$, at each frequency for which 90% of the exposed population will have no PTS or sensory cell loss (i.e., the x-intercept of the regression line); and (2) the rate at which PTS_{90}, OHC_{90} or IHC_{90} increases as the sound exposure level is increased above the threshold level at each frequency (i.e., the slope of the regression line). Two other useful relations that can be obtained from (1) and (2) above are: the total sound exposure level in a given octave band required to produce a criterion level of PTS_{90}, OHC_{90} or IHC_{90} at that octave band center frequency or conversely the PTS or cell loss that will not be exceeded by 90% of the exposed population for a specified exposure level in each octave band.

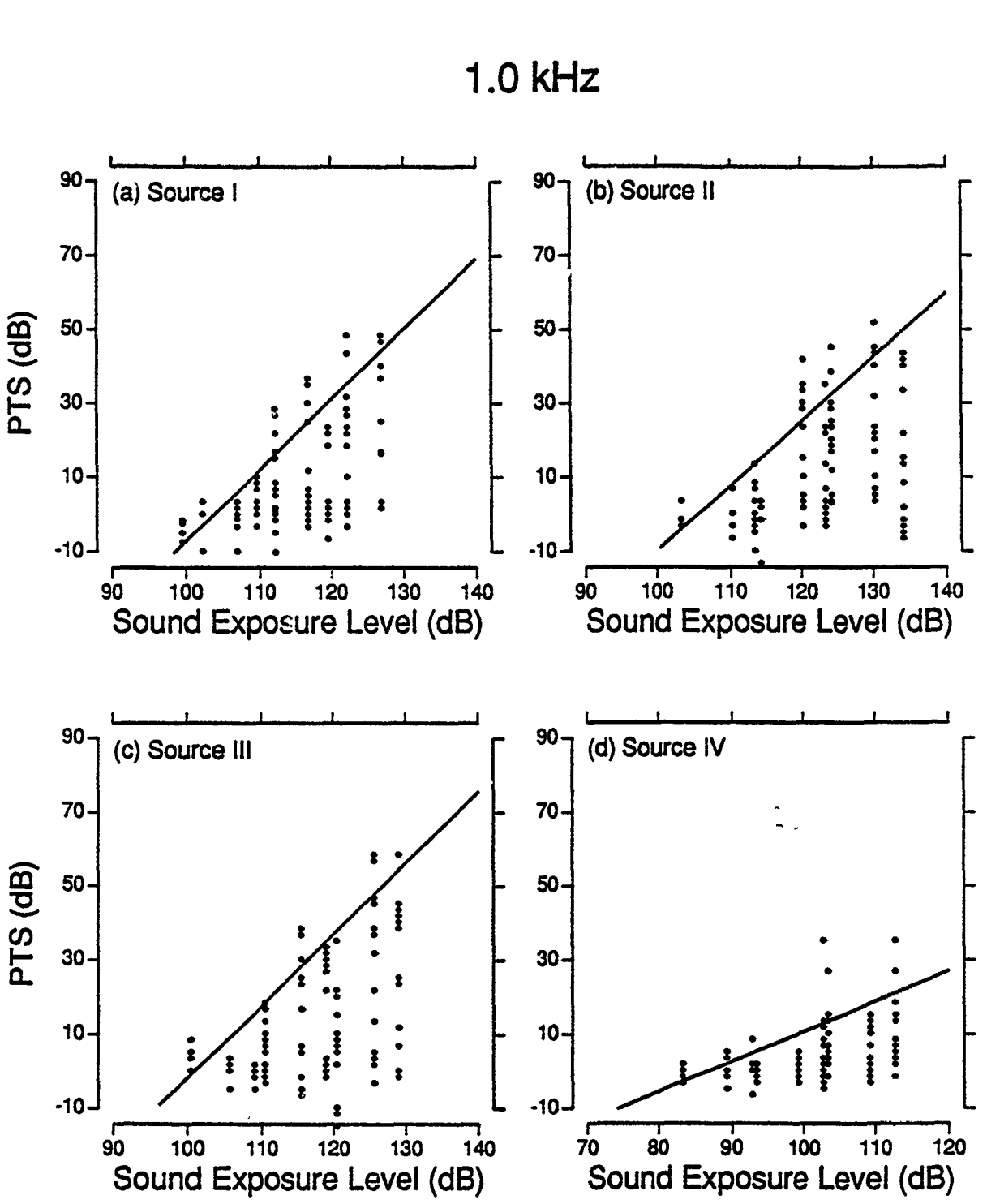

Figure 51. The PTS measured in individual animals at 1.0 kHz for all the animals exposed to impulses from the four different sources as a function of the total sound exposure level in the 1.0 kHz octave band of each exposure condition. The solid line represents the linear regression through the 90th percentile points in the PTS distribution for each exposure energy level.

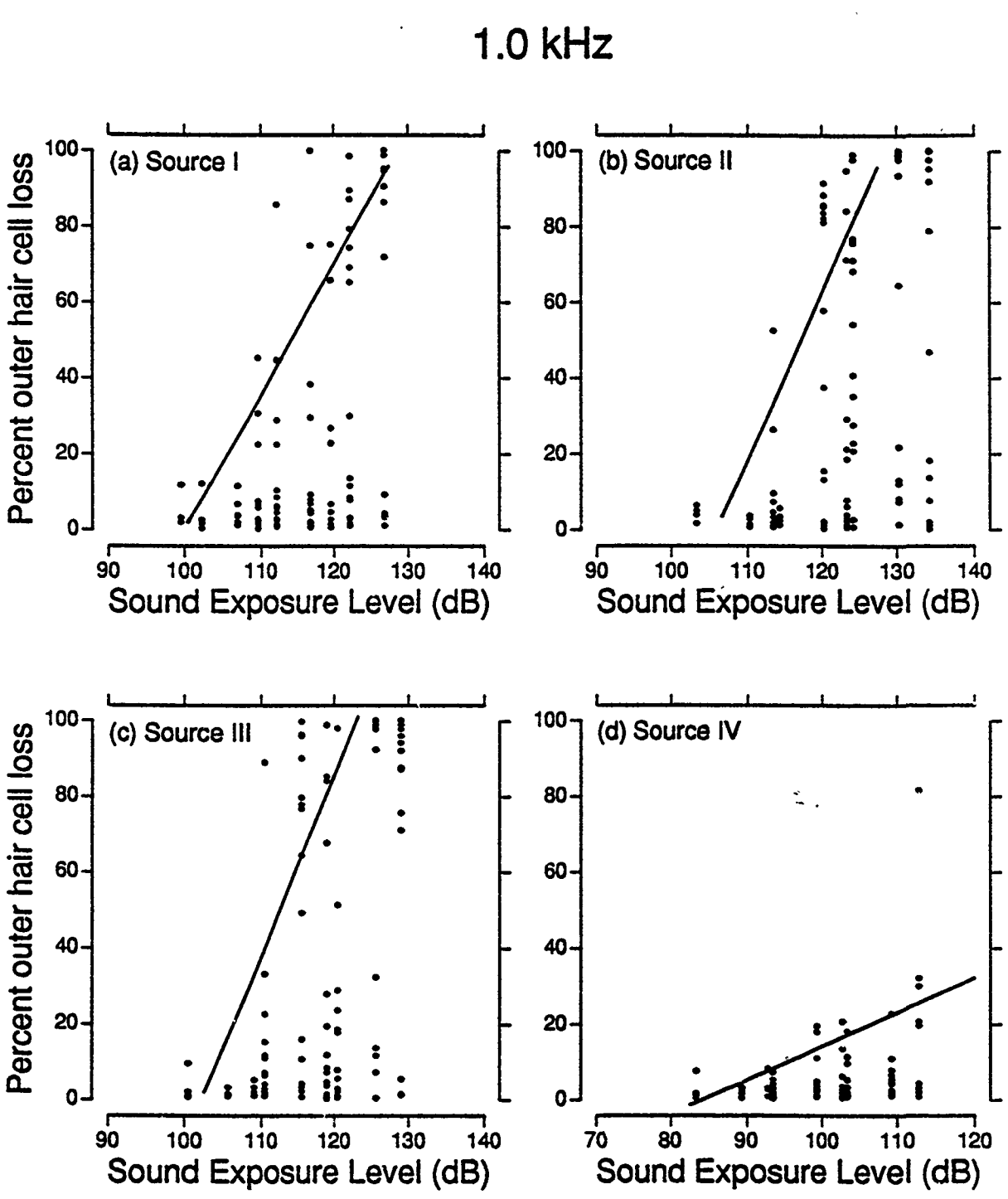

Figure 52. The percent outer hair cell loss (OHC) in the octave band length of the cochlea centered at 1.0 kHz for all the animals exposed to impulses from the four different sources as a function of the total sound exposure level in the 1.0 kHz octave band of each exposure condition. The solid line represents the linear regression through the 90th percentile points in the OHC distribution for each exposure energy level.

The results of the trauma versus energy analysis just described are summarized in Figures 53 and 54, and the slope and intercept values tabulated in Table 18. These figures illustrate the slope of the regression line and the intercept of this line with the abscissa for the three indices of trauma, PTS, OHC loss and IHC loss. That is, the figures illustrate: (1) how hearing loss and cell loss grows with increasing stimulus energy across the range of audible frequencies for the four classes of impulses and (2) the threshold energy, $E_0(f)$, below which there should be no PTS or sensory cell loss incurred in 90% of the exposed population. The following generalizations can be made from these figures: (1) At a given audiometric test frequency, hearing loss grows at a rate of between 0 and 3 dB of PTS for each dB increase in stimulus energy in that particular octave band while sensory cell losses grow at the rate of between 0 and 5% of loss per dB SEL. The above growth rates differ between sources and for each source the rates vary as a function of the audiometric test frequency.

The distinct trend in the growth rates is for the rates to be highest in the region of the spectral peak of the impulse and to fall off on either side. This fall off is greatest on the low frequency side of the spectral peak and very gradual or near zero on the high frequency side. The suggestion is that for a given impulse, hearing pathology will develop throughout the cochlea basalward of the spectral peak of the impulse. Thus, for Sources II and III whose spectral peak is in the 1-2 kHz region of the cochlea, the pathology is severe in the 1-2 kHz region and basalward of this region. While for Source IV, whose spectral peak is in the 4-8 kHz region peak, the pathology develops in the 4-8 kHz region and at higher frequencies, but falls off rapidly for the lower frequencies. Source I was interesting in that the general configuration of the slope-frequency function was similar to that of Source II and III, but was lower by 1-2% OHC loss/dB SEL across the range of test frequencies. Surprisingly this was also true at the high frequencies in the PTS/dB SEL function. Thus although the low frequency source had roughly the same energy as the other three sources at the higher frequencies, the slopes across all three measures of pathology were lower.

There was a surprising consistency in the threshold SEL at which trauma begins to develop for all three indices of trauma. For Sources I, II and III the threshold is around 105 dB SEL and is relatively independent of frequency. For Source IV, the threshold of trauma for frequencies above 2 kHz is also around 105 dB but falls off rapidly at and below 2 kHz. The Source IV impulses have the least energy below 2 kHz and the slope-frequency function is relatively flat and thus the SEL-intercept rapidly decreases. The thresholds for IHC loss tend to be more variable than PTS and OHC loss thresholds across both the source and frequency variables.

Using the data embodied in Figures 53 and 54, the amount of PTS, OHC loss and IHC loss at each test frequency that will not be exceeded by 90% of the exposed population, for a fixed amount of energy, can be estimated. The result of this exercise is shown in Figure 55 for a criterion SEL of 120 dB. The data in this figure indicate that: (1) the level of PTS generally increases with increasing frequency and (2) Source I generally produces the lesser amount of PTS, while Source III the greatest amount of PTS across the range of test frequencies. This figure also shows quite clearly that all energy is not equal in its ability to produce a PTS. At a given frequency, a 120 dB SEL in an impulse produced by Source III consistently produces more PTS than the same SEL from Source I by as much as 10 dB. At 2 and 4 kHz the differences in PTS between Sources I and IV are around 15 dB for the same SEL. Similarly, differences exist across sources for OHC and IHC loss. An

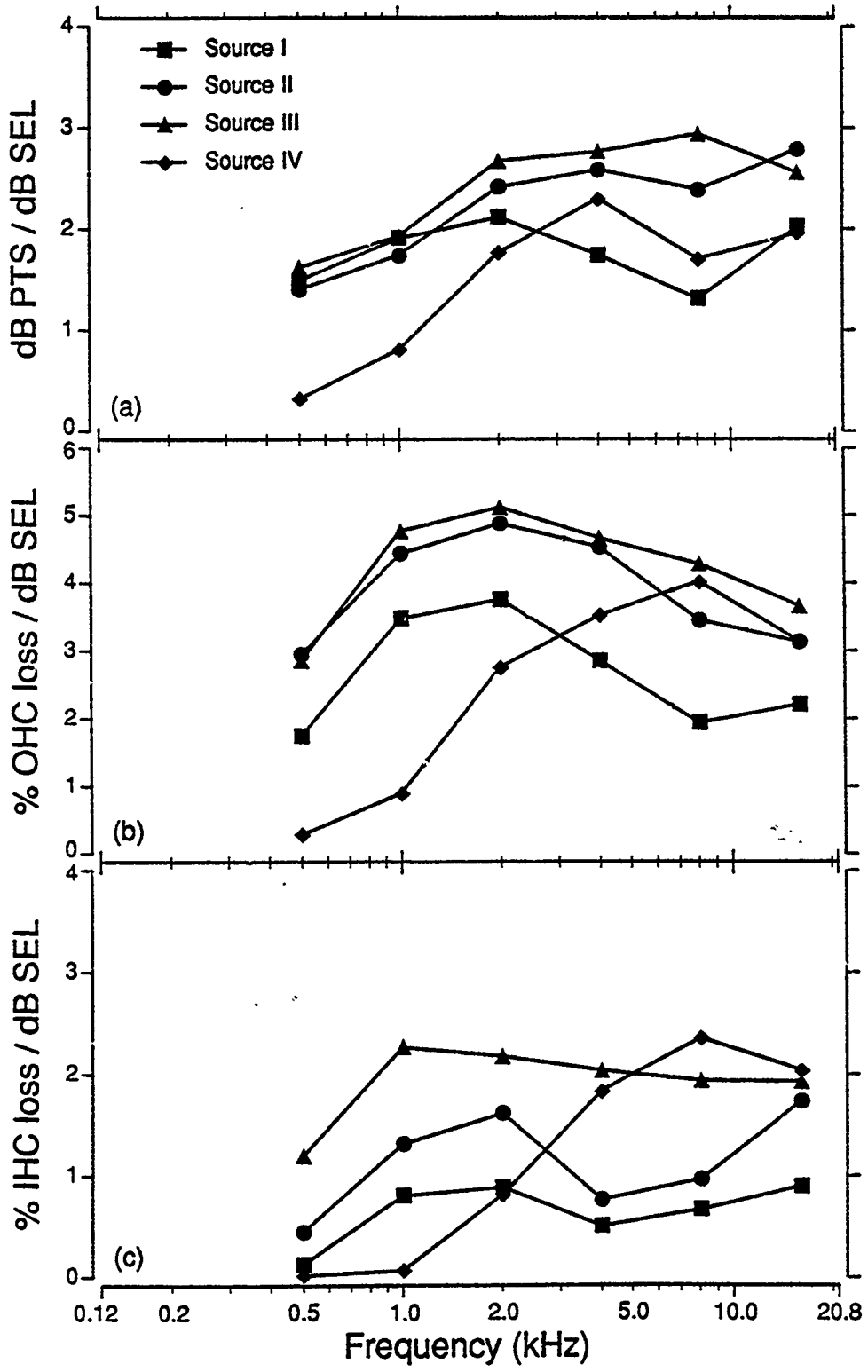

Figure 53. The slope of the regression line drawn through the 90th percentile points at each audiometric test frequency for all animals and each source showing the increase in (a) PTS, (b) percent outer hair cell loss and (c) percent inner hair cell loss for each dB increase in SEL.

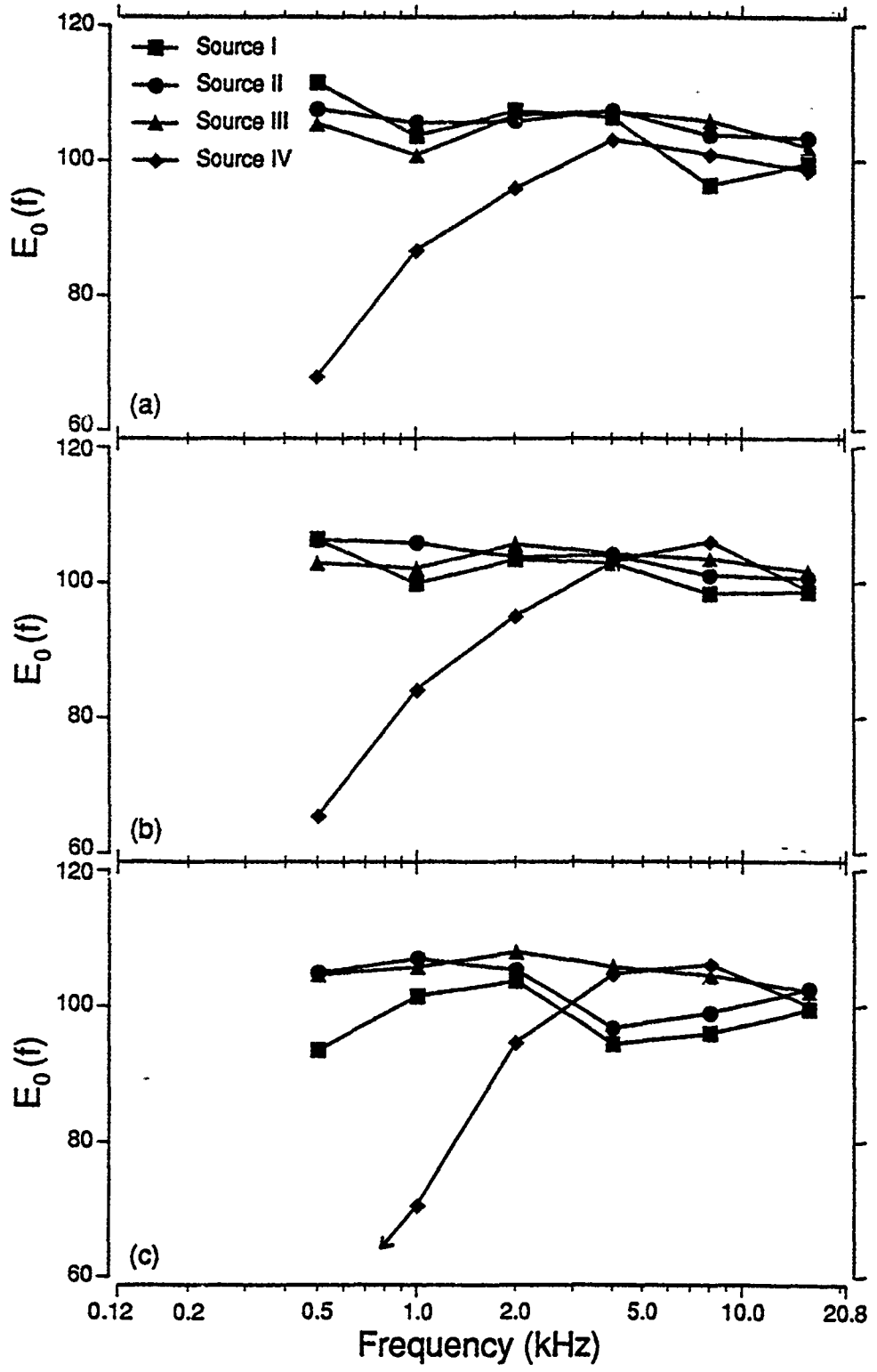

Figure 54. The predicted threshold energy, $E_0(f)$, obtained from the energy-axis intercept of the regression line through the 90th percentile points relating (a) PTS, (b) percent outer hair cell loss and (c) percent inner hair cell loss at each audiometric test frequency to the total SEL of the exposure.

Table 18

Slope (per dB SEL) and SEL intercept (dB) of the regression line drawn through the 90th percentile points for PTS and sensory cell loss at each audiometric test frequency for all animals for each source.

	Source I		Source II		Source III		Source IV	
kHz	Slope	Intercept	Slope	Intercept	Slope	Intercept	Slope	Intercept
				Permanent Threshold Shift				
0.5	1.5	111.5	1.4	107.7	1.6	105.5	0.3	68.0
1.0	1.9	103.7	1.7	105.6	1.9	100.9	0.8	86.7
2.0	2.1	107.4	2.4	105.9	2.7	106.8	1.8	95.9
4.0	1.7	106.4	2.6	107.4	2.8	107.3	2.3	103.2
8.0	1.3	96.3	2.4	103.9	2.9	105.9	1.7	101.0
16.0	2.0	99.7	2.8	103.4	2.6	102.1	2.0	98.6
				Percent Outer Hair Cell Loss				
0.5	1.7	106.4	2.9	106.4	2.9	102.9	0.3	65.6
1.0	3.5	99.8	4.4	105.9	4.8	102.1	0.9	84.2
2.0	3.8	103.4	4.9	103.8	5.1	105.7	2.8	95.1
4.0	2.9	102.8	4.5	104.1	4.7	104.2	3.5	103.0
8.0	1.9	98.3	3.4	101.0	4.3	103.5	4.0	106.0
16.0	2.2	98.6	3.1	100.6	3.7	101.6	3.1	98.9
				Percent Inner Hair Cell Loss				
0.5	0.1	93.6	0.5	105.0	1.2	104.7	0.0	-48.4
1.0	0.8	101.5	1.3	107.1	2.3	105.8	0.1	70.7
2.0	0.9	103.7	1.6	105.4	2.2	108.0	0.8	94.7
4.0	0.5	94.4	0.8	96.8	2.0	105.8	1.8	104.8
8.0	0.7	96.0	1.0	99.0	1.9	104.5	2.4	106.2
16.0	0.9	99.6	1.7	102.5	1.9	102.2	2.0	100.1

alternate way of stating this observation is that the energy, in a particular octave band, transported by an impulse whose spectral peak is at the very low end of the spectrum is less effective in producing a PTS than is the same amount of energy in the same octave band, transported by an impulse whose spectrum peaks at a higher frequency. One of the surprising features of the data presented in Figure 55 is the general absence of a "most sensitive" frequency in the sense indicated by Price (1983). Rather, the general impression is that there is an increase in susceptibility to trauma from the lowest to the highest audiometric frequencies and that this effect is further accentuated by 5 to 10 dB for the impulse produced by Source III (i.e., the source producing the impulse with the spectral peak located in the 2 kHz octave band frequency).

For a point of comparison, it should be noted that Sources I and II of this report produce impulses very similar to those produced by the 105-mm howitzer and the M-16 rifle, respectively, as reported by Price (1983). In the Price experiments, while the cat was used as the animal model, the conditions of the exposure were a subset of those described in this report. Although the audiometric techniques differed, the distribution of individual animal PTS and the degree of variability are similar. However, because of the the differences in the manner in which the data are presented, detailed comparisons between the two studies are difficult to make.

These same data were also analyzed by comparing the slopes and the SEL-intercepts of the linear regression line through the 90th percentile points of the distribution of individual animal $PTS_{1,2,4}$ and total sensory cell loss as a function of the total SEL for each exposure condition and source. The slope, in units of dB $PTS_{1,2,4}$/dB SEL, %OHC loss/dB SEL or %IHC loss/dB SEL for each of the respective dependent variables along with the threshold energy level $E_o(f)$ in dB for the on-set of trauma (SEL-intercept) are shown in Figure 56. As in the previous analysis in which test frequency was an independent variable, it is apparent that while the energy in a given exposure condition for Source I through IV continuously decreases, the threshold energy at which trauma begins to develop is highest for Source I and lowest for Source IV. This result clearly indicates the need to apply a frequency weighting function to the impulses before they can be evaluated for their relative effects on the auditory system. The difference in $E_o(f)$ between Sources I and IV shown in Figure 56 implies that the appropriate weighting function should show an approximately 15 dB differential for frequencies between 0.25 and 4.0 kHz.

The slopes of the various regression lines for each source and for each dependent variable also show some differences, but these differences are not very large, being on the order of approximately 1 dB $PTS_{1,2,4}$/dB SEL or 1.5% OHC loss/dB SEL. The effects are consistant across the three dependent variables. However, over a 10 dB increment in SEL damage to the auditory system can accumulate to yield a significant increase in trauma. The implication of these differences is that the growth of trauma is dependent not only on the total energy (weighted or unweighted) of the exposure, but is also dependent on the frequency distribution of the energy. That is, all energy is not equal; rather the effect of the amount of energy in a certain octave band is going to be dependent upon how the energy in the other octave bands is distributed.

While the above presentation of data for several different sources neglects some of the known characteristics of noise-induced hearing loss such as the half-octave shift, it is an approach that can be used to place bounds on the amount of pathology that can be expected from an impulse noise exposure on the basis of the spectral distribution of the energy of the exposure. If

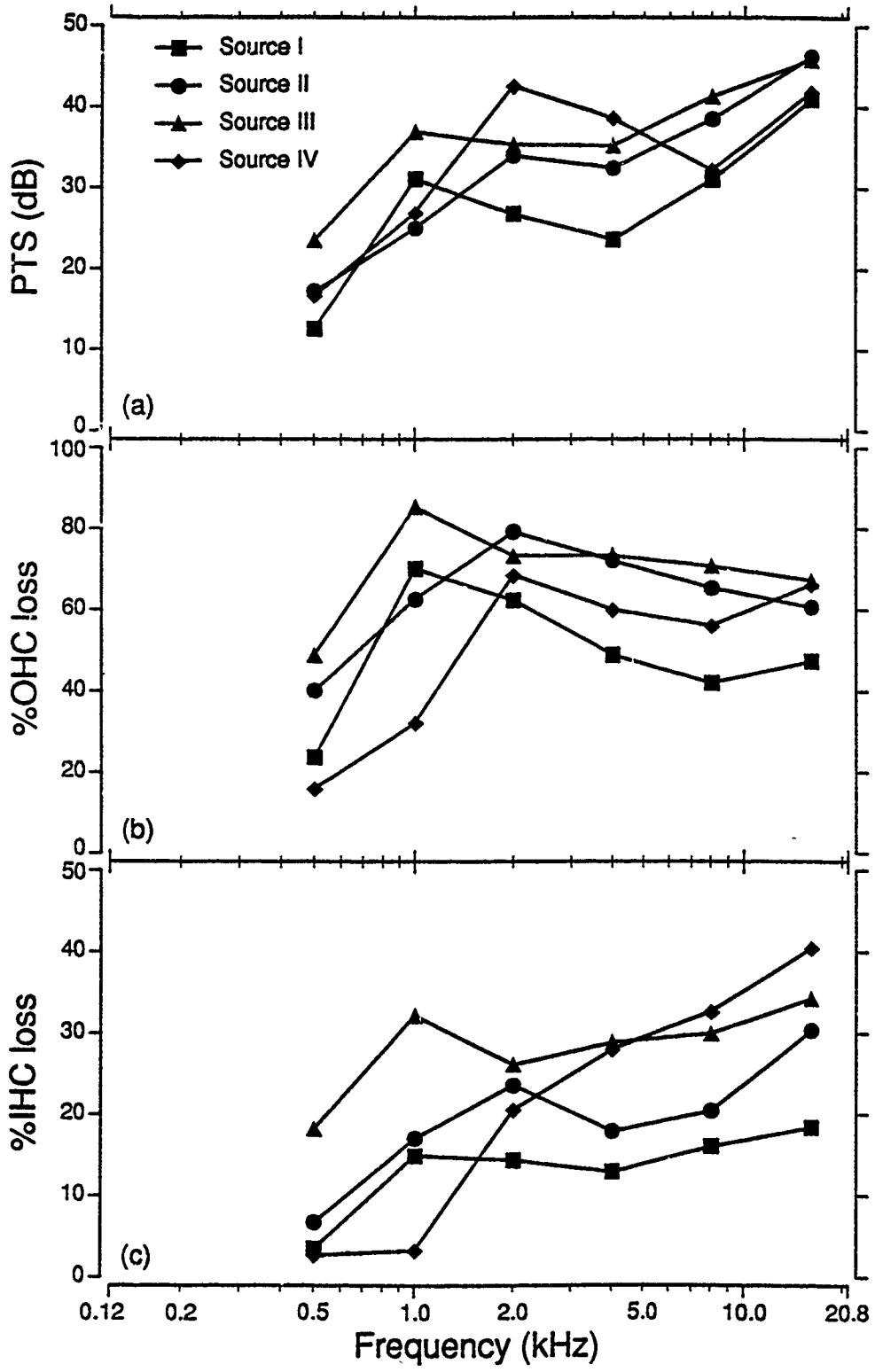

Figure 55. The predicted (a) PTS, (b) percent outer hair cell loss and (c) percent inner hair cell loss at each audiometric test frequency from an impulse having a total SEL of 120 dB. These predictions are based upon the data presented in Figures 53 and 54.

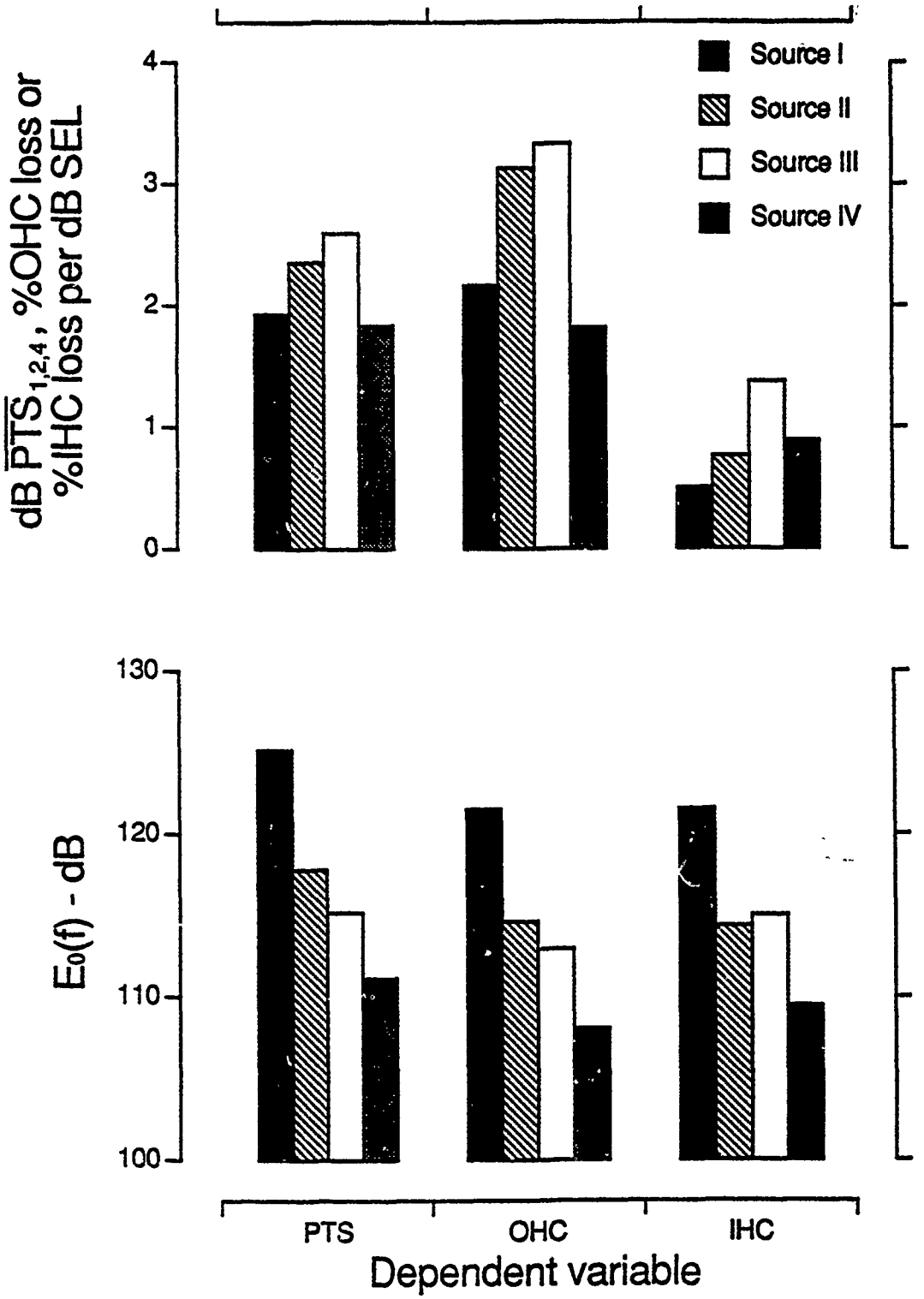

Figure 56. A comparison of the slopes and threshold energy intercept, Eo(f), of the regression line relating the 90th percentile mean PTS at 1, 2 and 4 kHz, the percent total outer hair cell loss or percent total inner hair cell loss to the SEL of the exposure for the different sources.

such an analysis is performed on a sufficiently large body of PTS and cell loss data obtained from sources which cover the range of audibility in their spectral peaks, upper and lower bounds on the indices of trauma can be established for the chinchilla. Such an approach would be quite similar to that suggested by Kryter (1970) except that PTS rather than some measure of TTS would be predicted.

E. The Relation Among Hearing Loss, Sensory Cell Loss and Tuning Curve Characteristics: Figure 57 illustrates the mean preexposure AEP TC's obtained on a total sample of 294 chinchillas at the probe frequencies of 0.5, 1.0, 2.0, 4.0, 8.0 and 11.2 kHz. The ordinate and abscissa represent the intensity and frequency, respectively, of a continuous tone that just masks the probe tone which is indicated with a solid symbol. (Although 294 animals constituted the population, tuning curves at some frequencies in a few animals were not measured for a variety of reasons, thus somewhat smaller sample sizes are to be found in the pre- and postexposure data. In the data plotted in Figure 57 the total sample size used in each calculation is shown.) The mean preexposure $Q_{10\ dB}$ and the slopes of these AEP tuning curves are similar to those reported by Salvi et al. (1982c) for the chinchilla. The sharpness of tuning and the low- and high-frequency slopes increase as the signal frequency is increased. The S_{LF} ranged from approximately 21 to 50 dB/octave and the S_{HF} ranged from approximately 27 to 95 dB/octave. This range of slopes is also in general agreement with the published behavioral data on the chinchilla (Salvi et al., 1982c). Table 19 presents the numerical values of $Q_{10\ dB}$, S_{LF}, and S_{HF}, for the entire population of preexposure tuning curves. The values shown were calculated using both the mean statistic and the mean tuning curve. There is a reasonably good agreement between the tuning curve variables calculated using the two different methods. Since the pattern of results obtained using the mean statistic of the individual tuning curves and the mean tuning curve statistic was similar, (Tables 19 through 22) the remaining figures present the analysis of the TC variables calculated from the mean tuning curves.

To get a visual impression of how the TC's change as PTS increases each animal was segregated at each frequency by the amount of PTS that the animal incurred. Bins containing animals that had PTS < 10 dB, $10 \leq$ PTS < 20, $20 \leq$ PTS < 30, $30 \leq$ PTS < 40 and PTS ≥ 40 dB, were formed for each probe frequency and mean tuning curves computed for each group. The results of this organization of the postexposure TC data are shown in Figure 58. From this figure the effect of an increasing PTS on the morphology of the mean TC at each probe frequency can be seen. When PTS is less than 10 dB, the morphology (namely the $Q_{10\ dB}$ the S_{HF} and S_{LF}) is virtually identical to the mean preexposure TC. In the $10 \leq$ PTS < 20 dB group there is a general elevation of the TC and only a slight reduction in $Q_{10\ dB}$. However, in the $20 \leq$ PTS < 30 dB group or higher the TC's are visibly broadened. Tuning is virtually eliminated for PTS greater than 40 dB and the data from those animals have not been shown. Beyond 40 dB, the TC's were either flat or beyond the range of the instrumentation's ability to completely mask the probe tone and provide no additional information. Thus, we can see a clear and systematic "detuning" of the mean TC as the degree of PTS increases across all the CF's. Listings of the numerical values for all the tuning curve parameters for the various PTS groupings are presented in Tables 20 through 22. As in the preexposure listing, two sets of quantitative values are presented; the mean tuning curve variables and the mean statistic calculated from individual TC's. Tables 19 through 22 may be used to find the $Q_{10\ dB}$, S_{HF} or S_{LF} of any tuning curve shown in Figures 57 or 58.

Figure 59 illustrates the percent change in the mean tuning curve characteristics (calculated from the data presented in Tables 19 through 22)

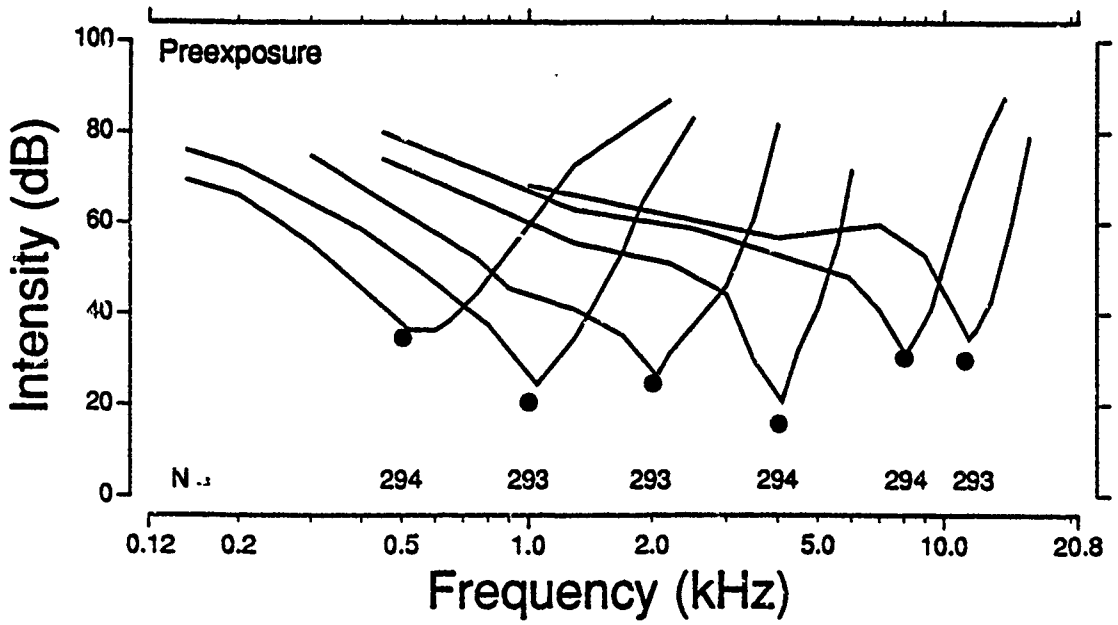

Figure 57. The mean preexposure tuning curves for the entire experimental population at each probe frequency. (N = sample size, ● = probe tone)

TABLE 19

The preexposure tuning curve variables, $Q_{10\ dB}$, high frequency slope (S_{HF}) (dB/octave) and low frequency slope (S_{LF}) (dB/octave)

Probe (kHz)	Mean Tuning Curve		Mean Statistic		
	$\tilde{Q}_{10dB}$	N	$\bar{Q}_{10dB}$	S.D.	N
0.5	1.340	294	1.579	0.716	275
1.0	2.400	293	2.489	0.969	289
2.0	2.414	293	2.813	1.656	291
4.0	4.147	294	4.326	1.752	293
8.0	3.428	294	3.711	1.947	284
11.2	3.759	293	5.359	3.850	283
	$\tilde{S}_{HF}$	N	$\bar{S}_{HF}$	S.D.	N
0.5	27.0	294	26.8	8.8	290
1.0	48.2	293	47.4	11.2	291
2.0	52.7	293	46.3	15.8	292
4.0	88.3	294	84.7	25.1	294
8.0	75.3	294	76.1	24.3	291
11.2	94.2	293	85.2	28.4	293
	$\tilde{S}_{LF}$	N	$\bar{S}_{LF}$	S.D.	N
0.5	23.8	294	24.0	7.9	293
1.0	26.6	293	26.6	8.6	293
2.0	21.6	293	21.7	12.1	292
4.0	52.5	294	52.5	19.2	294
8.0	37.0	294	37.4	22.5	292
11.2	51.4	293	52.0	29.5	292

Values calculated using the mean tuning curve (~) and the mean of all the individual tuning curves (-). (N = sample size, S.D. = standard deviation.)

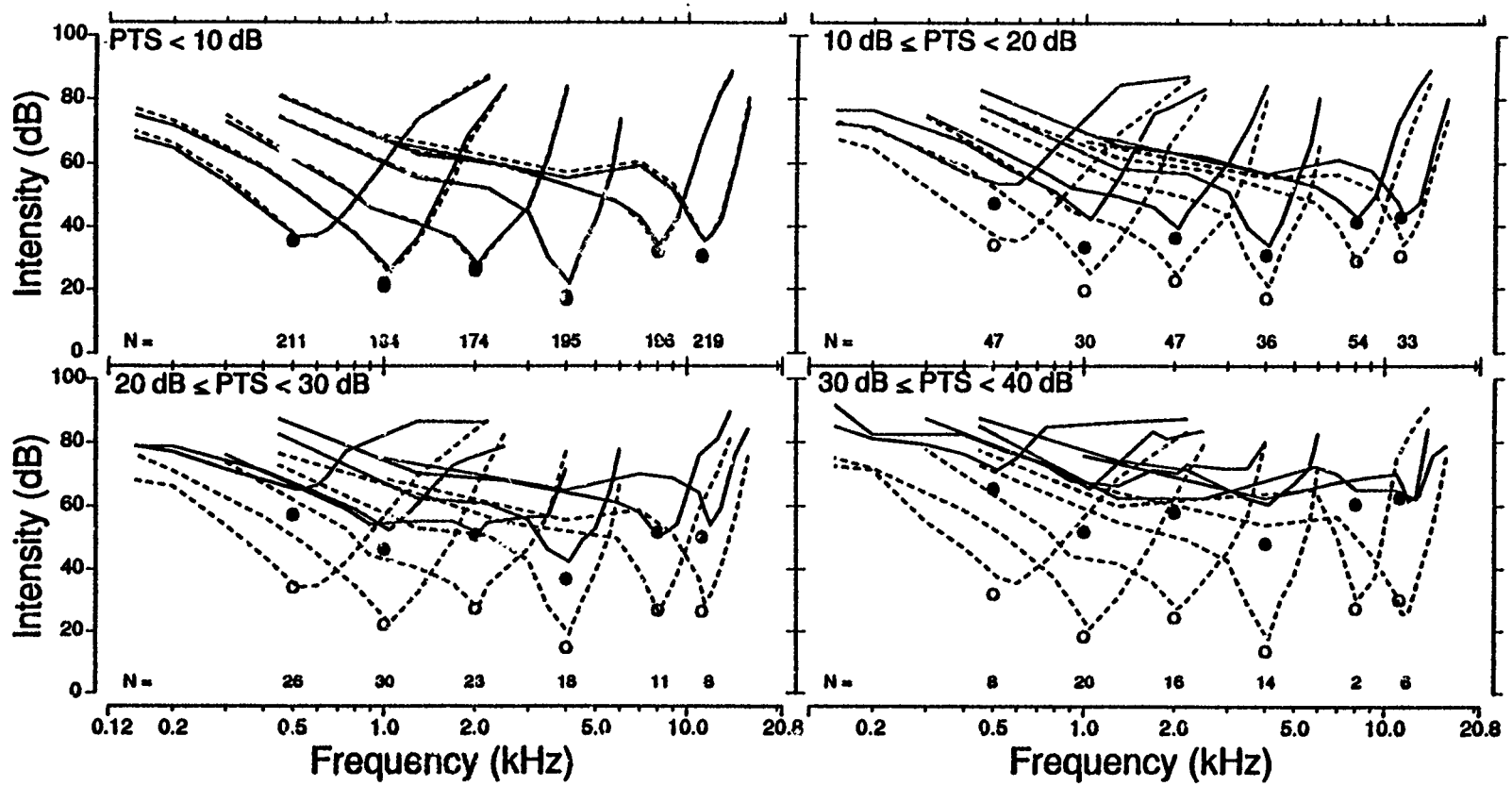

Figure 58. A comparison of the preexposure (dashed line) and postexposure (solid line) mean tuning curves obtained from groups of animals having various levels of PTS at a given probe frequency. (N = sample size, O & ● = probe tones)

Table 20

Mean Q_{10dB} Values ($\bar{Q}_{10}$) and Q_{10dB} for the mean tuning curves ($\tilde{Q}_{10}$)

Probe (kHz)	PTS	$\tilde{Q}_{10}$ Pre	Post	N	$\bar{Q}_{10}$ Pre	S.D.	N	Post	S.D.	N
0.5	PTS < 10 dB	1.367	1.351	211	1.643	0.769	198	1.548	0.692	203
	10 dB ≤ PTS < 20 dB	1.254	1.086	47	1.415	0.465	42	1.433	0.657	36
	20 dB ≤ PTS < 30 dB	1.370	1.058	26	1.518	0.609	25	1.587	0.743	19
	30 dB ≤ PTS < 40 dB	1.190	1.053	8	1.209	0.585	8	1.715	0.831	6
	PTS ≥ 40 dB	0.913	0.000	2	0.901	0.156	2			0
1.0	PTS < 10 dB	2.449	2.276	193	2.508	0.953	190	2.364	0.854	192
	10 dB ≤ PTS < 20 dB	2.368	2.139	30	2.561	1.138	29	2.231	0.925	29
	20 dB ≤ PTS < 30 dB	2.258	1.534	30	2.339	0.917	30	1.710	0.660	28
	30 dB ≤ PTS < 40 dB	2.553	1.402	20	2.639	1.024	20	1.611	0.708	12
	PTS ≥ 40 dB	2.054	0.952	20	2.277	0.915	20	3.268	2.682	3
2.0	PTS < 10 dB	2.517	2.200	174	2.975	1.813	173	2.899	1.773	169
	10 dB ≤ PTS < 20 dB	2.527	1.876	47	2.832	1.511	46	2.864	2.091	41
	20 dB ≤ PTS < 30 dB	2.439	0.685	23	2.527	1.651	22	2.681	2.541	15
	30 dB ≤ PTS < 40 dB	2.111	0.000	16	2.199	1.009	16	0.786	0.106	3
	PTS ≥ 40 dB	2.093	0.000	34	2.434	1.060	34	3.035	1.949	3
4.0	PTS < 10 dB	4.046	3.969	195	4.231	1.720	195	4.227	1.867	192
	10 dB ≤ PTS < 20 dB	4.124	3.228	36	4.208	1.704	35	3.362	1.449	35
	20 dB ≤ PTS < 30 dB	3.961	2.322	18	4.303	2.271	18	3.012	1.400	15
	30 dB ≤ PTS < 40 dB	4.892	1.288	14	4.784	2.135	14	2.326	1.648	11
	PTS ≥ 40 dB	4.747	0.796	31	4.861	1.438	31	1.317	0.448	8
8.0	PTS < 10 dB	3.237	3.055	196	3.611	1.977	191	3.350	1.878	188
	10 dB ≤ PTS < 20 dB	3.531	2.182	54	3.723	1.639	49	3.077	2.029	50
	20 dB ≤ PTS < 30 dB	4.473	2.292	11	4.604	1.831	11	3.438	1.258	8
	30 dB ≤ PTS < 40 dB	4.320	0.637	2	4.182	0.042	2	1.174	0.024	2
	PTS ≥ 40 dB	3.798	0.000	31	3.960	2.269	31	0.959	0.000	1
11.2	PTS < 10 dB	3.680	3.346	218	5.277	3.746	209	4.793	3.381	207
	10 dB ≤ PTS < 20 dB	3.918	3.051	33	5.394	3.833	33	4.817	4.079	29
	20 dB ≤ PTS < 30 dB	5.148	2.384	8	6.080	2.313	7	5.459	1.157	5
	30 dB ≤ PTS < 40 dB	4.583	0.000	6	6.073	4.740	6	2.597	1.286	4
	PTS ≥ 40 dB	3.766	0.000	28	5.597	4.857	28			0

Table 21

Mean S_{HF} Values ($\bar{S}_{HF}$) and S_{HF} for the mean tuning curves ($\tilde{S}_{HF}$) (dB/octave)

Probe (kHz)	PTS	$\tilde{S}_{HF}$ Pre	Post	N	$\bar{S}_{HF}$ Pre	S.D.	N	Post	S.D.	N
0.5	PTS < 10 dB	27.1	26.7	211	27.3	8.9	208	27.4	8.6	208
	10 dB ≤ PTS < 20 dB	26.6	18.8	47	25.5	9.8	46	21.4	13.3	46
	20 dB ≤ PTS < 30 dB	27.5	11.2	26	26.8	6.4	26	24.7	21.0	25
	30 dB ≤ PTS < 40 dB	24.8	7.0	8	24.4	8.8	8	19.9	23.2	8
	PTS ≥ 40 dB	27.9	0.2	2	23.7	11.4	2	0.0		1
1.0	PTS < 10 dB	48.6	48.4	193	48.3	12.1	192	50.0	13.3	192
	10 dB ≤ PTS < 20 dB	46.5	34.3	30	47.1	10.3	29	44.4	26.7	30
	20 dB ≤ PTS < 30 dB	48.2	21.9	30	46.8	9.4	30	22.3	14.4	30
	30 dB ≤ PTS < 40 dB	47.2	14.9	20	43.7	7.1	20	22.2	12.0	16
	PTS ≥ 40 dB	47.0	4.8	20	44.0	8.4	20	16.0	15.5	9
2.0	PTS < 10 dB	54.4	52.6	174	47.4	14.2	174	47.3	15.7	170
	10 dB ≤ PTS < 20 dB	52.8	44.2	47	45.3	13.1	46	49.9	36.9	46
	20 dB ≤ PTS < 30 dB	44.9	15.0	23	44.4	31.7	22	22.0	24.4	23
	30 dB ≤ PTS < 40 dB	49.8	6.2	16	43.2	12.3	16	12.0	18.1	13
	PTS ≥ 40 dB	49.9	0.8	34	44.9	14.0	34	9.7	25.9	14
4.0	PTS < 10 dB	90.9	87.3	195	86.7	25.0	195	84.2	24.3	192
	10 dB ≤ PTS < 20 dB	75.7	82.7	36	71.5	20.5	36	78.4	28.4	35
	20 dB ≤ PTS < 30 dB	81.8	61.1	18	80.9	19.2	18	55.3	32.1	18
	30 dB ≤ PTS < 40 dB	93.3	36.1	14	89.1	22.5	14	30.5	24.8	14
	PTS ≥ 40 dB	88.3	15.7	31	87.5	30.7	31	14.8	14.0	21
8.0	PTS < 10 dB	75.0	72.2	196	76.3	23.7	194	72.5	28.2	191
	10 dB ≤ PTS < 20 dB	75.2	62.9	54	72.6	26.4	53	64.4	28.0	52
	20 dB ≤ PTS < 30 dB	70.4	52.5	11	72.0	24.1	11	56.4	38.1	10
	30 dB ≤ PTS < 40 dB	85.3	16.0	2	104.8	31.0	2	7.1	9.2	2
	PTS ≥ 40 dB	79.1	1.8	31	80.9	23.1	31	51.2	98.0	9
11.2	PTS < 10 dB	94.8	90.3	218	84.9	29.1	218	84.8	27.8	213
	10 dB ≤ PTS < 20 dB	85.9	79.1	33	81.1	27.8	33	70.2	34.0	32
	20 dB ≤ PTS < 30 dB	97.1	62.5	8	87.9	36.0	8	47.2	37.7	8
	30 dB ≤ PTS < 40 dB	106.2	34.3	6	95.1	11.5	6	29.5	25.9	6
	PTS ≥ 40 dB	97.8	0.0	28	89.6	24.4	28	6.6	16.6	13

Table 22

Mean S_{LF} Values ($\tilde{S}_{LF}$) and S_{LF} for the mean tuning curves ($\tilde{S}_{LF}$) [dB/octave]

Probe (kHz)	PTS	$\tilde{S}_{LF}$ Pre	Post	N	$\tilde{S}_{LF}$ Pre	S.D.	N	Post	S.D.	N
0.5	PTS < 10 dB	24.6	22.2	211	24.5	8.0	211	22.2	8.6	210
	10 dB ≤ PTS < 20 dB	20.7	12.1	47	21.3	7.6	46	12.1	7.4	47
	20 dB ≤ PTS < 30 dB	24.7	7.9	26	24.7	5.3	26	9.7	7.4	26
	30 dB ≤ PTS < 40 dB	22.0	10.2	8	22.0	11.2	8	10.2	7.5	8
	PTS ≥ 40 dB	22.3	0.0	2	22.3	4.4	2	6.4		1
1.0	PTS < 10 dB	26.3	24.8	193	26.3	8.5	193	24.8	8.7	192
	10 dB ≤ PTS < 20 dB	26.1	17.2	30	26.1	9.1	30	17.1	5.7	30
	20 dB ≤ PTS < 30 dB	26.9	14.1	30	26.9	9.7	30	14.2	7.7	30
	30 dB ≤ PTS < 40 dB	31.2	12.2	20	31.2	6.8	20	13.0	6.9	17
	PTS ≥ 40 dB	25.5	10.8	20	25.5	7.9	20	10.8	11.7	9
2.0	PTS < 10 dB	21.7	19.2	174	21.7	12.3	173	19.5	11.4	170
	10 dB ≤ PTS < 20 dB	23.3	14.9	47	23.6	12.6	47	16.4	14.8	47
	20 dB ≤ PTS < 30 dB	19.2	5.4	23	19.3	11.9	22	6.8	7.9	23
	30 dB ≤ PTS < 40 dB	21.5	0.0	16	21.4	10.2	16	0.9	2.3	16
	PTS ≥ 40 dB	20.5	0.0	34	20.5	11.7	34	1.3	4.1	17
4.0	PTS < 10 dB	51.4	49.4	195	51.5	19.0	195	49.2	19.8	193
	10 dB ≤ PTS < 20 dB	51.2	38.3	36	51.5	19.6	36	38.4	20.3	35
	20 dB ≤ PTS < 30 dB	51.9	29.0	18	51.7	18.7	18	28.9	21.6	18
	30 dB ≤ PTS < 40 dB	56.3	10.4	14	56.2	18.1	14	13.5	14.5	14
	PTS ≥ 40 dB	59.2	0.0	31	59.3	20.5	31	3.8	5.3	23
8.0	PTS < 10 dB	33.7	29.2	196	34.1	21.4	196	29.7	20.7	192
	10 dB ≤ PTS < 20 dB	41.7	21.3	54	43.3	22.2	52	23.2	20.4	54
	20 dB ≤ PTS < 30 dB	51.6	23.5	11	51.4	19.0	11	24.7	18.5	11
	30 dB ≤ PTS < 40 dB	76.1	16.2	2	76.1	0.8	2	16.2	8.7	2
	PTS ≥ 40 dB	40.8	0.0	31	40.8	25.5	31	1.0	3.4	12
11.2	PTS < 10 dB	51.3	46.6	218	52.1	29.1	217	47.3	28.6	213
	10 dB ≤ PTS < 20 dB	49.0	37.7	33	50.1	34.7	33	38.4	26.7	32
	20 dB ≤ PTS < 30 dB	58.2	24.3	8	58.1	25.7	8	25.6	34.0	8
	30 dB ≤ PTS < 40 dB	51.7	4.1	6	51.7	30.1	6	15.0	20.7	6
	PTS ≥ 40 dB	51.8	0.0	28	51.9	28.3	28	4.6	10.4	10

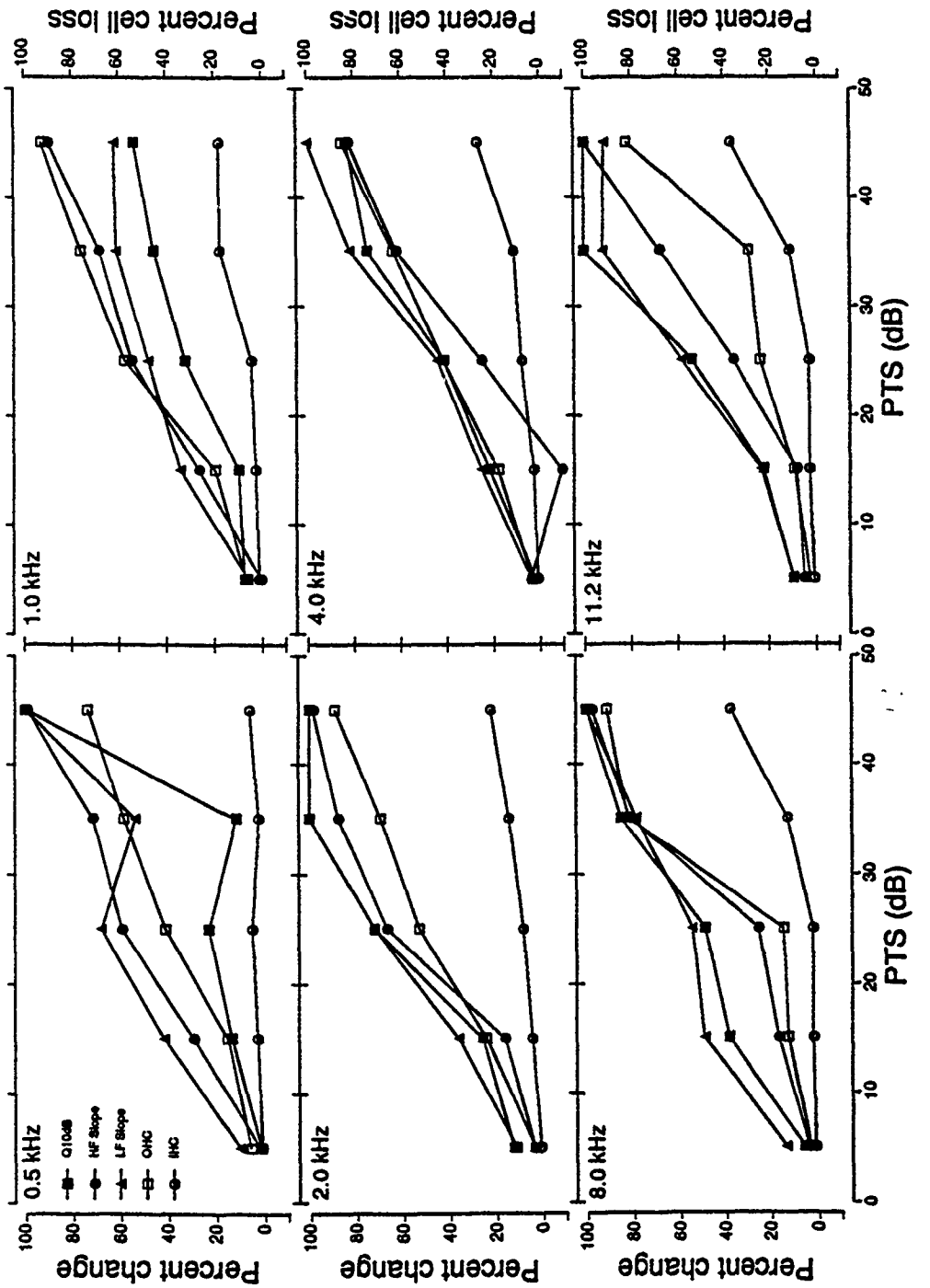

Figure 59. The percent change in the mean tuning curve variables compared with the extent of sensory cell loss for various amounts of permanent threshold shift.

as a function of PTS at various probe frequencies and is compared with the mean amount of sensory cell loss in those same animals in the octave bands centered around those probe frequencies. The total sensory cell loss was determined within the octave band region centered around the probe frequency for each particular PTS bin at that frequency. The IHC losses were much smaller than OHC losses for each PTS bin, being no greater than approximately 40% for PTS levels greater than 40 dB and usually much less. However, once the PTS exceeds approximately 30 dB the OHC's show large losses within the octave bands centered at 0.5 through 8.0 kHz. Below a PTS of 40 dB there was much less sensory cell loss within the octave band centered at 11.2 kHz than at the other frequencies. Generally, as the amount of PTS increases beyond 10 dB, the percent change in all three TC characteristics increases, reflecting a systematic reduction in tuning. Overall, it appears that the changes in TC characteristics are closely related to the increase in the amount of OHC loss over more than a 40 dB range of hearing loss at most probe frequencies. At the 8 and 11.2 kHz probe frequencies the percent change in $Q_{10\ dB}$ or the slope increases in the absence of substantial sensory cell loss for PTS up to 30 dB. At 8 kHz, the S_{HF} follows the trend in OHC loss and shows relatively little change across the first 30 dB of PTS while S_{LF} and Q_{10dB} show substantial changes. At 11.2 kHz, the S_{HF} also tends to broaden (becomes more shallow) despite a less severe sensory cell loss. Once PTS exceeds 40 dB however, all three TC characteristics show a large percentage increase concomitant with a fairly similar increase in the amount of OHC loss observed at the octave band regions centered at 8.0 and 11.2 kHz.

It is important to note that the level of the probe tone was fixed at 15 dB above the mean AEP threshold at each probe frequency for both the pre- and postexposure TC's. Thus the SPL of the probe could be up to about 50 dB higher in some postexposure animals. Since the probe level may present a confounding variable which can influence TC characteristics, we also examined the effects of a high probe level to determine to what extent the morphology of the TC was level dependent. Figure 60 shows the mean TC variables for the entire population of preexposure animals along with a control group (N = 9) whose TC's were obtained at 35 dB above the mean AEP threshold at each probe frequency. The results of t-tests (two-tailed) presented in Table 23 revealed no statistically significant difference ($\alpha = 0.05$) between the low and high probe level on TC characteristics across most probe frequencies. There were no statistically significant differences between probe levels for either the $Q_{10\ dB}$ or S_{LF} variables. A statistically significant steeper S_{HF}, caused by the high probe level, was measured at 11.2 kHz but at 1.0 kHz the S_{HF} was steeper for the low probe level. Thus, the higher probe level resulted in no consistent change in TC variables. Therefore, the changes previously described in the TC's measured from animals with PTS would tend to be representative of the effects of a PTS rather than probe level differences. (We recognize the inherent problems in using successive t-tests in this analysis. However, a repeated-measures analysis of variance could not be employed since missing data in any one cell of the high probe level frequencies resulted in all data being excluded from the analysis. The problem of "pyramiding alpha" would tend to underestimate the effects of a PTS on the tuning curve statistics.)

Studies by Ryan et al. (1979), Robertson et al. (1980), Harrison et al. (1981), Liberman and Dodds (1984), Smith et al. (1987) and others on the changes which occur in psychophysical and physiologic TC's measured from damaged cochleas have generally shown a reduced sharpness of tuning. On the other hand, Dallos et al. (1977) reported normal $Q_{10\ dB}$ with PTS of up to 50 dB from cochleas which had OHC losses only. Aside from the results of Dallos et al., the overwhelming evidence indicates that the quality of tuning is largely

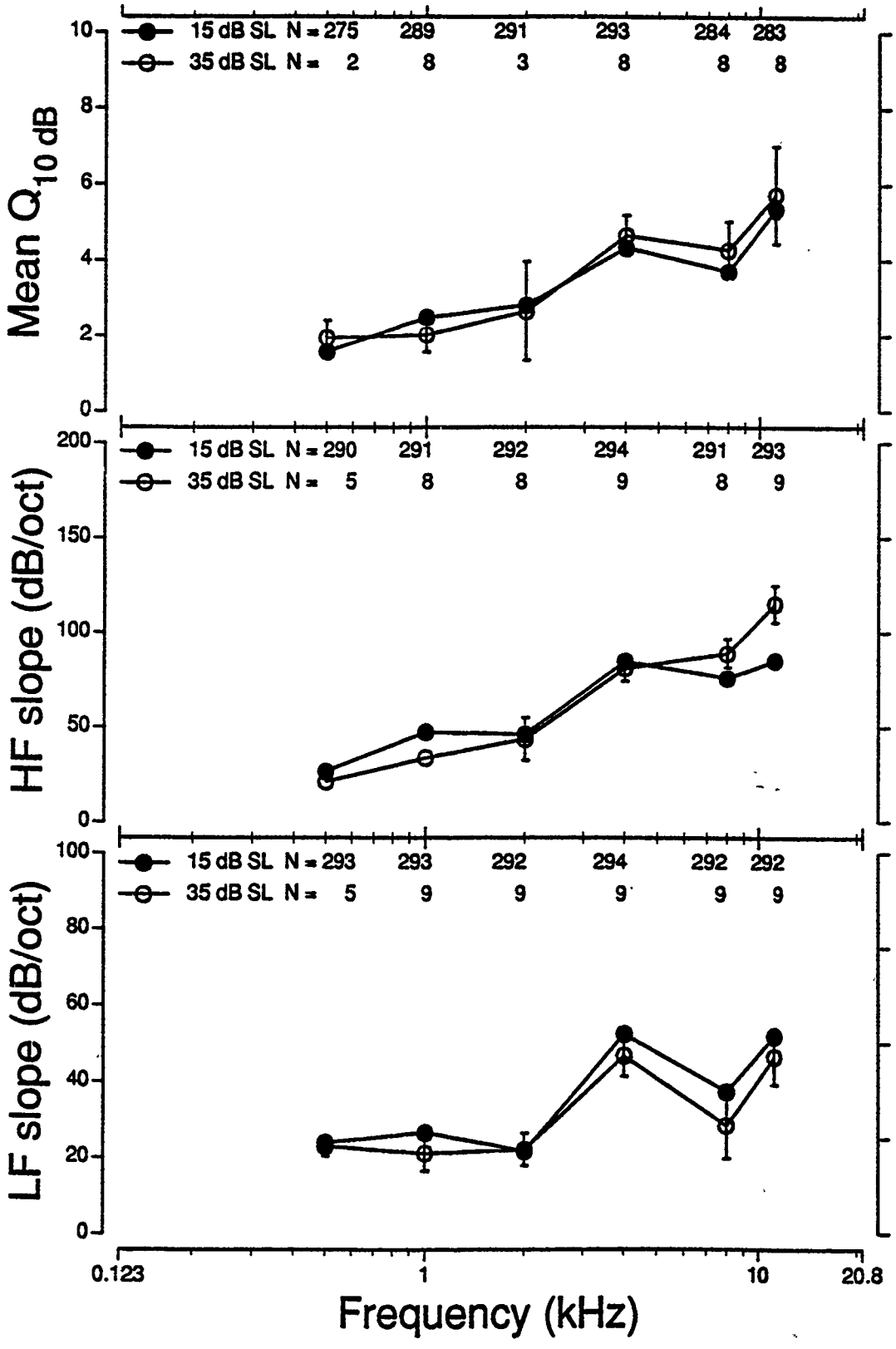

Figure 60. A comparison of tuning curve variables for probe tones presented at 15 or 35 dB above the mean AEP threshold at each probe frequency. (Error bars represent one standard error of the mean above and below the mean.)

Table 23

Summary of tuning curve characteristics for 35 dB SL probe

Statistic	kHz	Mean	s	N	t	df
Q_{10dB}	0.5	1.945	0.650	2	-0.721	275
	1.0	2.028	1.296	8	1.315	295
	2.0	2.644	2.263	3	0.175	292
	4.0	4.646	1.501	8	-0.511	299
	8.0	4.269	2.130	8	-0.798	290
	11.2	5.730	3.633	8	-0.269	289
S_{HF} (dB/octave)	0.5	21.4	11.0	6	1.481	294
	1.0	33.8	14.0	8	3.366*	297
	2.0	43.7	32.1	8	0.443	298
	4.0	81.1	20.7	9	0.426	301
	8.0	89.0	21.1	8	-1.486	297
	11.2	115.2	29.2	9	-3.119*	300
S_{LF} (dB/octave)	0.5	23.0	5.8	5	0.282	296
	1.0	21.1	14.5	9	1.845	300
	2.0	22.1	12.8	9	-0.098	299
	4.0	46.8	16.4	9	0.880	301
	8.0	28.5	26.5	9	1.163	299
	11.2	46.5	22.3	9	0.554	299

* $p < 0.05$ when compared with 15 dB SL results (Table 19)

dependent on the morphological integrity of the sensory cells, especially the outer hair cells. Thus, the issue is no longer whether TC characteristics are altered in damaged ears, but rather, to what extent can TC morphology in combination with the audiogram provide clinically useful information or to what extent can we estimate the condition of the sensory structures of the cochlea? Unlike the currently available studies which involved relatively few experimental animals, we expected that if a fairly large sample of TC's from normal and damaged ears could be assembled, this data base would provide a means of quantitatively relating the changes in frequency selectivity with measures of auditory threshold and the distribution of sensory cell loss. The results presented in this paper show a systematic relation between the degree of PTS, abnormal OHC populations and changes in the quality of tuning. The changes in the quality of tuning in pathologic cochleas cannot be accounted for on the basis of increases in probe level. Detectable changes can be measured, on average, in the three variables used to quantify the TC when the PTS exceeds 10 dB at any probe frequency. This result was somewhat surprising in light of the body of existing psychophysical data which indicates that it takes in excess of a 30 dB hearing loss before abnormal tuning can be consistently measured. However, given the sensitivity of the TC to threshold shifts seen in human studies (Mills, 1982) one might expect a similar sensitivity in an animal model. As PTS exceeds 30 dB, the data presented generally agree with the existing body of evidence which equates significant broadening of the TC with severe OHC losses. Given that IHC pathology was relatively small until PTS exceeded 30 dB, it appears, that the systematic changes in tuning are related primarily to effects arrising from losses of OHC's.

The results of these AEP generated TC data while qualitatively similar to much of the existing single unit data do however show some differences. For example, the physiological data of Harrison and Evans (1977) showed that for PTS below 30 dB there were distinct differences in the changes in tuning between low and high frequency fibers. Such clear frequency effects were not seen in the AEP data. In Figure 59, for example, we can see that as PTS increases most of the tuning curve variables are changed in a fairly similar fashion across the range of CF's that were tested. However there is good agreement between the general trends in our TC and PTS data and the comparable cochlear fiber TC data of Harrison and Evans. We did, however, observe large changes in tuning in the presence of relatively low level OHC losses in the region of 8.0 and 11.2 kHz. At the 8.0 kHz test frequency for instance, there is relatively little loss of sensory cells up to the $30 \leq PTS < 40$ dB bin. The S_{HF} for this test frequency is changed relatively little but the percent change in S_{LF} and $Q_{10\ dB}$ increases (i.e., an upward spread of masking). A similar effect may also be seen at the 11.2 kHz test frequency but at this test frequency S_{HF} shows more change despite the small losses of sensory cells. Thus, these two frequencies seem to show distinctive changes in tuning even though sensory cell losses are relatively small. Some caution, however, must be exercised in interpreting the data at the higher levels of PTS since the sample sizes are small and variability is large. The number of subjects in the lower PTS bins are more substantial but the tuning is still changed in spite of near normal sensory cell populations. The most parsimonious explanation of the abnormal tuning at 8.0 and 11.2 kHz is that it is probably due to the effects of an abnormal sensory cell population in the more apical regions of the cochlea, which is certainly the situation in our experimental population. This is an effect quite parallel to that reported by Liberman and Dodds (1984) when they showed that tuning of single VIII nerve fibers that originate from completely normal regions of the cochlea basalward of a lesion, could be altered. If a change in the masker's excitation pattern as a result of a lesion apical to the 8.0 kHz region alters the residual area of

excitation required for signal detection, we can expect changes in tuning to appear in areas remote from the lesion. A model for simultaneous masking (tone on tone) described by Johnson-Davies and Patterson (1979) for instance, shows that the unmasked area of the signal's pattern (i.e., the residual excitation) shifts toward the apex as the pattern of the masker shifts from below to above the signal frequency. Since the S_{LF} and S_{HF} of the tuning curve represent the high and low frequency side of the traveling wave pattern of the masker respectively (Van Heusden and Smoorenburg, 1981) a change in tuning may occur if the pattern of the masker is spatially altered and interferes with the residual excitation pattern of the signal. Thus, the shallow low frequency slope of the TC for regions of the cochlea with relatively small OHC losses would tend to imply that the traveling wave pattern of the masker is broadened or distorted on its high frequency side in such a manner that it reduces the residual excitation required for detection. This would explain the reduction of tuning in the presence of a normal S_{HF} at 8.0 kHz. The use of this model to produce a parallel explanation for the abnormal S_{HF} at 11.2 kHz when the corresponding region of the cochlea is relatively normal, however, is unsatisfactory. Another possibility is that extensive stereocilia changes within the octave bins might be responsible for the changes in tuning. Our histological method records missing cells and not subtle morphological changes which are known to affect sensory cell function (Liberman and Dodds, 1984). Other explanations that rely upon lesions which disrupt the innervation pattern to the normal outer hair cells basalward of a lesion are equally plausible.

The manner in which these data were analyzed (i.e., the assembly into PTS bins) ignores the status of the cochlea at regions removed from the particular bin being analyzed. Inherent in this approach is the unsuitable assumption of an independence between the various bins that are the basis of the analysis. Thus, potentially important characteristics of the innervation of the OHC's and traveling wave mechanisms are necessarily ignored. Despite this great simplification, the data clearly show that there are systematic changes in TC variables that begin to manifest themselves at relatively low levels of PTS and that these changes are related to the outer hair cell population.

V. REFERENCES

Bohne, B.A. (1974). Mechanisms for continuing degeneration in the Organ of Corti. Journal of the Acoustical Society of America. 55:77.

Burdick, C.K., Patterson, J.H., Mozo, B.T., Hargett, C.E. and Camp, R.J. (1977). Threshold shifts in chinchillas exposed to low frequency noise for nine days. Journal of the Acoustical Society of America. 62:S-95.

Carder, H.M. and Miller, J.D. (1972). Temporary threshold shift from prolonged exposure to noise. Journal of Speech and Hearing Research. 15:603-623.

CHABA (1965). National Research Council, Committee on Hearing Bioacoustics and Biomechanics. Hazardous exposure to intermittent and steady-state noise. Report Working Group 46, Washington, DC.

CHABA (1968). Proposed damage risk criterion for impulse nosie (gunfire). Report of Working Group 57, NAS-NRC Committee on Hearing, Bioacoustis. Washington, DC.

Coles, R.R.A., Garinther, G.R., Rice, C.G. and Hodge, D.C. (1968). Hazardous exposure to impulse noise. Journal of the Acoustical Society of America. 43:336-343.

Dallos, P., Ryan, A., Harris, D., McGee, T. and Ozdamar, O. (1977). Cochlear frequency selectivity in the presence of hair cell damage. In: Psychophysics and Physiology of Hearing, eds., E.F. Evans and J.P. Wilson, (Academic Press, London), pp. 249-262.

Davis, R. and Ferraro, J. (1984). Comparison between AER and behavioral thresholds in normally and abnormally hearing chinchillas. Ear and Hearing. 5(3):153-159.

Eames, B.L., Hamernik, R.P., Henderson, D. and Feldman, A. (1975). The role of the middle ear in acoustic trauma from impulses. Laryngoscope LXXXV 9:1582-1592.

Eldredge, D.H., Mills, J.H. and Bohne, B.A. (1973). Anatomical, behavioral and electrophysiological observations on chinchillas after long exposures to noise. In: Advances in Otophysiology, eds., J.E. Hawkins, M. Lawrence, W.P. Work, (S. Karger, Basel, Switzerland), pp. 64-81.

Eldredge, D.H., Miller, J.D. and Bohne, B.A. (1981). A frequency-position map for the chinchilla cochlea. Journal of the Acoustical Society of America. 69:1091-1095.

Engstrom, H., Ades, H.W. and Anderson, A. (1966). Structural Pattern of the Organ of Corti, (Almgvist and Wiksell) Stockholm, Sweden.

Fay, R.R. (1988). Hearing in Vertebrates, Hill-Fay Associates, Winnetka, IL.

Florentine, M., Buus, S., Scharf, B. and Zwicker, E. (1980). Frequency selectivity in normally-hearing and hearing impaired observers. Journal of Speech and Hearing Research. 23:646-669.

Friedlander, F.G. (1946). The diffraction of sound pulses. Proceedings of the Royal Society. Series A:322-367.

Giraudi, D., Salvi, R.J., Henderson, D. and Hamernik, R.P. (1980). Gap detection by the chinchilla. Journal of the Acoustical Society of America. 67:802-806.

Hamernik, R.P., Dosanjh, D.S. and Henderson, D. (1973). Shock tube application in bio-acoustic research. In: Recent Developments in Shock Tube Research, eds., D. Bershader and W. Griffith, (Stanford University Press, Stanford, CA), pp. 144-155.

Hamernik, R.P., Turrentine, G., Roberto, M., Salvi, R.J. and Henderson, D. (1984a). Anatomical correlates of impulse noise-induced mechanical damage in the cochlea. Hearing Research. 13:229-247.

Hamernik, R.P., Turrentine, G. and Wright, C.G. (1984b). Surface morphology of the inner sulcus and related epithelial cells of the cochlea following acoustic trauma. Hearing Research. 16:143-160.

Hamernik, R.P., Patterson, J.H. and Salvi, R.J. (1987). The effect of impulse intensity and the number of impulses on hearing and cochlear pathology in the chinchilla. Journal of the Acoustical Society of America. 81:1118-1129.

Hamernik, R.P., Ahroon, W.A. and Patterson Jr., J.A. (1988). Threshold recovery functions following impulse noise trauma. Journal of the Acoustical Society of America. 84:941-950.

Harrison, R.V. and Evans, E.F. (1977). The effects of hair cell loss (restricted to outer hair cells) on the threshold and tuning properties of cochlear fibers in the guinea pig. In: Inner Ear Biology, eds., M. Portman and J.M. Aran, Inserm, Paris.

Harrison, R.V., Aran, J.M. and Erre, J.P. (1981). AP tuning curves from normal and pathological human and guinea pig cochleas. Journal of the Acoustical Society of America. 69:1374-1385.

Henderson, D. (1969). Temporal summation of acoustic signals by the chinchilla. Journal of the Acoustical Society of America. 46:474-475.

Henderson, D., Hamernik, R.P., Woodford, C., Sitler, R.W. and Salvi, R. (1973). Evoked response audibility curve of the chinchilla. Journal of the Acoustical Society of America. 54:1099-1101.

Henderson, D., Hamernik, R.P. and Sitler, R.W. (1974). Audiometric and histological correlates of exposure to 1-msec noise impulses in chinchilla. Journal of the Acoustical Society of America. 56:1210-1221.

Henderson, D. and Hamernik, R.P. (1978). Impulse noise-induced hearing loss: An overview. In: Noise and Audiology, ed. D. Lipscomb (University Park Press, Baltimore, MD).

Henderson, D., and Hamernik, R.P. (1982). Asymptotic threshold shift from impulse noise. In: New Perspectives on Noise-Induced Hearing Loss, eds. R.P. Hamernik, D. Henderson, and R.J. Salvi (Raven Press, NY), pp. 265-281.

Henderson, D., Hamernik, R.P., Salvi, and Ahroon, W.A. (1983). Comparison of auditory-evoked potentials and behavioral thresholds in the normal and noise-exposed chinchilla. Audiology. 22:172-180.

Hodge, D.C. and McCommons, B.M. (1966). Reliability of TTS from impulse noise exposure. Journal of the Acoustical Society of America. 40:911.

Humes, L.E. (1984). Noise-induced hearing loss as influenced by other agents and by some physical characteristics of the individual. Journal of the Acoustical Society of America. 76:1318-1329.

Hunter-Duvar, I.M. and Elliott, D.N. (1972). Effects of intense auditory stimulation: Hearing losses and inner ear changes in the squirrel monkey. Journal of the Acoustical Society of America. 52:1181-1192.

Johnson-Davies, D. and Patterson, R.D. (1979). Psychophysical tuning curves: Restricting the listening band to the signal region. Journal of the Acoustical Society of America. 65:765-770.

Klein, A.J. and Mills, J.H. (1981). Physiological (waves I and V) and psychophysical tuning curves in human subjects. Journal of the Acoustical Society of America. 69:760-768.

Kryter, K.D., and Garinther, G.R. (1966). Auditory effects of acoustic impulses from firearms. Acta Otolaryngology. Suppl. 211.

Kryter, K.K. (1970). The Effects of Noise on Man. (Academic Press, NY).

Liberman, M.C. and Dodds, L.W. (1984). Single-neuron labeling and chronic cochlear pathology, III. Stereocilia damage and alterations of tuning curves. Hearing Research. 16:55-74.

Lindquist, S.E., Neff, W.D. and Schudnecht, H.F. (1954). Stimulation deafness: A study of hearing losses resulting from exposure to noise of blast impulses. Journal of Comp. Physiology and Psychology. 47:406.

Luz, G.A. and Hodge, D.C. (1971). The recovery from impulse noise-induced TTS in monkeys and men: A descriptive model. Journal of the Acoustical Society of America. 49:1770-1777.

Margolis, R.H. and Smith, P. (1977a). Tympanometric asymmetry. Journal of Speech and Hearing Research. 20:437-446.

Margolis, R.H. and Popelka, G.A. (1977b). Interactions among typanometric variables. Journal of Speech and Hearing Research. 20:447-462.

McGee, T., Ryan, A. and Dallos, P. (1976). Psychophysical tuning curves of chinchillas. Journal of the Acoustical Society of America. 60:1146-1150.

McRobert, H. and Ward, W.D. (1973). Damage-risk criteria: The trading relation between intensity and the number of nonreverberant impulses. Journal of the Acoustical Society of America. 53:1297-1300.

Miller, J.D. (1970). Audibility curve of the chinchilla. Journal of the Acoustical Society of America. 48:513-523.

Mills, J.H. (1973). Temporary and permanent threshold shifts produced by nine-day exposures to noise. Journal of Speech and Hearing Research. 16:426-438.

Mills, J.H., Adkins, W.Y. and Gilbert, R.M. (1978). Animal models of noise induced hearing loss: Correlations with human data and sensory cell functions. Midwinter Research Meeting of the Association for Research in Otolaryngology, St. Petersburgh, FL.

Mills, J. (1982). Effects of noise on auditory sensitivity, psychophysical tuning curves, and suppression. In: New Perspectives on Noise-Induced Hearing Loss, eds., R.P. Hamernik, D. Henderson and R. Salvi, (Raven Press, NY).

Moody, D.B., Stebbins, W.C., Johnsson, L.G. and Hawkins, J.E. (1976). Noise-induced hearing loss in the monkey. In: The Effects of Noise on Hearing, eds., D. Henderson, R.P. Hamernik, D.S. Dosanjh and J.H. Mills, (Raven Press, NY), pp. 309-325.

Morest, D.K. (1982). Degeneration in the brain following exposure to noise. In: New Perspectives on Noise-Induced Hearing Loss, eds., R.P. Hamernik, D. Henderson and R.J. Salvi, (Raven Press, NY), pp. 87-93.

Patterson, J.H., Jr., Lomba-Gautier, I.M., Curd, D.L., Hamernik R.P., et al. (1985). The effect of impulse intensity and the number of impulses on hearing and cochlear pathology in the chinchilla. USAARL Report No. 85-3.

Patterson, J.H., Lomba-Gautier, I.M., Curd, D.L., Hamernik, R.P., Salvi, R.J., Hargett Jr., C.E. and Turrentine, G. (1986). The role of peak pressure in determining the auditory hazard of impulse noise. USAARL Report No. 86-7.

Perkins, C., Hamernik, R.P. and Henderson, D. (1975). The effects of interstimulus interval on the production of hearing loss from impulse noise. Journal of the Acoustical Society of America. 57:S-62.

Pfander, F., Bongartz, H., Brinkman, H., and Kietz, H. (1980). Danger of auditory impairment from impulse noise: A comparative study of the CHABA damage-risk criteria and those of the Federal Republic of Germany. Journal of the Acoustical Society of America. 67:628-633.

Price, G.R. (1979). Loss of auditory sensitivity following exposure to spectrally narrow impulses. Journal of the Acoustical Society of America. 66:456-465.

Price, G.R. (1981). Implications of critical level in the ear for assessment of noise hazard at high intensities. Journal of the Acoustical Society of America. 69:171-177.

Price, G.R. (1983). Relative hazard of weapons impulses. Journal of the Acoustical Society of America. 73:556-566.

Price, G.R. (1986). Hazard from intense low-frequency acoustic impulses. Journal of the Acoustical Society of America. 80:1076-1086.

Ritsma, R.J., Wit, H.P. and van der Lans, W.P. (1980). Relations between hearing loss, maximal word discrimination score and width of psychophysical tuning curves. In: Psychophysical, Physiological and Behavioral Studies in Hearing, eds., G. Vanden Brink and F.A. Bilsen, (Delft University Press, Netherlands).

Roberto, M., Hamernik, R.P., Salvi, R.J., Henderson, D. and Milone, R. (1985). Impact noise and the equal energy hypothesis. Journal of the Acoustical Society of America. 77:1514-1520.

Robertson, D., Cody, A.R., Bredberg, G. and Johnstone, B.M. (1980). Response properties of spiral ganglion neurons in cochleas damaged by direct mechanical trauma. Journal of the Acoustical Society of America. 67:1295-1303.

Ryan, A. and Dallos, P. (1975). Effects of absence of cochlear outer hair cells on behavioral auditory thresholds. Nature. 253:44-46.

Ryan, A., Dallos, P. and McGee, T. (1979). Psychophysical tuning curves and auditory thresholds after hair cell damage in the chinchilla. Journal of the Acoustical Society of America. 66:370-378.

Salvi, R.J., Hamernik, R.P. and Henderson, D. (1978). Auditory nerve activity and cochlear morphology after noise exposure. 15th Workshop on Inner Ear Biology, Seefeld, Austria.

Salvi, R.J., Giraudi, D., Henderson, D. and Hamernik, R.P. (1982a). Detection of sinusoidally amplitude modulated noise by the chinchilla. Journal of the Acoustical Society of America. 71:424-429.

Salvi, R.J., Perry, J., Hamernik, R.P. and Henderson, D. (1982b). Relationships between cochlear pathologies and auditory nerve and behavioral responses following acoustic trauma. In: New Perspectives on Noise-Induced Hearing Loss, eds. R.P. Hamernik, D. Henderson, and R.J. Salvi, (Raven Press, NY).

Salvi, R.J., Ahroon, W.A., Perry, J.W., Gunnarson, A.D. and Henderson, D. (1982c). Comparison of psychophysical and evoked-potential tuning curves in the chinchilla. American Journal of Otolaryngology. 3:408-416.

Smith, D.W., Moody, D.B., Stebbins, W.C. and Norat, M.A. (1987). Effects of outer hair cell loss on the frequency selectivity of the patas monkey auditory system. Hearing Research. 29:125-138.

Smoorenburg, G.F. (1982). Damage risk criteria for impulse noise. In New Perspectives on Noise-Induced Hearing Loss, eds. R.P. Hamernik, D. Henderson, and R.J. Salvi (Raven Press, NY), pp. 471-490.

Spoendlin, H.H. (1976). Anatomical changes following various noise exposures. In: Effects of Noise on Hearing, eds., D. Henderson, R.P. Hamernik, D. Dosanjh and J. Mills, (Raven Press, NY), p. 69.

Tyler, R.S., Fernandes, M. and Wood, E.J. (1980). Masking, temporal integration and speech intelligibility in individuals with noise-induced hearing loss. In: Disorders of Auditory Function, eds., I. Taylor and A. Markides, (Academic Press, NY), Vol. III.

Tyler, R.S., Hall, J.W., Glasber, B.R., Moore, B.C.J. and Patterson, R.D. (1984). Auditory filter asymmetry in the hearing impaired. Journal of the Acoustical Society of America. 76:1363-1368.

Van Heusden, E. and Smoorenburg, G.F. (1981). Eighth-nerve action-potential tuning curves in cats before and after inducement of an acute noise trauma. Hearing Research. 5:25-48.

Ward, W.D., Selters, W. and Glorig, A. (1961). Exploratory studies on temporary threshold shift from impulses. Journal of the Acoustical Society of America. 33:781-793.

Ward, W.D. (1968). Susceptibility to auditory fatigue. In: Contributions to Sensory Physiology, ed. W.D. Neff, (Academic Press, NY), pp. 191-226.

Wightman, F.L., McGee, T. and Kramer, J. (1977). Factors influencing frequency selectivity in normal and hearing-impaired listeners. In: Psychophysics and Physiology of Hearing, eds., E.F. Evans and J.P. Wilson, (Academic Press, NY).

Young, R.W. (1970). On the energy transported with a sound pulse. Journal of the Acoustical Society of America. 47:441-442.

Zwicker, E. (1974). On a psychophysical equivalent of tuning curves. In: Facts and Models in Hearing, eds., E. Zwicker and E. Terhardt, (Springer-Verlag, NY), pp. 132-140.

VI. LIST OF PUBLICATION AND PRESENTATIONS SUPPORTED BY THIS CONTRACT.

I. Publications.

Davis, R.I., Ahroon, W.A. and Hamernik, R.P. (1989). The relation among hearing loss, sensory cell loss and tuning characteristics in the chinchilla. Hearing Research, 41:1-14.

Hamernik, R.P., Patterson Jr., J.H., Turrentine, G.A. and Ahroon, W.A. (1989). The quantitative relation between sensory cell loss and hearing thresholds. Hearing Research, 38:199-212.

Roberto, M., Hamernik, R.P. and Turrentine, G.A. (1989). Damage of the auditory system associated with acute blast trauma. Annals of Otology, Rhinology and Laryngology, 98:23-34.

Patterson Jr., J.H., and Hamernik, R.P. (1991). An experimental basis for the estimation of auditory system hazard following exposure to impulse noise. In: Noise-Induced Hearing Loss, eds. A.L. Dancer et al., (in press). B.C. Decker, Inc., St. Louis, MO.

Hamernik, R.P. and Hsueh, K.D. (1991). Impulse noise: Some definitions, physical acoustics and other considerations. Journal of the Acoustical Society of America, 90 (in press).

Hamernik, R.P., Ahroon, W.A. and Hsueh, K.D. (1991). The energy spectrum of an impulse: Its relation to hearing loss. Journal of the Acoustical Society of America, 90 (in press).

II. Presentations (Abstracts).

Davis, R.I., Ahroon, W.A. and Hamernik, R.P. (1988). Changes in frequency selectivity in the chinchilla following a noise induced permanent threshold shift. Journal of the Acoustical Society of America, 83:S116(A).

Hamernik, R.P. and Ahroon, W. A. (1988). Effects of high-level impulse noise intensity, number and rate on hearing. Journal of the Acoustical Society of America, 84:S75(A).

Davis, R.I., Hamernik, R.P., Turrentine, G.A. and Ahroon, W.A. (1990). Frequency selectivity in noise-exposed chinchillas. Journal of the Acoustical Society of America, 88:S19(A).

VII. LIST OF INDIVIDUALS SUPPORTED BY THIS CONTRACT

(1) Roger P. Hamernik, Ph.D. - Project Director
(2) William A. Ahroon, Ph.D. - Senior Research Scientist
(3) George A. Turrentine - Histologist
(4) Keng D. Hsueh, Ph.D. - Mechanical Engineer
(5) Robert I. Davis, Ph.D. - Audiologist
(6) Jeffrey Wells, M.S. - Engineer
(7) Sheau-Fang Lei, Ph.D. - Electrical Engineer
(8) Celeste Garganon - Secretary
(9) Roberta Chesbrough - Secretary
(10) Renee Johnston - Secretary
(11) Jennifer H. Johnson, B.A. - Graduate Student Assistant
(12) Randy Wetzel, B.A. - Graduate Student Assistant
(13) Andrea Kolz, B.A. - Undergraduate Student Assistant
(14) Lisa Valickus, B.A. - Undergraduate Student Assistant

DISTRIBUTION LIST

1 copy	Commander US Army Medical Research and Development Command Attn: SGRD-RMI-S Fort Detrick Frederick, Maryland 21701-5012
2 copies	Defense Technical Information Center (DTIC) ATTN: DTIC-FDAC Cameron Station Alexandria, Virginia 22304-6145
1 copy	Dean School of Medicine Uniformed Services University of the Health Sciences 4301 Jones Bridge Road Bethesda, Maryland 20814-4799
1 copy	Commandant Academy of Health Sciences, US Army ATTN: AHS-CDM Fort Sam Houston, Texas 78234-6100